NTNU

Norwegian University of
Science and Technology

Assessing Stability of Coastal Bluffs Due to Combined Actions of Waves and Changing Ambient Temperatures in the Arctic

Agnes Katharina Schneider

Civil and Environmental Engineering
Submission date: October 2017
Supervisor: Raed Khalil Lubbad, IBM
Co-supervisor: Ivan Depina, SINTEF
Mohammad Saud Afzal, IBM

Norwegian University of Science and Technology
Department of Civil and Environmental Engineering

NORWEGIAN UNIVERSITY OF SCIENCE AND TECHNOLOGY
DEPARTMENT OF CIVIL AND ENVIRONMENTAL ENGINEERING

Report Title:	Date:			
Assessing Stability of Coastal Bluffs Due to Combined Action of Waves and Changing Ambient Temperatures in the Arctic	Number of pages (incl. appendices): 91			
	Master Thesis	X	Project Work	
Name: Agnes Schneider				
Professor in charge/supervisor: Prof. Raed Lubbad				
Other external professional contacts/supervisors: Dr. Ivan Depina, Dr. Mohammad Saud Afzal				

Abstract:

The main objective of this thesis is the development of a numerical model with the software Plaxis, which simulates the thermodenudation, an erosion process in the Arctic which is mainly caused by the thawing of the permafrost soil. The developed model is a combination of a thermo-hydraulic model, which considers the cryogenic suction as an important process within frozen soil, coupled with a mechanical model via Python program codes to allow the analysis of slope stability and coastal retreat rates.

The model was calibrated and partly validated to the coastline of Baydara Bay in western Russia, showing good results regarding the active layer thickness, the coastal retreat rate and the volume of eroded soil, which were close to the measured data. To investigate the effects of climate change on this coastline and the applicability of the model for such a purpose, a temperature increase was simulated, according to predictions of the Intergovernmental Panel on Climate Change. The calculated results were reasonable and complied with predicted developments. Additionally, also the bearing capacity of the bluff at Baydara Bay was determined and the effects of a thermosyphon as a coastal protection measure were simulated, whereby the coastal erosion could be significantly reduced. A parameter variation was also conducted to identify modelling parameters with a high importance for the modelling results, which were the unit weight, the slope angle of the bluff and the positions of the boundary conditions and the water level.

In a conclusion, the limitations of the model are outlined and further research possibilities are proposed.

Keywords:

1. Coastal erosion/ thermodenudation
2.Modelling
3. Plaxis
4. Baydara Bay, Russia
5. Climate change

NTNU
Faculty of Engineering Science and Technology
Institute of Civil and Environmental Engineering

MASTER DEGREE THESIS

Autumn 2017

for

Student: Agnes Schneider

Accessing Stability of Coastal Bluffs Due to Combined Actions of Waves and Changing Ambient Temperatures in the Arctic

BACKGROUND

Bluff erosion is quite common in Arctic areas. Due to climate changes, an increase of the erosion rates is expected. This is mainly because the forecasted longer ice-free seasons lead to bigger sea-waves approaching the bluffs and warmer temperatures which will accelerate the thawing of the permafrost. Furthermore, warmer temperatures and a retreat of sea ice cover favour human activities in the Arctic regions, for example new shipping routes can be developed or natural resources can be used. That makes it important to develop reliable ways to model and forecast coastal erosion in the Arctic. There are two main processes, which are most important for coastal erosion in the Arctic regions: Thermodenudation and thermoabrasion. Thermodenudation is defined as the gradually thawing of permafrost bluffs due to solar radiation, warmer air temperature and snow melt. The thawing process reduces the strength of the soil, destabilizing the bluff and finally leading to its failure. The eroded sediment is deposited at the toe of the bluff wherefrom it is removed through the actions of waves and currents. Thermoabrasion is mainly caused by the erosive force of waves and currents at high water levels. The bluff then thaws quickly due to convective heat transport, whereby the melted sediment is transported off shore and out of the littoral system. This thawing process can lead to the formation of horizontal niches, the depth of which increases during several storms and years. When the so overhanging material becomes too heavy

and can’t be hold by the shear or bending strength of the soil it collapses as a block. The block is then exposed to wave forces and the influence of the warm seawater and is gradually removed.

TASK

This thesis shall focus on the modelling of the coastal erosion in the Arctic. The study is limited to the modelling of the thermodenudation process. The thesis shall include the following tasks:

- Literature review about coastal erosion processes in the Arctic and the available methods and tools that have been used to model these processes.
- Development of a numerical model to simulate the thermodenudation process and to determine the mass of the soil, which goes into the ocean/water body. Only the load due to linear waves shall be considered as far as hydrodynamic loading is considered, i.e. no modelling of wave propagation and the hydrodynamics is required. The program PLAXIS shall be used for the modelling.
- Investigate the possibilities to couple the thermodenudation model with a post-failure model, to simulate the total erosion processes.
- Review the literature about common protection measures against Arctic coastal erosion; and if time allows, use the numerical model developed during this study to model and asses some of these solutions.

General about content, work and presentation

The text for the master thesis is meant as a framework for the work of the candidate. Adjustments might be done as the work progresses. Tentative changes must be done in cooperation and agreement with the professor in charge at the Department.

In the evaluation thoroughness in the work will be emphasized, as will be documentation of independence in assessments and conclusions. Furthermore, the presentation (report) should be well organized and edited; providing clear, precise and orderly descriptions without being unnecessary voluminous.

The report shall include:

- Standard report front page (from DAIM, http://daim.idi.ntnu.no/)
- Title page with abstract and keywords.(template on: wiki page for students at CEE Departement)
- Preface
- Summary and acknowledgement. The summary shall include the objectives of the work, explain how the work has been conducted, present the main results achieved and give the main conclusions of the work.
- The main text.
- Text of the Thesis (these pages) signed by professor in charge as Attachment 1.

The thesis can as an alternative be made as a scientific article for international publication, when this is agreed upon by the Professor in charge. Such a report will include the same points as given above, but where the main text includes both the scientific article and a process report.

Advice and guidelines for writing of the report is given in "Writing Reports" by Øivind Arntsen, and in the departments "Råd og retningslinjer for rapportskriving ved prosjekt og masteroppgave" (In Norwegian) located at wiki page for students at CEE Departement

Submission procedure

Procedures relating to the submission of the thesis are described in DAIM (http://daim.idi.ntnu.no/).

Printing of the thesis is ordered through DAIM directly to Skipnes Printing delivering the printed paper to the department office 2-4 days later. The department will pay for 3 copies, of which the institute retains two copies. Additional copies must be paid for by the candidate / external partner. The master thesis will not be registered as delivered until the student has delivered the submission form (from DAIM) where both the Ark-Bibl in SBI and Public Services (Building Safety) of SB II has signed the form. The submission form including the appropriate signatures must be signed by the department office before the form is delivered Faculty Office.

Documentation collected during the work, with support from the Department, shall be handed in to the Department together with the report.

According to the current laws and regulations at NTNU, the report is the property of NTNU. The report and associated results can only be used following approval from NTNU (and external cooperation partner if applicable). The Department has the right to make use of the results from the work as if conducted by a Department employee, as long as other arrangements are not agreed upon beforehand.

Tentative agreement on external supervision, work outside NTNU, economic support etc.

Separate description is to be developed, if and when applicable. See wiki page for students at CEE Departement for agreement forms.

Health, environment and safety (HSE) http://www.ntnu.edu/hse

NTNU emphasizes the safety for the individual employee and student. The individual safety shall be in the forefront and no one shall take unnecessary chances in carrying out the work. In particular, if the student is to participate in field work, visits, field courses, excursions etc. during the Master Thesis work, he/she shall make himself/herself familiar with "Fieldwork HSE Guidelines".

NTNU student HSE policy is found here: https://innsida.ntnu.no/hms-for-studenter If you are doing labwork for your project og master thesis, you have to take an online e-course in lab HSE. To get link, email kontakt@ibm.ntnu.no.

The students do not have a full insurance coverage as a student at NTNU. If you as a student want the same insurance coverage as the employees at the university, you must take out individual travel and personal injury insurance.

Startup and submission deadlines

Startup and submission deadlines are according to information found in DAIM.

Professor in charge: Raed Lubbad

Other supervisors: Dr. Ivan Depina, Dr. Mohammad Saud Afzal

Department of Civil and Environmental Engineering

Acknowledgment

I would like to thank my supervisors at the NTNU for their excellent supervision of my Master thesis. Especially I would like to express my sincere gratitude to:

Associate professor Raed Lubbad, for his constant support, motivation and encouragement and his valuable comments on my thesis, which helped to improve it a lot and made the whole organisation easier.

Dr. Ivan Depina from SINTEF for sharing his vast knowledge about numerical modelling and programming in Plaxis with me, for his patience with my many questions and his helpful comments on my thesis. Without him, this thesis would not have been possible.

Dr. Mohammad Saud Afzal, for his good ideas about modelling possibilities, for providing the necessary data for the case study of Baydara Bay and for his support when it came to the evaluation of the results.

Finally, I would like to thank the first and second examiner of my thesis at my home university the RWTH Aachen, Univ.-Prof. Dr.-Ing. Holger Schüttrumpf and Univ.-Prof. Dr.-Ing. Heribert Nacken, for allowing me to write my Master thesis at the NTNU.

Abstract

This thesis focusses on the coastal erosion processes in the Arctic regions, which differ from erosion in temperate areas because of the presence of frozen soil. Due to this, the erosion is also influenced by thermal effects because of the warmer air or sea water temperature which leads to a thawing and thereby a destabilisation of the coastal bluff, whereas on temperate coastlines only erosion due to waves and currents is present. The Arctic coastal zone is characterized by high erosion rates, which are on average 0.5 m/year but can reach up locally to 25 m/year (Pearson 2015) and therefore endanger coastal infrastructure. Additionally, the global warming takes place twice as fast in the Arctic than in the rest of world, resulting in an expected increase of the erosion rates and a further acceleration of the climate change. Furthermore, warmer temperatures and a retreat of sea ice cover favour human activities in the Arctic regions. Therefore, it is very important to develop reliable ways to model and forecast coastal erosion in the Arctic (Zetsche, Faller and Broich 2005).

This thesis provides a new approach in simulating the thermodenudation, an erosion process which is mainly caused by the thawing of the permafrost soil, using the geotechnical software Plaxis. The developed Thermodenudation Model is a combination of a thermo-hydraulic model, which considers the cryogenic suction as an important process within frozen soil, coupled with a mechanical model via Python program codes to allow the analysis of slope stability and coastal retreat rates. The Mohr Coulomb soil model is used to simulate the stability of a thawing coastal slope. Excess pore pressure development due to the thawing of the soil is not considered. Additionally, a separate Excel sheet was developed to determine the volume of eroded soil. This model was then calibrated and partly validated to the situation at Baydara Bay a coastline in west Russia, obtaining good results, which are very close to measured data. To investigate the effects of climate change on Baydara Bay until the end of this century, the temperature increase predicted from the IPCC (Intergovernmental Panel on Climate Change) was simulated with the Thermodenudation Model in several scenarios, whereby the calculated results regarding the active layer thickness, the coastal retreat rate and the volume of eroded soil are reasonable and comply with predicted developments. The Thermodenudation Model was also used to determine the bearing capacity of the bluff, by placing loads on its top and to simulate the effects of a thermosyphon as a protection measure, whereby the erosion could be significantly reduced. Additionally, a parameter study was conducted to identify the most influential parameters.

Table of Contents

List of Figures

List of Tables

List of Abbreviations

ACIA	Arctic Climate Impact Assessment
BBM	Barcelona Basic Model
C	Carbon
CAD	Computer Aided Design
CO_2	Carbon dioxide
DGPS	Differential Global Positioning System
FS	Factor of Safety
GPS	Global Positioning System
IPCC	Intergovernmental Panel on Climate Change
K	Kelvin
MC model	Mohr Coulomb soil model
SAMCoT	Sustainable Arctic, Marine and Coastal Technology
SWCC	Soil water characteristic curve
Tg	Teragram
THM models	Thermo-hydro-mechanical models

List of Symbols

B_{DT}	Strain interpolation matrix
c'	effective cohesion
c	cohesion
C_w	specific heat capacity of water
d	thickness
D^e	elastic material matrix representing Hooke's law
D_v	vapour diffusion coefficient
D_{pv}	hydraulic diffusion coefficient
D_{Tv}	thermal diffusion coefficient
E	Young's modulus
e_v	internal energy in vapour
e_s	internal energy in the solid phase
e_w	internal energy in water
f	yield function
g	gravitational acceleration
g_p	plastic potential function
g_a	fitting parameter air entry
g_n	fitting parameter water extraction
g_c	fitting parameter used in the general Van Genuchten equation
g_l	fitting parameter
h	water depth
h_N	niche height
J_{Aw}	advective internal energy flux in water
J_c	conductive heat flow
J_v	mass flux of vapour
J_w	advective mass flux of water
K_w	bulk modulus of the pore fluid
k	coefficient of permeability
k^{int}	intrinsic permeability
k_{rel}	relative permeability
k_{sat}	permeability in the saturated state
k_x	horizontal permeability
$k_{y,}$	vertical permeability
M	material stress strain matrix
m	identity tensor
n	Porosity
p	average pore pressure
p_g	gas pressure
p_w	water pore pressure
Q_T	heat source
q	fluid velocity
S	degree of saturation
S_{res}	residual saturation
S_{sat}	saturated saturation
S_e	effective saturation
T	temperature
t	time
u	pore pressure

V_w	water phase velocity
x_m	niche depth
α	parameter MC model
β	constant Kobayashi 1985
ε	total strain
ε^e	elastic part of strain
ε^p	plastic part of strain
ϵ	surf zone eddy diffusivity
ν	Poisson's ratio
μ	dynamic viscosity
Λ	plastic multiplier
ψ_{sat}	unsaturated zone
ϕ_p	pressure head
ρ	density of the multiphase medium
ρC	heat capacity of the porous medium
ρ_g	gas density
ρ_s,	solid particle density
ρ_v	vapour density
ρ_w	density of water
τ	shear strength
σ'	effective normal stress
σ	total stress
λ	thermal conductivity
φ'	effective angle of friction
φ	angle of friction
ξ_m	temperature dependent parameter
ψ	angle of dilatancy
∇	gradient/divergence
χ	matrix suction coefficient

1 Introduction

1.1 Background and motivation

About 25 % of the land area are permafrost regions, mostly distributed in the northern hemisphere in Canada, Russia and China. Permafrost coastlines represent nearly 34 % of the worldwide coastlines and are exposed to increasing erosion rates endangering infrastructure such as roads and pipelines (Zetsche, Faller and Broich 2005). The average erosion rate in Arctic regions is 0.5 m per year but locally erosion rates up to 25 m per year are possible and due to climate change, a further increase of the erosion rate is expected (Pearson 2015). Additionally, warmer temperature will lead to increased thawing depths during the summer months, which will reduce the bearing capacity of the permafrost and lead to settlements and slope failure. The climate change takes place about twice as fast in Arctic areas than in the rest of the world leading to a temperature increase of about 4 °C in the last 50 years. The thawing of the permafrost could further accelerate the global warming, since about 25 % of the global terrestrial carbon is stored in the permafrost and will be released when it thaws (Zetsche, Faller and Broich 2005). Furthermore, warmer temperatures and a retreat of sea ice cover favour human activities in the Arctic regions, for example new shipping routes can be developed or natural resources can be used. That makes it important to develop reliable ways to model and forecast coastal erosion in the Arctic. There are two coastal erosion processes in Arctic regions, the thermoabrasion, which is mainly caused by waves and currents and the thermodenudation, which is thermally dominated and caused by the thawing and thereby destabilization of the permafrost soil. Whereas there are already numerical models to simulate the thermoabrasion erosion process e.g. Cosmos, simulating the thermodenudation process still is a challenge and no commercial software solutions are currently available.

1.2 Objectives

The main objective of this thesis is therefore the development of a model, which can simulate the thermodenudation erosion process using the geotechnical software Plaxis. Additionally, also the volume of eroded soil shall be calculated. This model shall then be calibrated and validated to the coast of Baydara Bay to investigate its applicability for the modelling of the effects of climate change scenarios regarding the active layer thickness, the coastal retreat rate and the volume of eroded soil. The modelling of protection measures shall be included in this investigation as well as a parameter variation, to identify the parameters, which have a

significant effect on the results. At the end, this thesis shall provide a model, which delivers reasonable results regarding the slope stability of coastal slopes, which are subjected to thermodenudation.

1.3 Structure

Chapter 2 provides an overview about the coastal erosion processes in Arctic regions, including parameters that influence them and their effects on a regional and global scale. Additionally, characteristics and processes related to frozen soil and permafrost are described as background information for the frozen soil modelling.

Chapter 3 deals with the protection measures against the erosion processes and presents besides general considerations some solution how to reduce coastal erosion in Arctic areas.

Chapter 4 focusses now on the already existing modelling possibilities of the erosion processes. Hereby mathematical models as well as available software is included.

In Chapter 5 the numerical Thermodenudation Model, which was developed in this study, is described. This chapter also includes a summary about the theoretical background of the used soil, thermal and hydraulic models.

Chapter 6 contains the case study of Baydara Bay, where the effects of climate change scenarios were investigated. The chapter includes descriptions of the study site and of the Thermodenudation Model, which was calibrated to the situation at Baydara Bay. Also, climate change projections and the selected climate change scenarios are presented.

In Chapter 7 the results of the calibration and validation of the Thermodenudation Model to the situation at Baydara Bay, as well as the results of the climate change scenarios are presented and discussed. Additionally, also results regarding the bearing capacity investigation and the protection measures are included.

Chapter 8 summarizes the main findings of this thesis, the abilities and limitations of the Thermodenudation Model and proposes further topics for research.

2 Coastal Erosion Processes in the Arctic

The coastal erosion in Arctic regions, differs from erosion in temperate areas mainly because of the presence of frozen soil. Nairn et al (1998) identified three aspects, which differentiate erosion at Arctic coastlines from that in more temperate climates: (1) thawing of the exposed frozen sediment by warmer seawater, (2) fine and ice rich sediment, which is common in Arctic areas does not contribute to the sediment balance of the littoral zone, and (3) subsidence of the littoral zone due to melting of ground ice. The coastal erosion in Arctic regions can be divided into two main processes, the thermodenudation and the thermoabrasion.

2.1 Thermodenudation

According to Pearson (2015) the thermodenudation is defined as the gradual thawing of permafrost bluffs due to solar radiation, warmer air and sea temperatures and snow-melt. The thawed sediment can become unstable and cause failure of a coastal slope, depositing sediment at the base of the slope. This sediment is then usually eroded and removed by waves and currents. Thermodenudation commonly takes place at coastlines with fine sediments and a high ice content. Figure 2-1 illustrates the thermodenudation process (Guégan and Christiansen 2016, Pearson 2015).

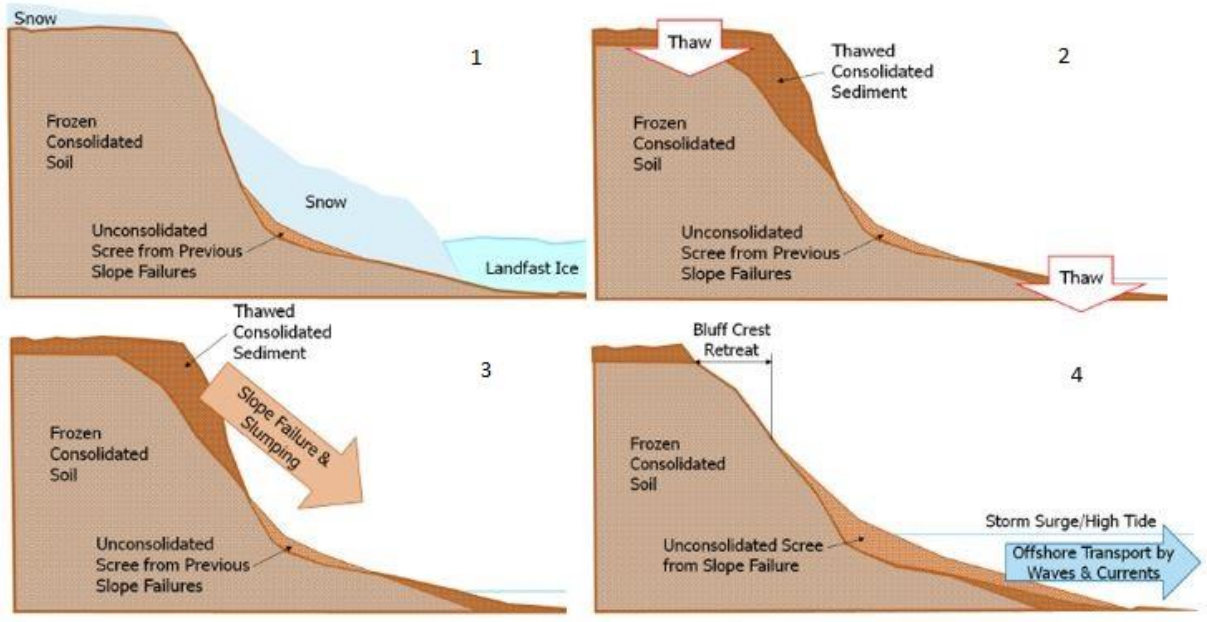

Figure 2-1: Illustration of the thermodenudation (According to Pearson 2015)

In contrary to thermoabrasion, thermodenudation is characterized by lower and consistent erosion rates and occurs mostly during calm weather conditions. Thermodenudation is mainly

dominated by thermal processes, since the sea water has no or only little contact with the frozen bluff and is just responsible for the removal of the deposited material at its toe. However, the deposited material can protect the bluff and slow down its erosion, when there are higher water levels or waves (Guégan and Christiansen 2016, Pearson et al. 2016, Pearson 2015).

There are several flow dominated soil mass movements of permafrost slopes such as solifluction, active layer detachment, bimodular flows and multiple retrogressive thaw slumps, which can be added to the thermodenudational processes, because they are mainly triggered by the thawing process and not by external forces e.g. waves (Morgenstern and McRoberts 1974).

Solifluction is a slow viscous downslope movement of saturated thawed soil due to gravitational forces. It is restricted to surficial materials with underlying frozen soil and occurs in frost susceptible fine-grained soils with a high-water content. The impermeable frozen soil acts as a barrier to water percolation leading to the down-flow of melted water together with soil. Solifluction is augmented by rainfall and snowmelt and usually initiated by frost action. There are different forms of solifluction depending on the slope angle, vegetation, and soil material. At slopes with little or sparse vegetation, the mass movement occurs in stripe forms, whereas at slopes with much vegetation constraining the soil movement, flat bulbous lobes are formed. The mass movement can vary in size depending on the slope angle and soil material, even mass movements on low angle slopes of 5 to 6 degrees are possible (Andersland and Ladanyi 2004, Morgenstern and McRoberts 1974).

Skin flows, also referred to as active layer detachments in the Arctic context are characterized by a detachment of a small layer of vegetation and soil and its movement over a planar inclined surface, which is usually the permafrost table. They form long and very shallow flow zones and can coalesce into broad sheets of instability. They are common at moderate to low angle slopes, when the effective shear stress is very low (Harris and Lewkowicz 2000, Morgenstern and McRoberts 1974). The mass movement described with the term bimodular flow has a biangular profile and involves two distinctly diverse types of movement. They are characterized by a steep head scarp and a low angle tongue. The head scarp servers as a source area for the colluvial material in the tongue, which can be both long and narrow shaped or wide and short. The tongue or lobe can occur on very low angle slopes of 1 to 2 degrees up to slopes with an angle of approximately 14 degrees depending on the grain size characteristics. (Harris and Lewkowitz 2000, Morgenstern and McRoberts 1974).

Figure 2-2 shows a picture of an active layer detachment slide in northern Canada.

Figure 2-2: Picture of an active layer detachment slide (Harris and Lewkowicz 2000)

Retrogressive thaw slumps are the most extreme form of thermodenudation. They develop along coastlines and streams in fine ice-rich soil and are often triggered by wave forces or active layer detachments (Pearson 2015). Retrogressive thaw slumps have a circular shape and consist of three main elements: a more or less vertical headwall formed by the active layer and ice poor material, a headslump, which moves landwards, due to the ablation of ice rich material and which has an inclination of 20 to 50 degrees and a slump floor, consisting of the thawed sediment, which has a liquid like consistence and flows out of the lobe formed by the headwall. Retrogressive thaw slumps occur when the erosion rate of the massive ice rich permafrost soil, which gets exposed due to wave action or active layer detachment, exceeds the erosion rate of the coastline. Figure 2-3 shows a front views and a cross section of a retrogressive thaw slump. (Pearson 2015, Lantuit and Pollard 2007)

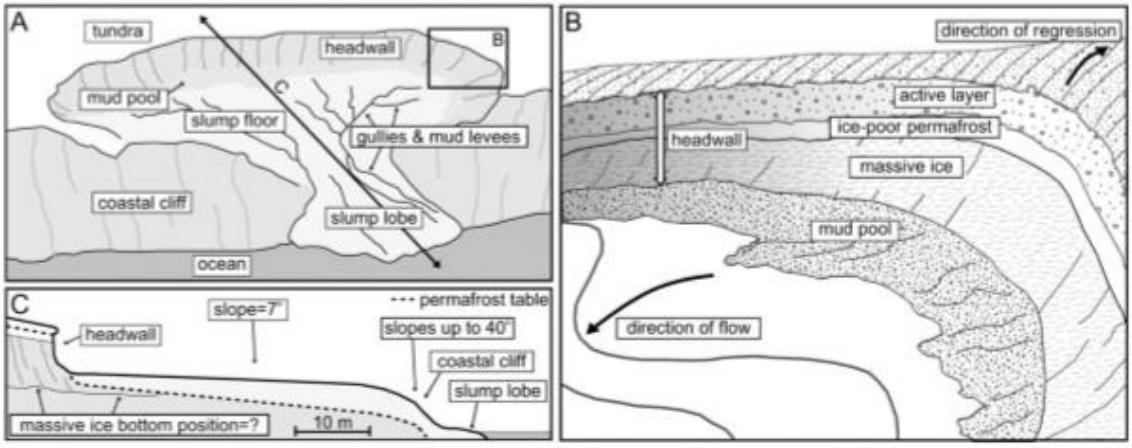

Figure 2-3: Different views of a retrogressive thaw slump (Lantuit and Pollard 2007)

2.2 Thermoabrasion

In contrary to thermodenudation, thermoabrasion occurs during storms and high-water levels, where deposited material at the toe of the slope is removed and the frozen bluff is directly exposed to the influence of the warm seawater. The bluff then thaws quickly due to convective heat transport, whereby the melted soil is transported offshore and out of the littoral zone by waves and currents. This thawing process can lead to the formation of horizontal niches, the depth of which increases during several storms and years. When the so overhanging material becomes too heavy and cannot be held by the shear or bending strength of the soil, it collapses as a block usually along an ice wedge. Typically, the block, consisting of frozen and unfrozen sediment, will gradually vanish because of warm water and wave forces. If the block remains in front of the bluff, it protects the bluff from further erosion. Figure 2-4 illustrates the process of thermoabrasion. (Guégan and Christiansen 2016, Pearson et al. 2016, Pearson 2015, Barnhard et al. 2013)

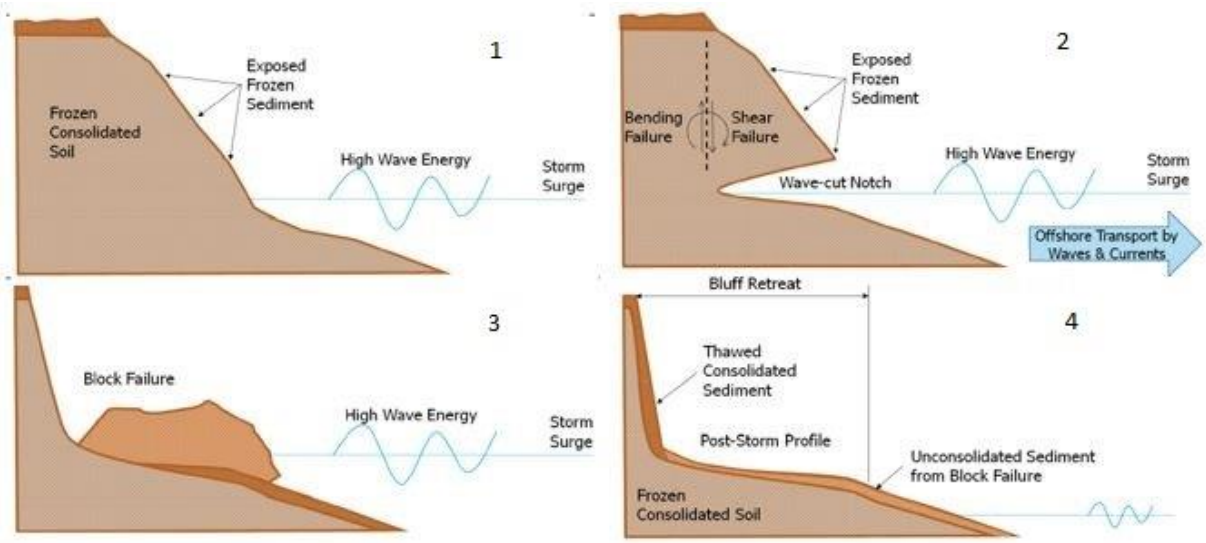

Figure 2-4: Illustration of the thermoabrasion (According to Pearson 2015)

Thermoabrasion is highly periodical and leads to very high and sudden land losses in coastal areas. Thermoabrasion is highly influenced by storm surges, because the corresponding rise in the seawater level exposes large amounts of the bluff to the seawater. Additionally, the warm seawater also erodes the coastal seabed, increasing the water depth in front of the bluff. This on the other hand makes the coastal area more accessible for longer and higher waves, accelerating the erosion process. Thus, also the temperature gradient between seawater and sediment is important for the erosion rate. (Guégan and Christiansen 2016, Pearson et al. 2016, Pearson 2015)

2.3 Parameters defining coastal erosion

Many parameters influence the coastal erosion processes in Arctic and temperate regions. The topography of the coastline is very important for the erosion processes. Higher cliffs need a longer time to retreat due to their bigger mass, which needs to erode, compared to lower coasts. Also, the slope angle has an influence, so steeper bluffs tend to erode more quickly than flatter bluffs. (Edil and Vallejo, 1979)

Very important for the hydrodynamic forces acting on the bluff is the bathymetry, the depth and shape of the seabed. This directly influences the wave transformation and breaking, tidal propagation, storm surge development, seawater temperature and sediment composition. The seabed in Arctic regions is usually very shallow with gentle slopes. (Pearson 2015, Edil and Vallejo 1979)

Also, the composition of the bluff influences the erosion rates. Bluffs made of fine, ice-rich material are expected to retreat faster, because the fine material is, after deposition in front of the bluff, transported out of the littoral system and cannot protect the bluff or account for bluff reconstitution. On the other hand, course material can form something like a small beach in front of the bluff, which protects it from further wave and current action. (Guégan 2015, Pearson 2015)

Furthermore, the erosion rates are influenced by sea-ice cover and snow. Both are expected to have a positive influence of the coastal erosion. The snow has insulating effects on the frozen bluff, preventing it from thawing (or slowing down the thawing process) and therefore from destabilization. Sea-ice, on the other hand, attenuates sea waves, so that erosion basically only takes place when the continuous sea ice cover has melted away. However, there are also effects of sea ice that can damage the bluff and increase the erosion, such as ice bulldozing or the development of frazil ice. (Guégan 2015, Pearson 2015)

Finally, the thermal conditions such as radiation energy, sunshine duration and the reflective surface properties of the soil affect the thawing of permafrost (Guégan 2015, Pearson 2015, Barnhart et al. 2013)

2.4 Consequences of coastal erosion in the Arctic

The consequences of coastal bluff erosion include socio-economic, climate and biogeochemical impacts and impacts on the marine ecosystem. Coastal erosion rates in Arctic regions can reach up to 25 m per year, which put at risk infrastructures such as roads, buildings and buried

pipelines (Fritz et al 2017). An increase of these erosion rates due to climate change is expected as a result of longer ice-free seasons. Therefore, the relocation of coastal communities and cultural heritage e.g. from early explorers or indigenous people might be necessary. (Fritz et al. 2017)

The climate and biogeochemical impacts consider the vertical transport of greenhouse gases into the atmosphere and the lateral transport of sediment and organic carbon of about 14,0 Tg organic matter per year into the water body due to the thawing of permafrost and thereby the release of previously bound carbon and nutrients (Fritz et al. 2017). This can lead to increased nutrient supply, ocean acidification, higher turbidity and decreased light transmission in the near shore ocean zone and therefore significantly influence the marine ecosystem. The liberation of nutrients like phosphorus and nitrogen can enhance the primary production leading to algal blooms in the summer, oxygen depletion in nearshore areas and an increase in phytoplankton production. On the other hand, the mineralization of organic carbon can strengthen the already ongoing ocean acidification. The ocean also absorbs carbon dioxide from the atmosphere during the ice-free seasons and the Arctic ocean contributes to that with 5 – 14 % of the global balance of CO_2 sinks and sources, absorbing 66 – 199 Tg C per year (Bates and Mathis 2009). The climate change also influences this process by reducing the period with a continuous sea ice cover where a CO_2 absorption is not possible. The lowering of the pH-value can create conditions in which some carbonate species like crabs or sea snails, which need a high enough saturation with calcium carbonate to build and maintain their shells, cannot survive due to the corrosion and dissolution of their shells. This can influence the food chain and decrease the number of fish, which depend on these species for food, effecting also the fishing industry in a negative way. Therefore, and to evaluate further land loss, it is important to develop methods to determine the amount of material which goes into the ocean due to the Arctic erosion processes. (Fritz et al. 2017, Mathis et al. 2015, Bates and Mathis 2009)

2.5 Frozen soil properties

One significant difference to temperate coastlines is the presence of frozen sediment in Arctic regions. Frozen soil is a four-phase continuum consisting of ice, unfrozen water, solid particles and air or gases. The unfrozen water forms a thin layer around the solid particles and is held there by strong intermolecular forces. The size of the particles, their surface area and the presence of solutes such as salt, directly influence the amount of unfrozen water in frozen soil, which is highest in very fine soils such as silt or clay. Higher unfrozen water contents lead to a

more plastic behaviour of the frozen soil, whereas with lower contents the behaviour becomes more brittle. (Andersland and Ladanyi 2004)

The freezing of the pore water leads to an increase in mechanical strength and reduces the hydraulic permeability, thereby stabilizing the soil body. Thus, the strength of frozen sand is about 8.5 times higher than of sand in confined unfrozen conditions, whereas the permeability approaches zero (Hoque and Pollard 2009). Clay shows a similar but moderate increase in strength. The strength of frozen soil is governed by its composition, for instance frozen coarse-grained soil shows a more brittle behaviour with less creep than fine grained soil. Also, temperature, and ice content influence the strength of frozen soil. Hereby a decrease of the temperature and an increase in ice content has a positive effect on the strength. For a grain volume fraction of about 0.4 the pore ice governs the behaviour of the frozen soil. For grain volume fractions between 0.4 and 0.6 the frictional resistance mobilized between particles becomes more important. For grain volume fractions above 0.6 an additional increase in strength can be noticed (Hoque and Pollard 2009). This is due to the dilatancy, which is caused by the interlocking of the densely-packed particles. The strength and the brittleness of the frozen soil increases with decreasing temperature. Also, confining pressure and deformation history have an influence on the soil strength. The tensile strength of frozen soil is 2 to 6 times smaller than the compressive strength (Hoque and Pollard 2009). Furthermore, phenomena such as pressure melting due to high hydrostatic pressures and dilatancy softening and hardening effects occur, influenced by the low compressibility of frozen soil. When exposed to a load frozen soil responds with an instant deformation and a time dependent deformation, which can be expressed through creep curves. The shape of these curves is influenced by the temperature, the magnitude of the applied stress, the soil type and the soil density. Ice rich soils show secondary creep dominated (time dependent) deformations. Under moderate stress conditions the primary creep can be neglected and the creep curve can be assumed as a linear line. In ice poor soil, there is little time dependent deformation, it is primary creep dominated. (Hoque and Pollard 2009, Andersland and Ladanyi 2004)

Since freezing of water is related to a volume increase of about 9 % it causes deformations of the ground surface (Andersland and Ladanyi 2004). This is increased by cryogenic suction, a process by which water migrates through soil pores to the freezing zone due to negative pressures resulting from the transformation of liquid water to ice, forming ice lenses within the soil body. The heave caused by ice lens formation is much bigger than from volume expansion, it can reach up to 20 % of the thickness of the frozen layer in frost susceptible soil and can

damage infrastructure through uplift and settlement (Andersland and Ladanyi 2004). However, ice lens formation only takes place in frost susceptible soil such as fine soils (clay, silt). This is because in coarser material like sand or gravel, water cannot migrate due to lower capillary action. Duration and intensity of freezing temperature strongly influence ice lens formation as well as the rate at which the temperature is lowered. (Pearson 2015, Zhang 2014, Hoque and Pollard 2009, Andersland and Ladanyi 2004)

2.5.1 Permafrost

Permafrost is perennial frozen sediment, the temperature of which remains below 0 °C for at least two consecutive years. In contrary to seasonal frozen sediment, which thaws during summer, only the upper layer of permafrost, called the active layer thaws each summer. When freezing the active layer freezes downward from the surface and upward from the underlying permafrost, which is referred to as two-sided freezing. When thawing permafrost loses much of its strength and impermeability. This can lead to slope failures due to reduced effective stresses because of excess pore pressures. Large magnitudes of excess pore water can occur due to trapped melted pore water, which leads to a further weakening of the soil. There might be also more melted water available than the soil can absorb leading to the development of thaw lakes and muddy soil with a very low bearing capacity. The presence of many thaw lakes characterizes the landscapes in permafrost areas, which is called thermocarst. Furthermore, the thawing of permafrost can cause ice wedges due to volume decrease. Ice-wedges are vertical ice-filled cracks which emerge due to thermal expansion. At low temperature, the soil contracts, and rips at several places and the thus developing cracks are filled with water from snowmelt during warmer seasons. Ice wedges can reach widths between one and three meters and are typically one cm to 10 m long. Block failures often occur at failure planes formed by ice wedges. (Pearson 2015, Zhang 2014, Andersland and Ladanyi 2004)

3 Erosion Protection Measures

3.1 General considerations in Arctic regions

Erosion protection measures depend on the features and triggers of the erosion processes at Arctic coastlines and the specific conditions and properties of the site. The aim of erosion protection measures protecting from the thermoabrasion is mainly the reduction of wave forces through e.g. breakwaters and influences due to high water level e.g. artificial beaches and to reinforce or armour the coastal cliff. Conversely, the erosion protection measures protecting from thermodenudation aim at preventing or slowing down the thawing of the frozen soil by means of cooling systems or insulation. Coastal protection measures should stabilize the coastal cliff and prevent sediment transport out of the littoral system. According to Leidersdorf, Gadd and McDougal (1990) problematic aspects regarding building measures in Arctic regions are:

- Lack of natural building material such as rocks and timber. Therefore, most of the building materials must be imported, which might increase the costs related to the construction of erosion protection measures.
- Building materials should be designed to withstand multiple freezing and thawing periods with low temperatures up to – 50 ° C, and loading from waves, ice, and snow.
- Building processes can disturb the fragile equilibrium condition of the permafrost and lead to additional settlements or heat development. This should be prevented using suitable equipment and technology.
- Lack of specialized construction equipment and high import costs.
- Construction of erosion protection measures must take place during the relatively brief open water summer season, usually within a time period between 60 and 90 days.
- Difficult transportation and depending on the site the lack of infrastructure to the building site.
- Paucity of available environmental data to define design loads or to predict extreme events.

All these aspects are site specific and should be considered when planning and building an erosion protection measure in Arctic environment. As a result, coastal slope protection structures should be simple and easy to construct with maximum use of locally available building material. (Leidersdorf, Gadd and McDougal 1990)

3.2 Erosion protection measures – Thermoabrasion

3.2.1 Seawall

A seawall is a massive free-standing structure, build parallel to the shore to prevent erosion and wave damage and to hold back the land behind. A seawall is designed to resist the full force of waves and storm surges and is therefore suitable for most wave conditions. A seawall is very effective against wave run off and impedes any sediment exchange between land and sea, which can decrease the local turbidity and improve the water quality. Another advantage is that they provide direct boat access to the shore. The erosion protection effect of seawalls is limited to the land directly behind. As a disadvantage, seawalls can increase the erosion down-drift and decrease and steepen a fronting beach. Additionally, the wave scour at the toe of the wall is increased and the access and use of the fronting beach is limited. Due to their massive structure and the need for pile driving seawalls are quite expensive to construct. (Depina, Guégan and Sinitsyn 2016, O'Neill 1986)

There are two distinct types of seawalls: cast-in-place concrete seawalls and rubble mound seawalls. Cast-in-place concrete seawalls can be constructed with a smooth, stepped or curved face. Smooth faced seawalls are restricted to low to moderate wave climates and constructed with a low to vertical angle and a very wide base, to prevent it from settling due to the large bottom surface area. The base can either extend a little at the toe of the structure, rest on a foundation or on vertical drilled piles. The wave run up of this type of seawall can be quite high due to the low frictional resistance of the smooth concrete surface. An increase in the steepness of the wall leads to an increase in wave run up and scour erosion, since considering vertical walls nearly the same amount of wave energy is directed downwards than upwards. The surface of the stepped face seawall provides much higher frictional resistance and therefore reduces the wave run up significantly. Apart from the surface the design is quite like the smooth faced seawall, it is suitable for moderate wave climates. Curved face seawalls are designed to withstand high wave energy and minimize wave run up and overtopping. Due to their concave form the wave is turned back on top of itself, which also prevents scour erosion. Curved face seawalls are the most massive type of seawalls and suitable for severe wave climates. (Depina, Guégan and Sinitsyn 2016, O'Neill 1986)

Rubble mound seawalls consist of heavy stones, the weight of which is chosen depending on the severeness of the wave climate. They provide the least wave run up, due to their rough surface which leads to a high dissipation of wave energy. Additionally, rubble mound seawalls are less vulnerable to scour erosion and undercutting because the structure is flexible and

individual stones can readjust to a changing bottom profile. Another advantage is that failure usually happens gradually and not catastrophic. Figure 3-1 shows a stepped face sea wall (a) a curved face seawall (b) and a rubble mound seawall (c).

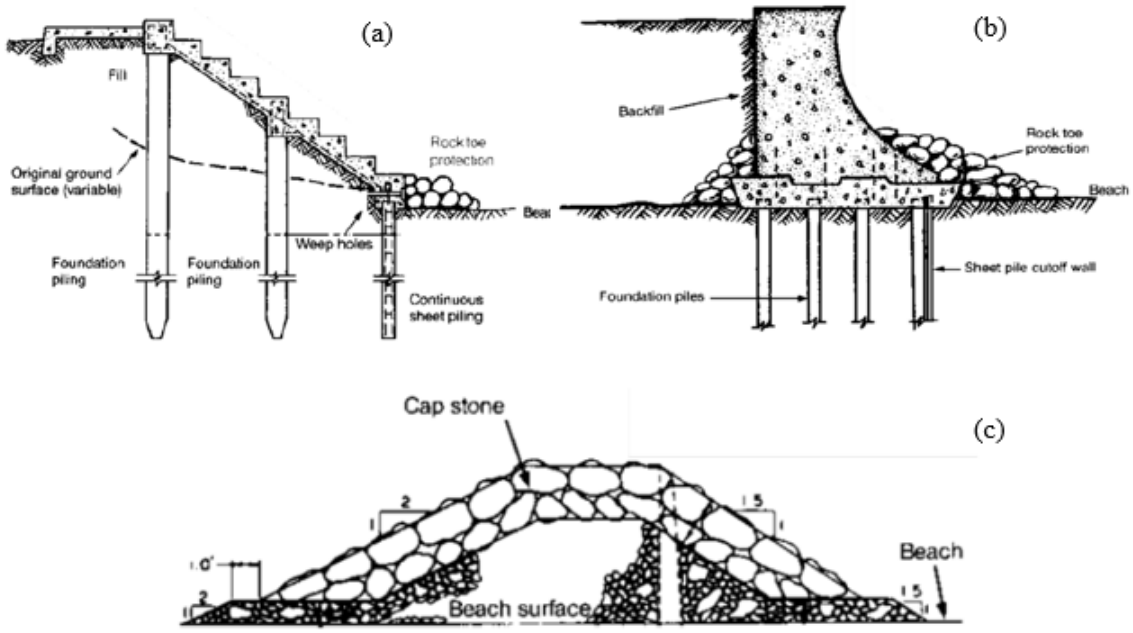

Figure 3-1: Different types of seawall (Depina, Guégan, Sinitsyn, 2016)

Seawalls should be equipped with a scour protection to minimize erosion and prevent undercutting. Additionally, the development of water pressure behind the wall, due to rainwater or thawing should be prevented with a drainage system, e.g. weep holes with filter material (O'Neill 1986). In Arctic context forces induced through frost heave and thaw settlement behind the wall should be considered in the design process. (Depina, Guégan and Sinitsyn 2016)

3.2.2 Bulkheads

Bulkheads are a structure parallel to the shoreline, the main purpose of which is the retention of the soil behind and not especially the protection against high waves or current induced forces or the stabilization of the bluff. Bulkheads are constructed of lighter materials than seawalls and therefore less massive. Advantages and disadvantages are quite similar to the seawall only they are less expensive and the repair is fairly easy. On the other hand, bulkheads may be susceptible to severe wave conditions. (O'Neill 1986)

Sheet pile bulkheads are composed of interlocked vertical sheets of steel, concrete or wood, which are drilled into the ground and held together with horizontal beams, called wales, which prevent the structure from bending outward. Sheet piles can be equipped with anchors to increase the strength and reduce the bonding depth, which should be in this case 1½ to 2½ times

the height of the structure above the predicted erosion scour depth in front of the wall. Without anchors the depth of penetration should be at least 2½ times (better 3) the height of the structure in front of the wall to prevent overturning by waves or undercutting by wave scour at the toe. (Depina, Guégan, Senythsin 2016, O'Neill 1986)

Cellular sheet pile walls are advantageous compared to normal sheet piles. They can be filled with local material and placed directly on the permafrost. They provide good erosion protection and can serve as a foundation as well. However cellular sheet piles are associated with high transport and installation costs. (Depina 2017)

Bulkheads made of wood are composed of vertical log piles, which are horizontally secured with steel ties and founded on a buried anchor plate and horizontal planks behind. Advantages of wooden protection walls are the long lifetime since wood is durable in Arctic climate, the environmental friendliness and modest maintenance costs, due to easy substitution of damaged timber piles. However, if it comes to a loosening of the structures anchoring, maintenance work can be more demanding and expensive. Negative aspects usually are the need for importation and transportation of the timber piles and the difficult installation and anchoring of the wall, since for sufficient stability the piles should be founded into the permafrost or at least with a depth of 2 m. Another disadvantage is the sediment removal in front of the wall through the reflection of waves, this can be reduced by installing the wall slanted and not vertical. Then more of the wave energy is absorbed but the maintenance costs are higher (Linzbach 2013). Figure 3-2 shows the principle of an anchored wooden bulkhead.

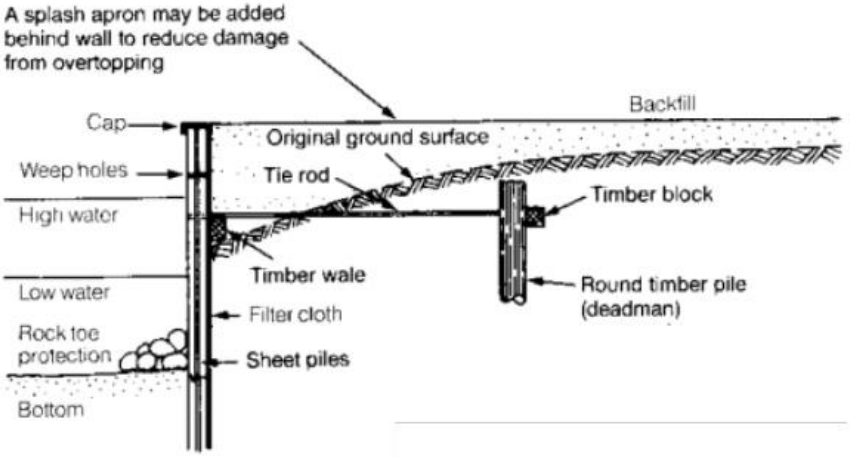

Figure 3-2: Principle of wooden bulkhead (Depina, Guégan and Sinitsyn, 2016)

Also, Gabions can be used to construct a Bulkhead, they consist of wire mesh structures which are filled with small rocks and need a toe protection, because they do not penetrate the soil.

Gabions are susceptible to ice damage and corrosion due to the sea environment. Geocells function on the same principle. They can be used to stabilize nearly vertical slopes and consist of a series of three dimensional cells made of polyethylene or polyester. When filled they resemble the shape of a honey comp. Geocells increase the resistance of the slope towards wave forces and prevent downward movement of soil. Advantages of gabions and geocells are the low transportation costs, the easy replacement and construction and the use of locally available soil. (Depina, Guégan and Sinitsyn 2016, Linzbach 2013)

3.2.3 Revetment

A revetment is a structure, consisting of a filter layer, an armour layer of rock or concrete and a toe protection, which is built at and parallel to the toe of a bluff or embankment or on a beach to protect the slope against the erosive forces of waves and currents. It is suitable for a moderate wave climate. The purpose of the filter layer is to prevent the washing out of fine soil materials and the resulting settling of the armour layer. The filter layer also allows drainage of water behind the revetment and can consist of graded gravel or a filter fabric such as a geosynthetic layer. On the amour layer the wave energy dissipates, it can be built as a rigid or flexible structure and should be placed on a slope flat enough to prevent down sliding of the structure. At the toe of the revetment a protection in form of heavier stones should be installed to prevent scour erosion. The revetment should be built high enough to minimize wave overtopping (O'Neill 1986). Figure 3-3 shows a cross section of a typical revetment.

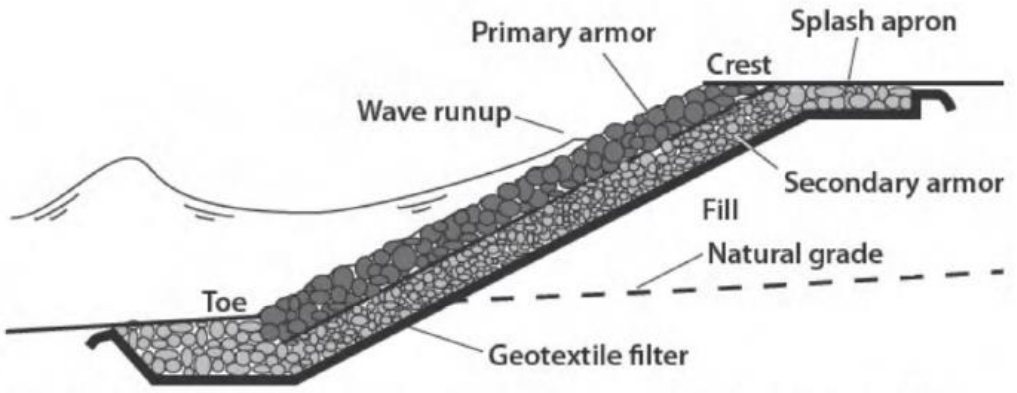

Figure 3-3: Cross section of a typical revetment (Depina, Guégan and Sinitsyn 2016)

Rigid revetments consist of cast in place concrete elements, which form a thin layer on the slope, by which there are supported. Special attention should be paid to the drainage of the soil behind the elements and the prevention of settlements, which can lead to cracks in the concrete. Flexible revetments can adjust to settlements of the ground to a certain degree without losing

their protective function. Two versions of the amour layer are possible. The type rock rip rap consists of large angular rocks, which are placed loosely on the filter layer. Due to the rough surface a high amount of the wave energy dissipates and the run off is low. Additionally, hydrostatic pressure can easily dissipate through the porous structure. This type is also suitable for the most extreme wave climates. A flexible amour layer can also consist of prefabricated concrete blocks which are interlocked with each other. Compared to the rock rip rap revetment they can endure less settlement and experience higher wave run up, due to their smoother surface, which on the other hand can reduce ice forces on the structure. Other flexible amour layer materials are sandbags and gabions, but there are vulnerable to ice action and their durability in Arctic environment is not ensured. Advantages of revetments are the reduction of scour erosion and the erosion of the fronting beach, compared to seawalls and bulkheads, relative easy construction and repair and lower construction costs, depending on the selected type of revetment. Additionally the failure usually is progressive. Disadvantages are the possible reduction of the size of the fronting beach and its increase in steepness, the limited use and access to the fronting beach and they may be hazardous for people walking on them. (Depina, Guégan and Sinitsyn 2016, O'Neill 1986)

For the use in Arctic areas settlement due to the thawing of permafrost slopes and ice induced forces should be considered in the design process as well as freeze thaw effects in the backfill. (Depina, Guégan and Sinitsyn 2016)

3.2.4 Groin

A groin is a rigid, perpendicular to the shoreline oriented structure, which interrupts the longshore water flow thereby limiting the sediment transport and protecting the beach against erosion. Groins can be designed as high structures to prevent all littoral drift or as lower ones, which are temporarily or always submerged and allow a certain longshore sediment transport. It is recommended to build groins as impermeable structures, since permeable ones show a low effectivity (O'Neill 1986). Groins can be arranged as a single structure or as a group, called a groin field. Groins usually lead to a sawtooth shaped beach with accumulation of sediments at the up-drift side and erosion at the down-drift side of the groin. The accumulated sand fillets protect the beach by absorbing storm wave impacts and preventing erosion of the beach itself as long as they are present. They are suitable for areas with a unidirectional longshore transport and a beach made of sand, because finer materials like clay or silt will not settle down at the up-drift side, remain in suspension and will be carried away by currents. In areas with fine materials, which are present at many Arctic coastlines artificial sand supply is necessary to

protect the beach with groins (Depina, Guégan and Sinitsyn 2016, O'Neill 1986). Figure 3-4 shows the effect of a groin field on the coastal development.

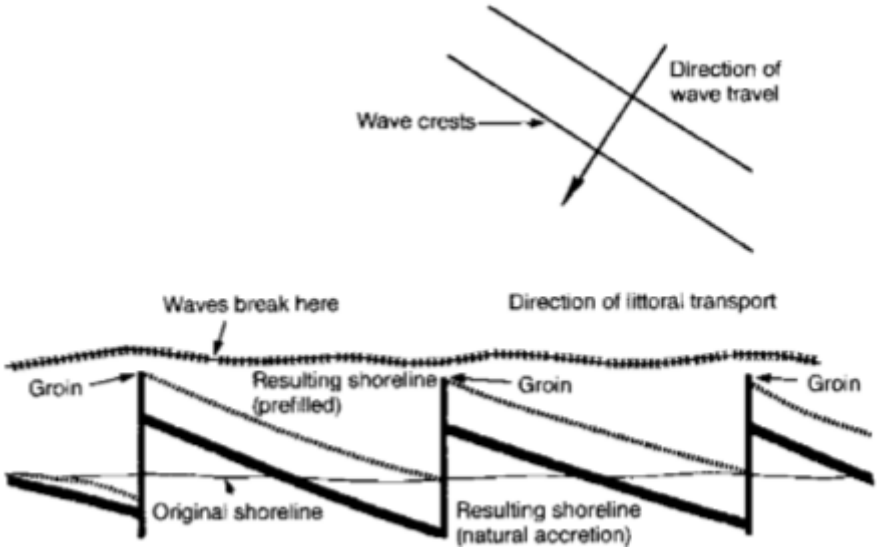

Figure 3-4: Schematic representation of a groin field (O'Neill 1986)

The effectivity of a groin is mainly influenced by its length, height and spacing. A groin should be long enough to create sand accumulation, but not that long that the down-drift erosion is too high, usually a length from the top of the berm to the breaker zone or less is sufficient. Too long groins, which exceed the breaker zone will direct bypassing sediment into deeper water, where it is lost for the system. On the other hand, too short groins will not trap enough sediment to make sand accumulations possible. The spacing is a very difficult criterium when designing a groin. Usually the space between groins should lead to a development of an up-drift fillet which reaches the up-lift groin, when filled to capacity. If the spacing is too wide, excess erosion takes place between the groins, whereas groins arranged too close to each other might lead to too little time or space for the sand to be transported back to the beach to form a fillet. In general, the spacing should be 2 to 3 times the length of the groin from the berm crest to the waterward end (O'Neill 1986). Groins can be made of timber, steel, concrete, rubble mound or gabions and sandbags. The durability of the used materials in Arctic conditions should be considered, e.g. gabions should only be used in ice free areas, with low wave action (Depina, Guégan and Sinitsyn 2016). Advantages of groins are the possible expansion of the beach; additional fish habitats may be provided and the access to the beach is not limited. Disadvantages are the limited travel along the beach and the submerged end of the groin, which might be hazardous to navigation. Furthermore, the down-drift erosion is increased and a depletion of down-drift beaches might take place. Additionally, groins can lead to rip currents, which might be hazardous to swimmers. (Depina, Guégan and Sinitsyn 2016)

3.2.5 Breakwater

A breakwater is a structure placed offshore from or connected to eroding coastlines, that protect the coastlines or harbour areas from wave action. Offshore breakwaters are commonly constructed parallel to the shoreline. Since the sediment transport rate is a function of the wave height squared, breakwaters reduce the sediment transport and thereby the erosion by creating calm water conditions. This can lead to the deposition of sediment. There are three types of breakwaters: the rubble mound breakwater, which is most commonly used, the caisson breakwater and the floating breakwater. The last one is only suitable for Arctic regions if there is a certain water depth > 6 m, long wave periods and less ice. Advantages of this type are the flexibility and the low impact on the natural ecosystem. They can also be applied in areas with poor foundation possibilities. The rubble mound breakwater is a rubble of layers of progressively larger and heavier stones or various angular concrete units, founded on a layer of crushed stone. The surface of the structure is capped with a layer of massive amour stones. It can be used in any depth and wave climate. The caisson breakwater usually has vertical sides is made of concrete or steel, filled with local material, to ensure stability and it is suitable for moderate wave climates. Breakwaters can also be made of gabions or sandbags, however then they are only suitable for sheltered shores without ice and with low wave forces. A breakwater only protects the coast on its lee side and may lead to increased erosion rates in down drift areas, because the sediment transport is interrupted. The height of the breakwater mainly influences the erosion protection and the down-drift erosion (O'Neill 1986). The erosion protection will be most effective when all waves are blocked, but this will increase the down-drift erosion. Breakwaters are vulnerable to ice action and may be subjected to foundation failures (Depina, Guégan and Sinitsyn 2016). Advantages of breakwaters are that they provide sheltered mooring areas and do not limit the access to the beach. Additionally, they influence a long section of the shoreline and lead to an increase of the beach. Disadvantages are the high construction costs and the difficult maintenance as well as the erosion on the down-drift side. (Depina, Guégan and Sinitsyn 2016)

3.2.6 Protective beach

Protective beaches can provide shore protection by significantly reducing the wave energy before the wave reaches upland areas. Sediment which gets eroded by waves is transported down-drift by the longshore current and accumulates at nearby beaches, filling up eroded sediments there. Sediment which is transported offshore might deposit and form bars, which also protect the beach from erosion. Waves tend to break at bars, whereby a large portion of the

wave energy dissipates before the wave reaches the shore. There are two strategies of coastal protection with protective beaches: beach restoration and beach nourishment. In the term beach restoration are all measures included which are necessary to maintain the natural state of a beach or create a beach artificially. Beach nourishment means a continuous or periodic supply of sediment, which replaces the eroded sediment and prevents beach erosion. Usually the used fill material should comply with the material at the beach but the use of coarser material can extend the time between supply measures. A dynamic beach consists of sand and gravel, which is significantly coarser than the natural beach material, but less coarse than the material for revetments. Due to wave and current action on the beach the shape of the added material adjusts to the conditions at the shoreline and is dynamically stable. A dynamic beach is considered to be cost efficient, because it lasts longer (Smith and Hendee 2011). However too coarse material can be washed offshore by storm waves and remain there, because lower energy waves are not able to transport it back to the shore (O'Neill 1986). The fill material can be obtained by dredging on- and off-shore. Advantages of protective beaches and beach nourishment are the big section of the shoreline, which can be positively affected by this measure, the extension of the beach shoreline and the unlimited access to the beach. Additionally, this measure is insusceptible against ice action. Disadvantages are the requirement of maintenance, the need for specialized equipment and the increase in turbidity. Furthermore, the effect is not long lasting and expensive especially at remote sites. For sites with extreme wave conditions this measure seems uneconomic due to the high erosion and frequent replacement of eroded fill material (Depina, Guégan and Sinitsyn 2016).

3.3 Erosion protection measures – Thermodenudation

3.3.1 Reduction of heat intake in summer

To reduce the heat intake in summer a thermal insulating material (e.g. polystyrene) can be placed on the slope. A disadvantage of this method is the reduction of heat loss during winter. An alternative is the installation of sun sheds, which allow free circulation of cold air along the slope during winter, while during summer the surface temperature of the permafrost is reduced. Also, reflective layers, with a high albedo can be used. Thereby the amount of heat energy which is transmitted into the ground by absorption and transmission is reduced. (Depina, Guégan and Sinitsyn 2016)

3.3.2 Activation of heat exchange during winter.

3.3.2.1 Air convection embankment

The activation of heat exchange during winter can be achieved by adding an additional layer of highly porous, but poorly graded materials such as crushed stones on the slope surface. This method also is referred to as air convection embankment. Due to the high permeability, natural air convection occurs in the insulating layer during the cold seasons where unstable air density gradients exist. The cold air at the ground surface will settle down whereas the warmer air within the soil body will rise due to its lower density and an air circulation is established. Due to stable air density gradients, there is no air circulation during warm summer periods. Applying insulation measures such as a layer of crushed stones on a permafrost slope leads to an increase in the heat resistance of the slope, a reduction of its mean annual temperature, an acceleration of refreezing and a slowed down thawing. Thereby the permafrost layer can be maintained or even lifted compared to the pre-construction level. Studies of a railway embankment in Fairways, Canada showed that by using an insulation of crushed stones the mean annual temperature could be reduced by 4 °C. (Jørgensen et al. 2007, Weihong et al., Cheng et al. 2004)

3.3.2.2 Passive cooling techniques

As cooling techniques, thermosyphons and ventilated shoulders are used to stabilize highway and railway embankments in Arctic areas and they might be also applicable for coastal slopes. A two phase thermosyphon is a passive heat transfer device which does not require external power sources to operate. It consists of an airtight vacuum tube filled with a low boiling point liquid such as ammonia or freon. Most of the tube is filled with the gaseous state of the liquid whereas its liquid form only exists at the bottom. The tube is equipped with a radiator on its top. The lower part of the thermosyphon is embedded into the permafrost layer and functions as an evaporation part, whereas the middle part up to the soil surface acts as a thermal insulation. The upper part, which lies above the soil surface, is responsible for condensation processes. Figure 3-5 shows the principle of a two-phase closed thermosyphon.

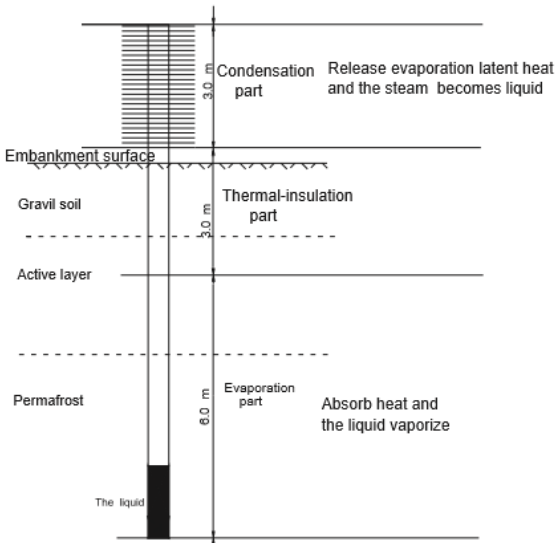

Figure 3-5: Principle of two-phase closed thermosyphon (Zhi et al. 2004)

During the winter when the air temperature is below the ground temperature the cold air cools and condensates the gaseous media which flows down to the below ground level, where it is subjected to warmer temperature. It then vaporizes and rises to the radiator, releasing its heat energy through the radiator to the surrounding air during phase change. Thereby, the soil temperature gets lowered, the permafrost layer can rise and thawing in the following warmer period is slowed down. (Jørgensen et al. 2007, Zhi et al., 2004)

Figure 3-6 shows a picture of thermosyphons arranged at a railway embankment in China.

Figure 3-6: Thermosyphons at railway embankment (Yandong et al. 2013)

A heat drain is a device that extracts heat from the soil body and raises the permafrost table. It consists of a drainage geocomposite with high permeability that goes from the top of the slope in a L shaped course within the soil body to the bottom of the slope. There an air intake system is placed at the lower outcome of the drain to enable upward movement of air due to temperature induced density changes, which is also referred to as the chimney effect. Initially the heat flows

to the drain by conduction and is then expelled of the slope by convection. The effects of a heat drain are concentrated around the geocomposite and at the upper part of the slope. At the lower part temperatures are only slightly colder than without the heat drain. Additionally, the heat drain requires more construction efforts, since drilling of twisted boreholes is more difficult. (Yandong et al. 2013, Jørgensen et al. 2007)

3.3.3 Coastal slope reshaping

Coastal slope reshaping is actually not a solution to coastal erosion but it can stabilize a slope and reduce the effects of thermodenudation, e.g. active layer detachments. Coastal slope reshaping usually evolves the decrease of the slope angle by cutting back the slope. To decrease the amount of land loss due to this measure it can be combined with a retaining structure such as bulkheads or gabions by constructing a terraced slope (Depina, Guégan and Sinitsyn 2016). Figure 3-7 shows a cutback slope (a) and a terraced slope (b).

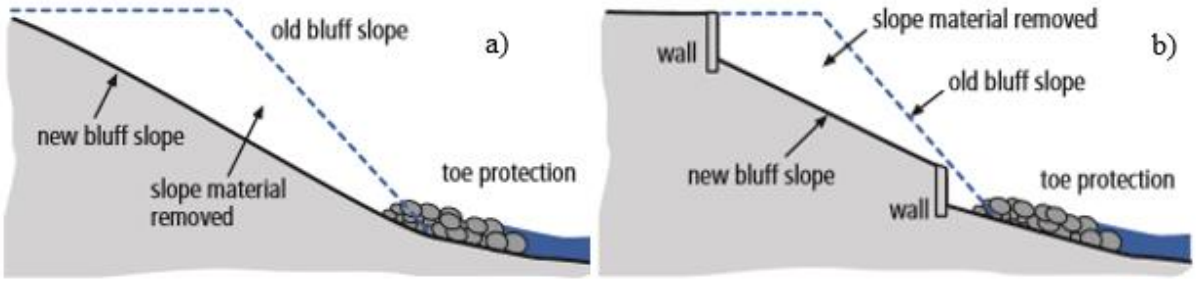

Figure 3-7: Figure of a cutback slope (a) and a terraced slope (b) (Depina, Guégan and Sinitsyn 2016)

If a loss of land is not possible the slope can also be filled with granular material until a certain slope angle is reached. This method is however better suitable for coasts where a beach is present, to avoid high water levels at the toe of the bluff. A toe protection is constructed to reduce the erosion and prevent the soil from sliding down. To further improve the stability the slope can be reinforced with geogrids or geotextile layers. Reinforced fills can also be used to replace a retaining structure. (Elias and Christopher 1997)

A coastal slope reshaping measure is usually followed by revegetation. This however can be difficult in Arctic areas, since local plants usually have a slow grow rate and might be susceptible towards saltwater and the growing season is short. The advantages of this measure are the relatively low costs, the use of the frontal beach is not affected and the access to it often improved. Additionally, the overgrown slope blends well into the surrounding. The main disadvantage is the reduction of usable land on top of the slope. (Depina, Guégan and Sinitsyn 2016)

4 Mathematical Modelling of Arctic Coastal Erosion Processes

4.1 Thermoabrasion

4.1.1 Block failure models

Thermoabrasion processes are usually simulated with Block failure models, which describe the development of niches, the block failure, and the block erosion after the failure of the bluff.

Hoque and Pollard (2009) developed an analytical bluff erosion model, which can be used to analyse the block failure mechanisms for varying cliff heights, long-term strength, and ice-wedge locations of permafrost coasts. The modelling approach consists of the following steps: an examination of the bluff stability without the influence of horizontal niche or ice-wedges and the determination of the factor of safety, using known strength properties of the soil is conducted. Then the development of a horizontal niche is modelled, taking different cliff heights into account. In the following step this is combined with the influence of ice wedges, investigating changes in failure conditions and mechanics. The cliff is assumed to be near vertical and the niche growth is formulated according to the approach of Kobayashi (1985). Two different failure planes are considered, a vertical failure plane and an inclined failure plane based on the Culmann's method of slope stability (Carson 1971), which is parallel to the initial failure plane. Figure 4-1 (a) and (b) show sliding without and with ice wedge, respectively. Figure 4-1 (c) and (d) show rotation without and with ice wedge, respectively. (Hoque and Pollard 2009)

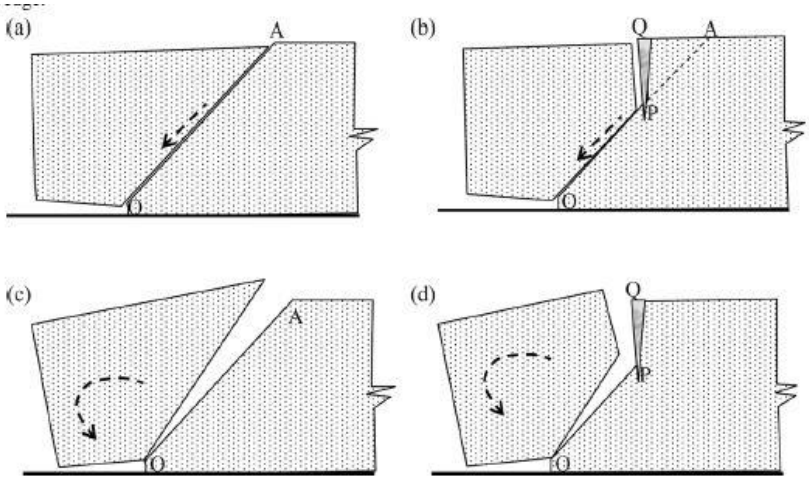

Figure 4-1: Potential failure modes at an inclined plane (Hoque and Pollard 2009)

Figure 4-2 shows the failure modes along a vertical failure plane, here ice wedges do not have an influence, therefore only sliding (a) and rotation (b) are considered.

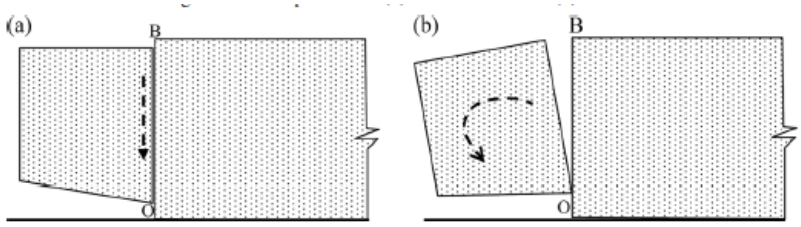

Figure 4-2: Potential failure modes at a vertical plane (Hoque and Pollard 2009)

Both shear and moment failure modes are considered. The earlier leads to block sliding and the latter causes block overturning. It could be shown that smaller cliffs tend to fail along a vertical failure plane whereas higher cliffs tend to collapse along an inclined failure plane (Hoque and Pollard 2009). In the case of a vertical failure plane, smaller cliffs collapse due to bending and higher cliffs due to shear. In the presence of an ice-wedge the failure plane also is inclined, following the ice-wedge. The critical niche depth, which causes block failure, was found to depend on the distance of the ice-wedge from the cliff face, the height of the cliff, the soil properties and the failure mode (bending or shearing). Requirements to predict the failure mode and critical niche depths are the cliff geometry, properties of the cliff soil and the location of the ice-wedges. (Hoque and Pollard 2009)

Ravens et. al. (2012) developed a coastal/shoreline erosion model for the Beaufort Sea. Figure 4-3 shows the steps of the model, which consists of several coupled models simulating specific processes.

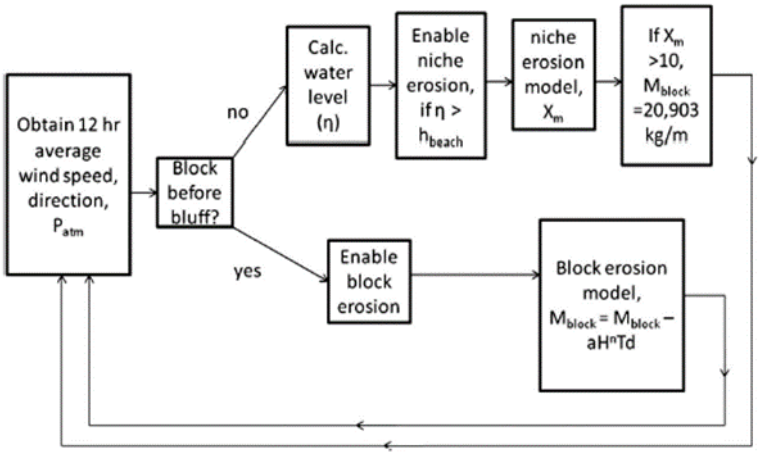

Figure 4-3: Principle of a Block Erosion Model (Ravens et al. 2012)

In the model developed by Ravens et al. (2012), the wind speed and direction are determined in 12-hour periods, because this is approximately a storm period in the Beaufort Sea. The model

usually starts assuming no block in front of the bluff. Then the changes in the water level due to the wind conditions (i.e. storm surge) are calculated. The niche growth starts when the water level becomes high enough to reach the bluff. The niche growth is modelled according to Kobayashi (1985), which assumed the niche as an unsteady boundary, which moves landwards, depending on the sediment and salt concentration, the water temperature and the horizontal fluid velocity and physical and thermal properties of the seawater and the frozen sediment. The height of the niche is formulated as a function of the water depth h at the base of the bluff, which is assumed as constant, and a constant β with a nominal value of 2.

$$h_N = \beta h \tag{4-1}$$

The depth of the niche x_m is formulated according to Kobayashi (1985) with the following equation:

$$x_m = 2\xi_m\sqrt{\epsilon t} \tag{4-2}$$

where ξ_m is a temperature dependent parameter, ϵ is the surf zone eddy diffusivity and t the time.

When the niche reaches a critical depth, which is in the case of the model developed by Ravens et al. (2012) a fixed value of 10 m, the bluff collapses. The weight of the bluff can be calculated taking the distance between ice wedges and other data into account. Then the simulation starts again, assuming now a block in front of the bluff, which enables the block erosion. Therefore, another specific model was applied, which takes the water temperature relative to the melting point and the wave height into account (Ravens et al. 2012, Kobayashi 1985)

Barnhart et al. (2013) developed a model, which captures the submarine and subaerial erosion, notch formation and force balance of the bluff and the failure tracks of the bluff. The model is quite similar to that of Ravens et al. (2012) though there are some improvements. Thus, shorter time steps of only one hour are used, to capture also storms with a shorter duration, a different block degradation model is implemented, which considers also field- and time-lapse imaginary observation and three different formulations of the impacts on submarine erosion are assessed. Additionally, the model is evaluated through a comparison of its results with long and short-term erosion rate observations.

Besides the Kobayashi formula, there are also other approaches to model the submarine erosion for example the Russel-Head formulation and the White Formulation (Barnhart et al 2013). Both are empirical formulations, which describe the melting of an iceberg. Through a factor, these formulas can be adapted to the melting process of the bluff consisting of ice and soil

material. All these formulations are implemented in the model developed by Barnhart et al. (2013) and their accuracy and applicability is evaluated. To predict the short and long term subaerial erosion, the White formulation delivers best results, whereas the erosion predicted with the Russel-Head formulation is too low. A reason for that might be the fact that the Russel-Head formulation does not consider the effects of waves on the submarine erosion. The Kobayashi formulation predicts a faster bluff erosion rate especially with small notch widths. (Barnhart et al. 2013)

Hoque and Pollard (2016) developed a model to assess the influences of ice wedges and horizontal niches on the coastal erosion, which is based on their earlier model (Hoque and Pollard 2009). In this model, block failure occurs along a failure plane which goes from the end of the niche to the bottom of the ice-wedge. The failure happens when the depth of the thermoerosional niche and the location and depth of an ice-wedge reach a critical situation. The failure mode is considered to be an overturning around the end point of the niche. In contrary to the earlier model, this model takes the influence of pore water pressure in the active layer into account. Through this pressure, an additional driving force is exerted on the collapsing block. The model is formulated in FORTRAN using cliff heights between 2 and 20 m. For every cliff height, the development of a thermoerosional niche is simulated by increasing the niche depth in incremental steps of 0.25 m from 0 up to 10 m. Then this is combined with the effects and location of ice-wedges and the critical situation when failure occurs is determined. Finally, an examination of the model sensitivity to different inputs is conducted. (Hoque and Pollard 2016)

4.1.2 Available software

To predict coastal erosion due to thermoabrasion, the abovementioned theoretical models must be implemented in suitable software. While there are many mechanical erosion models for coastlines in temperate climates, only a few consider thermal induced mechanism. Additionally, models to simulate wave conditions and sediment transport in Arctic regions might be necessary to obtain input variables for the niche development and block erosion models due to a paucity of available observed data, which is often present in Arctic areas.

4.1.2.1 COSMOS

COSMOS is a coastal profile model, which can model thermoabrasion. The model consists of three components according to Pearson (2015):

- Hydrodynamic component to simulate waves and currents for 2D profiles on uniform coastlines. It captures processes like shoaling, refraction, Doppler shifting and wave energy dissipation, including both alongshore and cross-shore currents.
- Sediment transport module to model both alongshore and cross-shore sediment transport, taking tidal influences into account. This module was developed to simulate bluff erosion on cohesive coastlines, considering erosion due wave orbital velocity and the breaking of waves.
- Thermal erosion model, which enables COSMOS to model thermo-mechanical erosion. The soil is specified according to two conditions: frozen or unfrozen. The fraction of coarse material can be determined, thereby is it possible to estimate the amount of soil, which remains in the littoral system.

COSMOS was extensively used to model coastal and sediment erosion in temperate and tropical climates. The thermo-erosion module was successfully developed and used to predict bluff erosion at coastlines of the Canadian Beaufort Sea (Pearson 2015, Nairn et al., 1998) and it also was used to simulate thermomechanical erosion at a coastline in Russia. Because COSMOS does not consider air temperature and radiation effects, it cannot be used to model particularly the thermodenudation processes. (Pearson 2016, Pearson 2015)

COSMOS is currently the only software, which can simulate the thermoabrasion process. However, there are other software that can be used to model the coastal erosion during ice-free periods. (Pearson 2015)

4.1.2.2 SCAPE

SCAPE (Soft Cliff and Platform Erosion) is a software developed to model short and long-term erosion processes and glacial tilt of soft rock coasts (clay). It is possible to simulate nearshore wave transformation, sediment transport along-, on- and off-shore, beach- and cliff evolution. Horizontal niching is specified in SCAPE, bud fewer mechanism and effects are considered in the modelling than in COSMOS. Because there are analogies between glacial tilt and thermomechanical erosion of permafrost coasts it might be possible to use SCAPE also for such a purpose, even though this is not yet verified. (Pearson 2015)

4.1.2.3 Other software packages

Other coastal erosion software packages for temperate climates are for example **XBeach** and **UNIBEST-CL+ (CITE)**. These models cannot simulate thermoabrasion but might be applicable during ice-free summer periods when the active layer is thick enough that thermal influences on the erosion process can be neglected. (Pearson 2015)

WAVEWATCH III is a software that can be used to model waves for example as an input for coastal evolution models, in Arctic regions. It is capable of simulating refraction and straining due to currents of mean water level changes, influences of wind and bottom on wave growth and dissipation and depth induced wave breaking and shattering. The model includes a dynamically updated ice coverage, which also considers wave-ice interactions in the marginal zone. WAVEWATCH has already been used to model changes in the significant wave height due to climate changes in Arctic regions. (Wavewatch III 2017, Pearson 2015)

Delft 3D is a 3D modelling tool, which can be used to investigate sediment transport, hydrodynamics including wave and currents, morphology and long-term morphodynamical change and water quality for fluvial, estuarine, and coastal environments. (De Goede and De Graff 2014)

The software also contains an ice module, which is able to simulate ice growth and transport processes as well as snow fall and snow related processes, for example insulation. The ice growth, modelled in Delft 3D, depends on the salinity and temperature of the water, the frequency and height of waves and currents and the atmospheric conditions, described through wind, solar radiation, and temperature. Effects of snow on the ice cover can be considered as well as the presence of oil, which can also change the properties of the water. The numerical implementation of the ice model in Delft 3D is a combination of a thermodynamic model, assuming a single ice layer with snow on its top and a dynamic model based on the elastic-viscous-plastic (EVP) sea-ice rheology and the second-generation Louvain-la-Neuve Ice-Ocean Model code. It is also possible to model ice-structure interactions. The ice model predicts ice growth/melt and thickness with sufficient accuracy for lakes and shallow seas. Although the model has already been used in studies of Arctic coastal regions, mainly for simulating hydrodynamic and sediment transport, the ice module of Delft 3D is not yet suitable for Arctic regions (Pearson 2015, De Goede and De Graff 2014)

4.2 Thermodenudation

4.2.1 Thermo-hydro-mechanical models

Thermodenudation is an erosion process, which is mainly caused by the presence and behaviour of permafrost. To simulate this erosion process, models must be established which describe the complex influences and interactions permafrost usually is exposed to. In general, thermo-hydro- and mechanical aspects must be considered. For example, temperature changes within the frozen soil body can lead to thermal dilatation as a mechanical aspect. This on the other hand directly influences the permeability as a hydraulic aspect. The presence of water within the soil body influences the convective heat transport and heat conduction. Furthermore, the thawing of the ice within the soil body leads to a loss of strength. Thermo-hydro-mechanical models (THM models) must be able to take all these interactions into account and describe them with governing and constitutive equations. These are then usually implemented in suitable software to solve the problem numerically and asses for example the slope stability of a permafrost slope. In Figure 4-4 some interactions of a THM model are presented. (Zhang 2014)

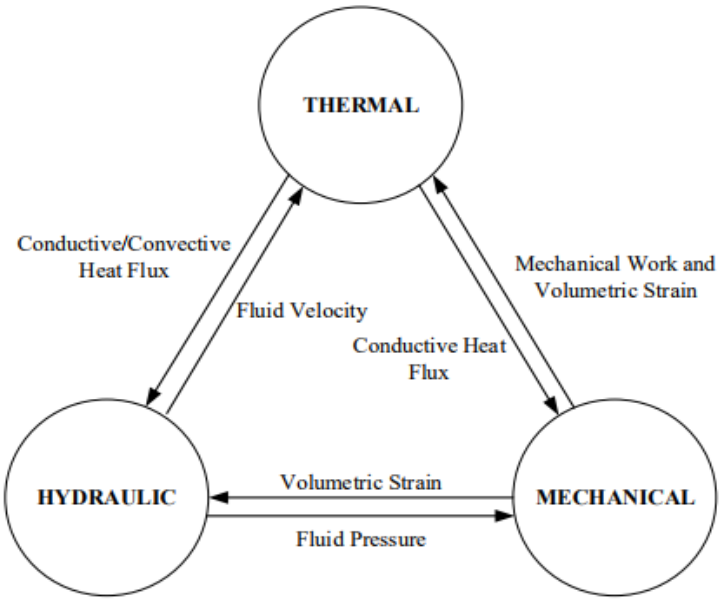

Figure 4-4: Principle of a THM model (Zhang 2014)

There are three basic approaches to couple the different processes in THM models. In the one-way coupling, the equations of different fields are solved independently in several steps using the output from the previous field as the input for the following. No information is passed back. This is the easiest and least computationally expensive way to couple different fields together, most suitable for applications where one process dominates the other processes. For very complex processes with mutual influences, the fully coupled method is more suitable. In the

fully coupled method, all variables are included in one set of equations, which are solved simultaneously providing most realistic results. However, the computational expense may be high due to large matrixes formed by the set of equations. A method in between one-way and fully coupling is the loose coupling (sequential coupling). Thereby the equations of different fields are solved independently but some information are passed back sequentially. The result is not as accurate as with the fully coupled method, but it is faster and less computational expensive, providing solutions with sufficient accuracy (Zhang 2014). Some fully coupled and recently developed models for frozen soil are shortly presented in the following.

Nishimura et al. (2009) developed a coupled THM finite element analysis for frozen soil. The model considers freezing and thawing in water saturated soils and can be applied to analyse frost heave, foundation stability or mass movements in cold regions. The governing equations include the thermodynamic equilibrium of frozen soil, which is expressed through the Clausius-Clapeyron equation (equilibrium between liquid water and ice phase). A freezing characteristic function, described through the van Genuchten model, is established to model the relation between unfrozen water and the saturation to the soil's thermo-dynamic properties. To model fluid transfer, Darcy's law is used and Fourier's equation is applied to calculate the conductive heat flux. The mechanical equilibrium is finally formulated considering both total stresses and body forces. Besides the governing equations, this model also contains some constitutive equations. Due to the analogy between frozen-saturated and unfrozen-unsaturated soils, the elasto-plastic Barcelona Basic model (BBM) for unsaturated soils is used to describe the essential features of frozen and unfrozen soil behaviour. If the soil is unfrozen; the model reacts similar to the effective-stress based critical state modified Cam Clay model. Under frozen condition, the model increases the yield stress and strength of the soil, taking hardening effects into account. The accuracy of the model to simulate the field pattern of pipeline heave, water migration and ice accumulation was validated through field tests and experiments, see Nishimura et al. (2009).

Liu and Yu (2011) developed a coupled THM model for porous materials under frost action. To model the thermal field, the Fourier's equation with convection and conduction terms is used to describe the energy transfer in porous materials. The hydraulic field is formulated using the mixed-type Richard's equations for fluid flow in unsaturated media. To take the ice formation into account, a specific term was added to the Richard's equation. The van Genuchten's or Frelund's equation was used to describe the soil-water characteristic curve (SWCC), which describes the relationship between soil, unfrozen water, and matrix potential

and allows the prediction of the hydraulic conductivity. To model phase change and the co-existence of water and ice, the Clapeyron equation was formulated. Thereby also the freezing point of pore fluid and the ice content could be obtained, (assuming thermodynamic equilibrium conditions). To take the stress and strain field into account, the Navier's equation was applied. Thereby the equation of motion, strain displacement correlation and constitutive relationship was incorporated. The presented model was validated against measured data at an example of a pavement under different climate conditions. It provides reasonable results according to Liu and Yu (2011).

Zhang (2014) developed a THM model for freezing and thawing of soil using the governing equations: Equilibrium equation, including stress and body forces, the conservation of mass, describing the water flux with Darcy's law and a conservation of energy equation. Special effort was paid to the description of the porosity and an implementation of a thermal model with phase change. A porosity rate function is implemented to describe the thermally induced increase of the porosity during ice lens formation, which was also found to contribute to the volumetric strain, which thus is expressed by the change of porosity. The thermal model takes thermal properties for the soil mixture, the volumetric heat capacity, and the effective heat into account. Also, equations to express latent heat are included and especially addressed, since the calculations distinguish between pore ice and ice in ice-lenses. The model was successfully used to simulate a footing on frost-susceptible soil and it provided good results for frost heave and thaw settlement, see Zhang (2014).

Amiri, Kadivar and Grimstad (2015) developed a constitutive THM model for saturated frozen soils, which are assumed to be a combination of solid grains, unfrozen water, and ice. The part of the stress carried by the solid grains is considered to be responsible for any deformation due to mechanical loading. Besides the solid phase stress, a cryogenic suction is implemented in the model. As in the model developed by Nishimura et al. (2009), the yield surface equations are formulated according to the BBM. Two equations for the strain are developed, the elastic strain due to the suction variation and the plastic strain associated with the flow rule. To validate the results of the presented model, triaxial compression tests of frozen soil were conducted under different temperatures and it was shown that the model can provide sufficient results. The model is also able to capture behaviour related to pressure melting, modelling the interactions between soil strength increase due to mechanical effects and soil weakening due to thermodynamic effects at higher pressures. According to Amiri, Kadivar and Grimstad (2015), it is expected that this model can also simulate ice segregation although this could only be investigated in a

qualitative approach without comparison with laboratory data. (Amiri, Kadivar and Grimstad 2015)

Amiri et al. (2016) recently developed a constitutive model for frozen and unfrozen soil, which expresses the behaviour of the frozen soil as a function of the temperature. It is a critical-state elasto-plastic time-independent mechanical soil model, which follows a similar approach as the soil model developed earlier by Amiri, Kadivar and Grimstad (2015). Thus, it is formulated in the framework of two-stress-state variables, the solid phase stress and the cryogenic suction. The solid stress is formulated in a way that the effect of frozen water on the soil behaviour is described using the Bishop single effective stress. The Clausius-Clapeyron equation is used to obtain the cryogenic suction that is the difference between the ice- and the pore water pressure. Through the cryogenic suction, the effects of ice content and temperature variations can be considered. The calculation of the elastic part of the strain due to solid phase stress is based on the Hooke's law, using a Young's modulus, that takes the temperature dependent behaviour of ice into account. Equations for the calculation of the elastic part of the strain due to suction are also implemented in the model. For the unfrozen state, the simple Cam-Clay model describes the soil behaviour, whereas for the frozen conditions two suction dependent yield functions are used. One of them is based on the loading collapse yield function of the BBM, taking the influence of the unfrozen water saturation into account. The other considers deformations due to ice lens formation and soil expansion and is formulated according to the Grain Segregation yield criterion. The model requires several parameters, some of them are difficult to determine from laboratory tests. The model was used to simulate frost heave and thaw settlement at the example of a buried pipeline in unfrozen soil and a footing on frozen ground, see Aukenthaler et al. (2016) and Amiri et al. (2016).

Na and Sun (2017) developed a stabilized thermo-hydro-mechanical finite element model to simulate the freezing and thawing of porous media, in the finite deformation range. Whereas earlier models often neglect the flow of unfrozen water, energy dissipation due to phase transition and geometry nonlinearity, this model takes all these mechanisms into account. The conservation laws include the kinematics of the frozen media, which is assumed as a fully saturated mixture of solid soil, ice and unfrozen water, using the Clausius-Clapeyron equation to describe the behaviour of crystal ice through the thereby obtained ice pressure. By using the kinematics, movements of water or ice are described as their relative movements with respect to the solid particles. The balance of linear momentum is based on the Bishop's effective stress theory and the interactions between ice and unfrozen water are described with a freezing

retention curve. The balance of mass is formulated using three variables, the temperature, solid displacement, and liquid phase pressure. The last conservation law is the balance of energy, which was formulated assuming that all constituents behave according to Fourier's law. In contrary to many earlier models the derivation of the balance of energy presented by Na and Sun (2017) also considers heat convection, mechanical dissipation, structural heating and the geometrical nonlinearity. Thereby it is for instance possible to take the generation of heat due to friction or effects of fluid flow with a different temperature into account. Besides the conservation laws there also are several constitutive laws implemented in this model. The behaviour of the soil is modelled based on a finite strain Cam-Clay model and the basic Barcelona model with an associative hardening rule and coupled to a freezing retention model. The flow of unfrozen water is formulated according to Darcy's law with a saturation dependent relative permeability and a temperature dependent viscosity. Na and Sun (2017) conducted four numerical examples to validate the applicability and robustness of the presented model.

4.2.2 Available software

The above presented thermo-hydro-mechanical models describe the processes in frozen soil mathematically, but due to their complexity it is very difficult to solve frozen soil related problems analytically without making simplifying assumptions. Therefore, these thermo-hydro-mechanical models are implemented in suitable software, which solve the complex equations numerically by approximation. Some available programs are presented in the following.

4.2.2.1 GeoStudio

GeoStudio is a geotechnical software that can be used to analyse a wide range of geotechnical problems including ground freezing and engineering problems in permafrost areas. GeoStudio offers several integrated products, which are designed to solve specific problems. For problems related to ground freezing, the following modules can be used:

- TEMP/W to simulate and analyse thermal changes in the soil body
- SIGMA/W to assess changes of the strength and simulate deformations
- SLOPE/W to evaluate the stability of the soil body
- SEEP/W to simulate groundwater flow
- VADOSE/W to take interactions at the ground surface such as infiltration or snow melt into account

GeoStudio is however not capable of solving the problem in a fully coupled manner. In fact, each module solves one partial problem separately and is then coupled with another module

using the results of the previous model as a boundary condition for the following model, see GeoStudio (2017).

Tsegaye & Nordal (2014) developed a frozen soil model, which can be used in GeoStudio and is based on a finite element geotechnical model. The strength of the frozen soil is determined and applied to a finite equilibrium or finite element stability model. Thus, the soil, which potentially will fail can be determined. This model only takes the loss of strength linked to the thawing of the soil into account and not mechanical erosion processes triggered by the thawing for example the flushing out of fine sediment due to the drainage of melted water. Also, it is not possible to simulate the actual failure or deformation of the soil. (Pearson 2016)

4.2.2.2 CODE_BRIGHT

CODE_BRIGHT (COupled DEformation, BRIne, Gas, and Heat Transport problems) is an open source program, capable of dealing with coupled thermo-hydro-mechanical problems in geotechnical media. It has been developed at the Department of Geotechnical Engineering and Geo-Sciences of the Polytechnic University of Catalonia and works in combination with GiD. GiD is a pre-and postprocessor for geometrical modelling, mesh generation, definition and transfer of data and the visualization of the results. CODE_BRIGHT uses the finite element method to solve a set of governing equations, which are associated with a variable.

- Equilibrium of Stresses – Displacements
- Balance of water mass – liquid pressure
- Balance of air mass – gas pressure
- Balance of internal energy – temperature

The code solves the equations, obtaining the corresponding variable, which usually is the unknown of the problem. CODE_BRIGHT can solve coupled and uncoupled problems in one (uni-axial confined strain and axi-symmetric), two (plane strain and axi-symmetric) or three dimensions. The following boundary conditions are available:

- Mechanical problem: forces and displacement rates in any spatial direction and at any node
- Hydraulic problem: mass flow rate of water and air prescribed and liquid/gas pressure prescribed at any node
- Thermal problem: heat flow rate prescribed and temperature prescribed at any node

CODE_BRIGHT can model all interactions between thermal, hydraulic, and mechanical processes.

CODE_BRIGHT has already been used to model geotechnical problems related to permafrost or freezing and thawing processes of saturated and unsaturated soil. So, it was used in a study to assess the impact of global climate change on infrastructure in cold regions, to model freezing ground water migration problems like frost heave around chilled pipelines. Also, three-dimensional ground-structure interactions could be considered. (Code Bright 2017, Clarke et al. 2008)

4.2.2.3 Abaqus

Abaqus is a powerful, commercial, finite element method based program, which can simulate a wide range of engineering problems. As a multipurpose software, it can solve more than only mechanical (stress/displacement) thermal (heat transfer) and hydraulic problems (fluid dynamics). For example, acoustic or electrical aspects can also be considered. However, to simulate the behaviour of frozen soil or permafrost slope failures a coupled thermo-hydro-mechanical model is sufficient. Abaqus can simulate the behaviour of a wide range of engineering materials like steel, polymers, concrete and geotechnical materials such as rock or soil. The software consists of three programs, which are used for the three different stages of the simulation. In the pre-processing stage, a model must be designed using Abaqus/cae. For the simulation Abaqus/standard or Abaqus/explicit can be chosen to solve the numerical problem. The results of the calculation can be evaluated and visualized in the postprocessing stage using again Abaqus/cae.

Abaqus was used to model a frost bulb and its degradation under a road embankment in northern Canada. Furthermore, it was used to simulate the freezing of an unpaved road above a culvert in frost susceptible soil. Thereby initial distribution of the temperature and of geo-static vertical stress could be obtained as well as temperature distribution, vertical displacements and excess pore pressure distribution and pore pressure after several time-steps up to one year. Also, the effect of insulation of the culvert could be investigated. Furthermore, Abaqus was used to model the frost heave and thaw settlement around a chilled pipeline and behind a retaining wall. (Gholamzadehabolfazl 2015, Zhang 2014)

4.2.2.4 COMSOL Multiphysics

COMSOL Multiphysics is a commercial multipurpose software similar to Abaqus, which has a modular structure. To simulate the behaviour of permafrost the modules geomechanics, heat transfer and subsurface flow can be used. The geomechanics model, an add-on to the structural mechanical module, can be used to model various geotechnical problems like slope stability,

embankments, foundations, and tunnels. Additionally, it offers a wide range of material models e.g. Clam Clay, Mohr Coulomb and using the interface function in COMSOL Multiphysics it is also possible to adapt the material models to special needs and extend them to versatile applicable material classes. The module heat transfer can simulate the effects of heating and cooling on devices and processes as well as the mechanisms of heat transfer, convection, conduction, and radiation. There also are interfaces available to model the heat transfer in porous media, which is especially important for geotechnical applications. Furthermore, phase changes and latent heat can be modelled as well as volume changes due to these processes. The module subsurface flow can model fluid flow in fully or variable saturated porous media. Using this function ground water flow, spread of contaminants, material- and heat transport can be considered. Also, free channel flow can be simulated. (COMSOL 2017)

Additionally, COMSOL Multiphysics offers a material library, which provides the properties of more than 2.500 materials, including soil types and rocks. There are many interfaces available to provide easy connections to other programs like CAD, Excel or MATLAB. (COMSOL 2017)

COMSOL Multiphysics is capable of simulating permafrost which was verified by Dagher et al. (2014) using it to model the conductive heat transfer with phase change in geological formations covered in permafrost and surrounding a shallow thaw lake. Furthermore, COMSOL Multiphysics was used in the validation of a THM model and produced reasonable results (Dagher et al. 2014, Liu and Yu 2011)

4.2.2.5 COMPASS

COMPASS is a numerical finite element model which was developed by the University of Cardiff to simulate freeze thaw behaviour of soil and the development of ice lenses but also hot temperature phenomena of soil for example gas pressure. Compass is in fact a thermo-hydro-chemo-mechanical model with the following key features according to the official website of the Cardiff University:

- Heat transfer: conduction, convection, and latent heat
- Liquid transfer: due to pressure or gravitational gradients, chemical thermal osmosis
- Mechanical deformation/behaviour: elastic and elasto - plastic
- Vapor transfer: due to vapor pressure gradients, thermal effects, and chemical osmosis.
- Gas (air) transfer: bulk flow of dry air from pressure gradients and dissolved gas.
- Multicomponent transport of chemical species: by advection, dispersion, and diffusion in both liquid and gas phases.

- Geochemical reactions: due to heterogeneous and homogenous reactions between/in solid, liquid and gas phases and under both equilibrium and kinetic conditions.

Additionally, COMPASS offers a widespread library of finite elements to design 1D, 2D and 3D geometrics, a wide range of boundary conditions and a pre-and postprocessing package, which allows mesh generation, definition of initial and boundary conditions and material parameters and the results are presented in a user-friendly way. (COMPASS 2017)

The basic input variables for the governing equations are pore-water pressure, the temperature, the pore air pressure, the displacement, and a chemical component concentration. The governing equations for the flow are mainly formed by conservation of mass/energy whereas the mechanical formulation considers the stress equilibrium. (COMPASS 2017)

COMPASS can be used for modelling both one and two-sided freezing as well as ice segregation and cryogenic processes, the development of heaving strain and latent heat in saturated and unsaturated soils. Laboratory experiments confirmed the results. (Thomas et al. 2009, Glendinning 2007)

4.2.2.6 PLAXIS

PLAXIS is a commercial geotechnical finite element software with versatile application possibilities. It offers a user-friendly interface, enabling a fast and easy model creation and powerful post processing abilities. The software can be used for two-dimensional deformation and stability analysis in geotechnical engineering and rock mechanics, but there also is a three-dimensional version available. Plaxis provides many predefined structural elements, loading types, and boundary conditions which makes the model and geometry implementation as well as the definition of soil layers through the borehole function time efficient. Calculation results like deformation and stresses can be presented in many forms, e.g. contour vector or isosurface plots. There also is a curve manager for creating graphs available. (Plaxis (1) 2017)

An add-on module to Plaxis 2D is Plaxis 2D Thermal. With this module, it is possible to simulate the influence of thermal effects and heat flow on complex geotechnical problems e.g. temperature distributions and expansion, soil freezing etc., which makes the software applicable for simulations in Arctic regions. The Thermal 2D module contains soil models for frozen and unfrozen soil, such as the Barcelona Basic Model or the user defined Frozen and Unfrozen Soil Model, temperature dependent water properties and the ability to simulate phase change and the thermal expansion of soil and structures. The thermal conditions can be defined with time dependent or constant boundary conditions including thermosiphon. As a result, ice saturation

plots, temperature and heat flux distributions and curves in soil and structures can be obtained. (Plaxis (1) 2017)

The Add-on module, Plaxis 2D PlaxFlow can be used to take ground water flow into account. The module contains various soil water characteristic curves with predefined data sets and boundary conditions for flow. Fully coupled flow deformation analysis is possible, but there also is an only flow option. The module can calculate suction, permeability, and groundwater head as well as the degree of saturation and Darcy's velocities. The results come in addition to displacements and stresses. (Plaxis (1) 2017)

Plaxis 2D, Plaxis 2D Thermal and Plaxis 2D PlaxFlow offer the possibility of coupled thermo-hydro-mechanical modelling.

Plaxis was already successfully used to model problems related to frozen soil and cold climate engineering. So, the software was used to simulate frost heave around a chilled pipeline, obtaining temperature distributions, ice saturation and deformations. It was also used to model thaw settlement due to a footing on frozen soil during a warmer period. (Aukenthaler et al. 2016)

5 A New Model for Thermodenudation

In this chapter the development of a numerical model to simulate the thermodenudation process is described. For that the software Plaxis is used. The newly developed numerical Thermodenudation Model in Plaxis consists of a conventional Mohr Coulomb soil model to model the response of the unfrozen soil and a combination of the Mohr Coulomb model with the cryogenic suction in the frozen domain. This modelling approach is developed to simulate instabilities of coastal slopes and coastal retreat rates. The modelling approach is developed under the assumption that the slope failure leading to coastal retreat occurs in the unfrozen soil domain. The reason for adopting this modelling approach and the consequent assumption originates in the limitations of the Frozen and Unfrozen Soil Model in Plaxis, which does not support the 'c phi' algorithm, commonly employed to evaluate slope stability.

5.1 Model description

To describe the behaviour of frozen soil Plaxis offers a user-defined soil model, the Frozen and Unfrozen Soil Model, which was developed by Amiri et al (2016). The model distinguishes between soil in frozen and unfrozen state, applying different soil models to describe its behaviour. In the frozen state, the mechanical strength of the soil is described in terms of the cryogenic suction and the solid phase stress, which is formulated as the combined stress in solid particles and ice. Thereby it is possible to take effects of ice and unfrozen water content as well as temperature variations into account. If the soil is present in an unfrozen condition the Modified Cam Clay model is applied.

To analyse slope stability and obtain global safety factors and failure planes, which are needed to assess coastal retreat rates, a safety analysis in Plaxis must be conducted. The safety analysis is a calculation type in which the cohesion c, the friction angle φ and the tensile strength are needed as input parameters because they are gradually reduced during the analysis to obtain a global safety factor. These parameters are not explicitly defined in the Frozen and Unfrozen Soil Model, which therefore cannot be used in a straightforward way for slope stability analysis and the calculation of safety factors. Therefore, a new modelling approach was implemented in this study with the conventional Mohr Coulomb soil model, simulating the response of the

unfrozen soil and a combination of the Mohr Coulomb soil model and cryogenic suction in the frozen domain as defined in the following equation:

$$\tau = c' + (\sigma - u)tan\varphi'; \begin{cases} u \geq 0 & T \geq 0\,°C & pore\ pressure \\ u < 0 & T \geq 0\,°C & suction \\ u < 0 & T < 0\,°C & cryogenic\ suction \end{cases} \quad (5\text{-}1)$$

Where τ is the shear strength, c' is the effective cohesion, σ is the total normal stress, φ' is the effective friction angle, u represents the pore pressure, suction and cryogenic suction, and T is the temperature in °C. Due to the focus on slope stability analysis, which is determined by the soil strength, the effects of temperature on soil stiffness were not examined.

The THM coupling necessary to evaluate slope stability analysis was implemented in two steps: (1) flow analysis and (2) stability analysis as illustrated in Figure 5-1. More detailed presentation of the model follows in Section 5.2.

(1) In the flow analysis, a coupled thermal and hydro analysis is performed according to the algorithms implemented in Plaxis (Plaxis 2015, Plaxis (3) 2017). Inputs to the flow analysis include slope geometry, thermal and hydraulic soil properties, thermal and hydraulic boundary conditions. The outputs of the flow analysis include the fields over the model domain of pore pressure, saturation, temperature, groundwater flow, suction in the unfrozen subdomain and cryogenic suction in the frozen subdomain. The cryogenic suction is calculated according to the Clausius-Clapeyron equation (Thomas et al. 2009). The outputs of the flow analysis are mapped to the stability analysis via Python scripting.

(2) In the stability analysis, the mechanical part of the THM coupling is performed. The stability model shares the geometry with the flow model. The inputs to the stability model include soil parameters required to specify the Mohr Coulomb soil model and the mechanical boundary conditions, specifying deformations and loads applied at model boundaries. The thermal and hydraulic boundary conditions and field variables are mapped from the flow model via Python scripting, as illustrated in Figure (5-1). In addition to the outputs of the flow model, the outputs of the stability model include displacements and stress fields over the model domain. Additionally, slope stability analysis is performed to determine the global factor of safety and the failure plane with the 'c-phi' algorithm. The development of excess pore pressures, due to the thawing of the soil in the stability model is not considered.

5.2 Model setup

The newly developed Thermodenudation Model consists of two models, which are coupled together with Python program codes. The programming was done with the open source Python language development environment Spyder. Figure 5-1 shows the main elements of the thermodenudation model.

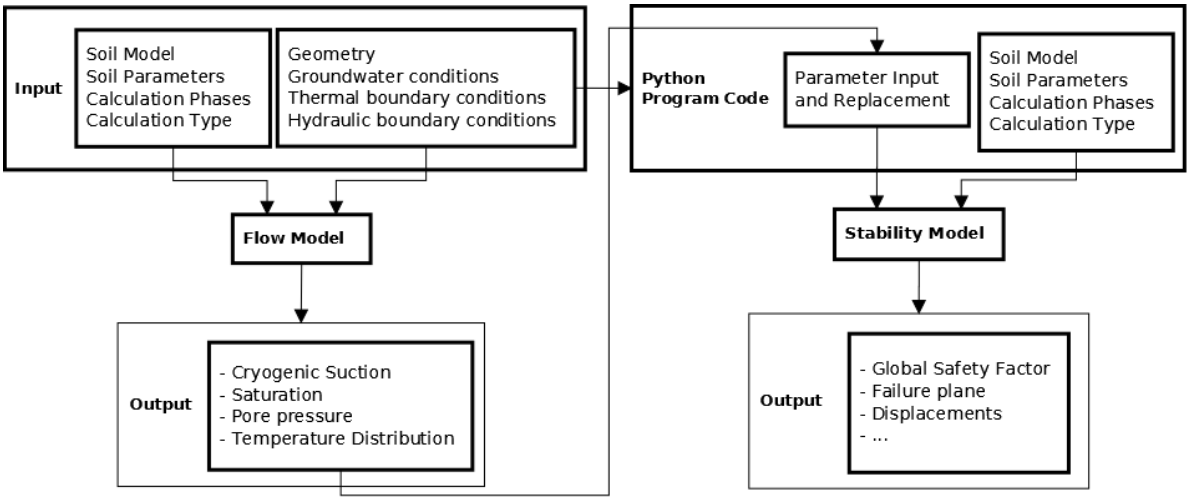

Figure 5-1: Principle of the Thermodenudation Model

The **Flow Model** is used to define the geometry and the boundary conditions. In the Flow Model, the effects of freezing and thawing periods on the groundwater flow and porewater processes are simulated. Mechanical responses of the soil are not considered. The cryogenic suction is used to consider effects of ice content and temperature variations. The cryogenic suction leads to negative pore water pressures within the soil, which are caused by the migration of pore water to the freezing zone because of the transformation of liquid water to ice. These negative pore pressures increase the effective stress of the soil, leading to higher stabilities and they are therefore important for the stability analysis. Within the Frozen and Unfrozen Soil Model, the cryogenic suction is described as the pressure difference between ice and liquid water phases and this formulation is also used in the Thermodenudation Model. The Flow Model consists of three calculation phases:

- *Initial phase* to simulate the mainly frozen state of the soil, according to the thermal boundary conditions. The initial pore pressure distribution due to phreatic water level and the initial temperature distribution are calculated.
- *Two years phase* to simulate freezing and thawing cycles of the soil. The pore pressures of the initial phase are used as input values and transient thermal flow, according to non-constant thermal boundary conditions, are applied. This phase also correctly displays the two-sided freezing of the active layer and is added because when thawing the soil is

not always completely frozen and to give more realistic input conditions for the following thawing period.

- *Quarter year cycle* is used to simulate one thawing period. The input pore pressures are taken from the previous phase and the temperature distribution is calculated according to time dependent boundary conditions.

In **Spyder** programmed Python codes copy the geometry and boundary conditions of the Flow Model to the Stability Model and define the calculation phases for the Stability Model. Also, the values for the cryogenic suction, the saturation, initial and boundary water pressure and Darcy flow velocities, which are calculated in the *Quarter year cycle* phase of the Flow Model, are transferred to the Stability Model with Python codes.

The **Stability Model** simulates the mechanical responses and the slope stability of the soil due to the freezing and thawing cycles. The soil strength is described with the Mohr Coulomb model shown in Equation 5-1. The linear elastic perfectly plastic Mohr Coulomb model is computationally efficient, which leads to relatively fast computation of results. The effects of soil freezing and thawing are implemented in the Stability Model importing the thermal and hydro field variables and boundary conditions. For example, the imported values of the cryogenic suction, lead to negative pore pressure values in the frozen part of the soil. The negative values of cryogenic suction increase the strength of the frozen soil, as interpreted from Equation 5-1, and the stability of the frozen soil domain. Consequently, this means that the slope failure is likely to occur in the thawed soil domain. It is important to note that pressure in Plaxis is considered to be negative, which means that in Plaxis the thawed part of the soil has negative active pore pressure values. A pore pressure distribution as an output of the Stability Model is presented in Figure 5-2.

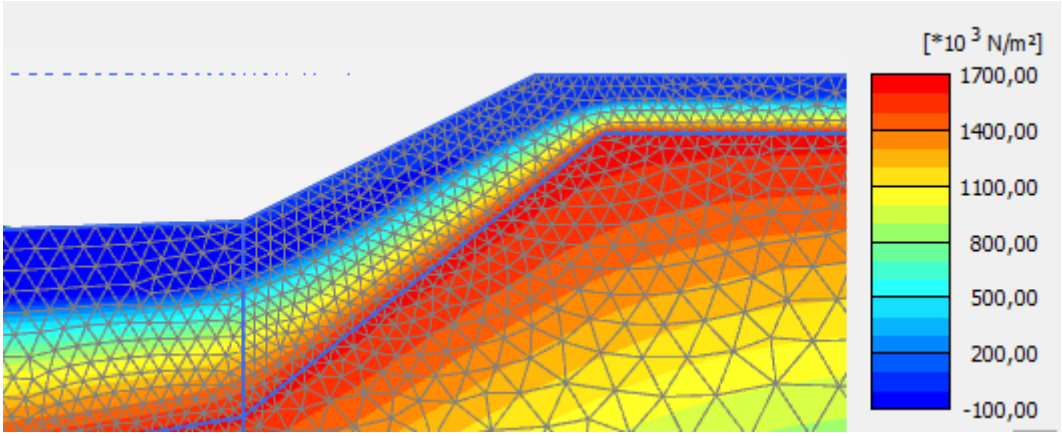

Figure 5-2: Distribution of the active pore pressures

As shown in Figure 5-2 there is a clear distinction between the thawed part of the soil, indicated with negative pore pressures (blue) and the frozen part with positive pore pressures, where suction is present (red). To implement the calculated values for the pore pressures in Equation (5-1) the signs must be reversed, due to the different sign convention of Plaxis.

The Stability Model also includes three calculation phases:

- *Initial phase* to calculate the initial effective stress field as well as pore pressures and state parameter, due to the self-weight of the soil body and the loading history. The thermal and hydraulic field variables and boundary conditions from the flow analysis are mapped to this calculation phase.
- *Equilibrium phase* to carry out elastic plastic deformation analysis. The time dependent change of pore pressures is not considered, because the pore pressure values are imported from the Flow Model. This phase is mainly added to establish equilibrium conditions within the soil for the following safety analysis
- *Safety phase* to compute global safety factors by successively reducing the Mohr Coulomb shear strength parameters (tan φ, and c'). Thereby deformations, total displacements and failure planes can be obtained.

To investigate influences on the slope stability which are independent from the frozen state of the soil, e.g. loads, they must be defined in the geometry of the Flow Model to be copied to the geometry of the Stability Model. To include them into the slope stability calculation they must be applied which certain values in the Stability Model, then the *Equilibrium* and *Safety phase* of the Stability Model must be run separately. This is necessary since only the values of parameters related to the frozen state of the soil are automatically transferred to the Stability Model and not the values of parameters related to loading conditions.

5.3 Calculation of the mass of eroded material

To calculate the mass of eroded material a separate Excel sheet was developed. As the output of the Stability Model, the total displacements of all nodes are available, which were used for this purpose. In Plaxis the model geometry is divided into several triangular elements, which are defined during the meshing process and the size of which depend on the refinement of the mesh. These elements are all equipped with 15 nodes, at which calculations are conducted. All elements, of which at least one node experiences a certain displacement are included in the calculation of the mass of eroded material by summing the areas which corresponds to the elements. The thereby calculated area is the area of displacement. The specific element areas are also given in form of a table in the output results of the Stability Model. In the Excel sheet

a limit value for the displacement can be defined and the required data must be imported from Plaxis, then the area of displacement can be calculated. The area of displacement is not automatically the area, which erodes due to the erosion processes. This area is usually much smaller and can be obtained by defining a high limit value, to just include elements in the calculation which experience a high displacement. The thereby calculated area is usually situated at the toe of the bluff, which also is the part of the slope, which gets eroded first. The mass of the eroded material per m length of the bluff can be calculated by multiplying the area with the soil density.

5.4 Theoretical background

5.4.1 The Mohr Coulomb soil model

The linear elastic, perfectly plastic Mohr Coulomb model (MC model) uses five input parameters to describe the behaviour of soil and rock in a first order approximation. The Young's modulus *E*, as the stiffness modulus and the Poisson ratio v are used for soil elasticity whereas the cohesion *c*, the angle of friction φ and the angle of dilatancy ψ describe the soil plasticity. The angle of dilatancy is used to model positive plastic volumetric strain increments which can occur in dense soil, which dilates under load. Figure 5-3 shows the basic idea of an elastic perfectly plastic model.

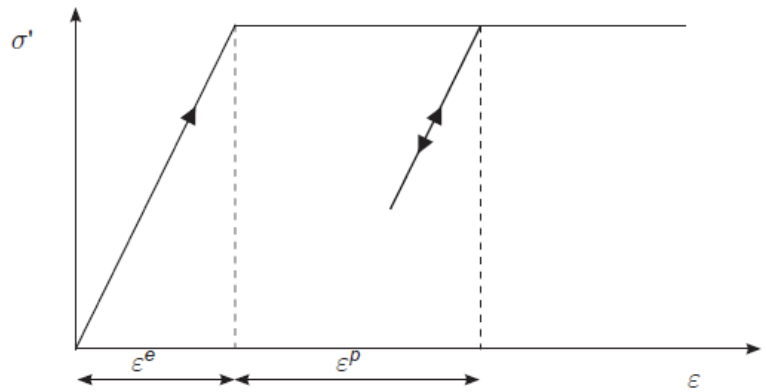

Figure 5-3: Basic idea of an elastic perfectly plastic model (Plaxis (3) 2017)

The plastic part of the stain involves the development of irreversible deformations. The MC model uses a constant average stiffness or a depth depending linearly increasing stiffness for the soil layers, which lead to relatively fast computation results and deformation estimations. In the MC model, the strain and strain rates consists of an elastic ε^e and a plastic part ε^p:

$$\varepsilon = \varepsilon^e + \varepsilon^p \tag{5-2}$$

The elastic part is described with Hooke's law of isotropic elasticity, which relates the stress rates to the elastic strain rates:

$$\sigma' = D^e \cdot \varepsilon^e \tag{5-3}$$

Where $\sigma'$is the effective stress and $D^e$is the elastic material matrix representing Hooke's law. The plastic strain part is based on the MC failure criterion and formulated according to the classical theory of plasticity, where the plastic strain rates are proportional to the derivative of the yield function with respect to the stresses also referred to as associated plasticity. Because for MC type yield functions the classical theory of plasticity overestimates the dilatancy, in the MC model a plastic potential function is introduced. The term non-associated plasticity is used in the case the plastic potential function is unequal to the yield function. In general, the plastic part of the strain can be formulated as follows:

$$\varepsilon^p = \Lambda \frac{\partial g_p}{\partial \sigma'} \tag{5-4}$$

Where g_p is the plastic potential function and Λ is the plastic multiplier, which is zero for purely elastic behaviour and positive otherwise. The relationship between the effective stress rates and the strain rates can be written as:

$$\sigma' = \left(D^e - \frac{\alpha}{d} D^e \frac{\partial g_p}{\partial \sigma'} \frac{\partial f^T}{\partial \sigma'} D^e \right) \varepsilon \tag{5-5}$$

Where f describes the yield function and d the thickness, expressed as:

$$d = \frac{\partial f^T}{\partial \sigma'} D^e \frac{\partial g_p}{\partial \sigma'} \tag{5-6}$$

The parameter α functions as a switch, for elastic behaviour it is zero, whereas for plastic behaviour it equals unity. It can be calculated with the following equation:

$$\alpha = \frac{\partial f}{\partial \sigma'}^T D^e \varepsilon^e \tag{5-7}$$

For elasticity, the result of the equations is equal or below zero, for plasticity it is positive. The theory of plasticity is restricted to smooth yield surfaces. Because the MC model also involves multi surface yield contours, the theory was extended by Koiter (1960) through the introduction of two more plastic potential functions to account for flow vertices and several quasi-independent yield functions to determine the magnitude of the multiplier.

In the MC model implemented in Plaxis the yield condition is defined with six yield functions, formulated in principal stresses and six plastic potential functions. In soils, which may also fail in tension instead of in shear the tension cut off function in the MC model in Plaxis can be used to model such a soil behaviour. Then three additional yield functions are available, which

establish relationships between the tensile stress and the principal stresses. (Plaxis (1) 2017, Plaxis (3) 2017)

5.4.2 The hydraulic model

Plaxis offers several data sets and hydraulic models. In the Thermodenudation Model the standard option, which offers several basic soil types such as coarse or fine soil was used and medium was selected as a soil type. The particle fractions are then automatically defined or can be entered manually. Other input parameters are respectively the horizontal and vertical permeabilities, k_x and k_y, and the unsaturated zone ψ_{sat}, which is set by default to a very large value, indicating that the unsaturated zone is unlimited. The Van Genuchten model is used to describe the shape of the soil water characteristic curve (SWCC), which describes the hydraulic behaviour of unsaturated soil and can be used to estimate several soil hydraulic parameters. The equation which was proposed by Van Genuchten (1980) contains three parameters and relates the saturation S to the pressure head ϕ_p, which is the negative quotient of suction pore stress to unit weight of pore fluid:

$$S(\phi_p) = S_{res} + (S_{sat} - S_{res})\left[1 + (g_a|\phi_p|)^{g_n}\right]^{g_c} \quad (5\text{-}8)$$

S_{res} is the residual saturation, which describes the part of the water which remains in the pores even at high suction heads, S_{sat} is the saturation at saturated conditions. Because although in saturated conditions air can still be trapped in the pores and they are therefore not completely filled with water the value for S_{sat} usually is less than one. g_a, g_n and g_c are fitting parameters. g_a takes the air entry into the soil into account, g_n is a function of the rate of water extraction of the soil once g_a has been exceeded. g_c is used in the general Van Genuchten equation, in Plaxis it is expressed through a formulation containing g_n and g_c, which thereby reduces the equation for the Saturation to a two-parameter equation.

The effective Saturation is expressed with the following formulation:

$$S_e = \frac{S - S_{res}}{S_{sat} - S_{res}} \quad (5\text{-}9)$$

Using the effective saturation, the relative permeability can be formulated according to Van Genuchten as follows:

$$k_{rel}(S) = \max\left[S_e^{gl}\left(1 - \left[1 - S_e^{\left(\frac{g_n}{g_n - 1}\right)}\right]^{\frac{g_n - 1}{g_n}}\right), 10^{-4}\right] \quad (5\text{-}10)$$

g_l is a fitting parameter, which must be measured for a specific material as all other fitting parameters as well. The Van Genuchten model provides reasonable results for low and moderate suction values, for high suction values the saturation remains the residual saturation.

Transient flow in a porous medium is in Plaxis in general described with Darcy's law, which is for three dimensions:

$$q = \frac{k}{\rho_w g}(\nabla p_w + \rho_w g) \tag{5-11}$$

q is the fluid velocity (specific discharge), g is the acceleration vector due to gravity, ρ_w is the density of water and ∇p_w is the gradient of water pore pressure, which is responsible for groundwater flow. k is the coefficient of permeability, which can be expressed through the ratio of permeability at a given saturation k_{rel} and the permeability in fully saturated soil k_{sat}:

$$k = k_{rel} k_{sat} \tag{5-12}$$

The mass concentration in each elemental volume of the soil is equal to the product of porosity and saturation of the soil and the density of water. Changes in the mass concentration are equal to the flow out of the medium, which also is equal to the divergence of the specific discharge. Using Boussinesque's approximation by neglecting the gradients of the density of water and the deformations of solid particles the continuity equation is given by:

$$\nabla^T \cdot \left[\frac{k_{rel}}{\rho_w g} k_{sat}(\nabla \rho_w + \rho_w g)\right] + Sm^T \frac{\partial_\varepsilon}{\partial t} - n\left(\frac{S}{K_w} - \frac{\partial S}{\partial p_w}\right)\frac{\partial p_w}{\partial t} = 0 \tag{5-13}$$

Where m^T= (111000). The first term describes the divergence of the specific discharge, the second term accounts for the displacements of solid particles and the last term describes changes in the mass concentration. Considering transient groundwater flow the second term can be neglected and for steady state flow the last term equals zero, because $\frac{\partial p_w}{\partial t} = 0$.

Plaxis offers several boundary conditions but only the types closed and head were used in the Thermodenudation Model. The type closed means that there is zero Darcy flux and dissipation of excess pore pressure over the boundary, whereas in the type head an external water pressure is generated for the boundary, which is treated as a traction load from the analysis program in Plaxis. (Plaxis (1) 2017, Plaxis (2) 2017, Plaxis (3) 2017)

5.4.3 Soil thermodynamics

In Plaxis, non-isothermal unsaturated groundwater flow, heat transport and deformation are considered, assuming a constant gas pressure and thermodynamic equilibrium. The isothermal

unsaturated flow is described with the Richard's model with the following equation for the advective mass flux of water, which is based on Darcy's law:

$$J_w = \rho_\omega \left(\frac{k_{relL}}{\mu} \kappa^{int} (\nabla p_w + p_w g) \right) \tag{5-14}$$

κ^{int} is the intrinsic permeability of the porous medium, which is a function of the porous structure, μ is the dynamic viscosity, which depends on the temperature and the type of the fluid. k_{rel} is the relative permeability, which is a function of the Saturation and p_w is the water pressure, g the gravitational acceleration and ρ_w the density of water.

Because of different temperatures the transformation from liquid to vapour must be considered and the mass flux of vapour can be formulated according to Rutqvist et al. (2001) and based on Fick's law:

$$J_v = -D_v \nabla p_v = D_{pv} \nabla p_w - D_{Tv} \nabla T \tag{5-15}$$

D_v is the vapor diffusion coefficient in porous material, which depends on gas pressure, medium tortuosity and temperature. D_{pv} is the hydraulic and D_{Tv} the thermal diffusion coefficient. T is the temperature of the porous medium at local equilibrium in Kelvin.

The mass balance can also be formulated according to Rutqvist et al. (2001):

$$n \frac{\partial}{\partial t} \left(S_{\rho w} + (1 - S) \rho_v \right) + \left(S_{\rho w} + (1 - S) \rho_v \right) \left[\frac{\partial \varepsilon_v}{\partial t} + \frac{1 - n}{\rho_s} \frac{\partial \rho_s}{\partial t} \right] = -\nabla \cdot (J_w + J_v) \tag{5-16}$$

Where n is the porosity. The term $(1 - S)\rho_v$ can be neglected, because it will be very small compared to S_{ρ_w} if the soil is saturated and low temperatures are present.

The linear momentum balance for a representative elemental volume of the soil can be expressed with the following equation:

$$\nabla \cdot \sigma + \rho g = 0 \tag{5-17}$$

$$\rho = (1 - n)\rho_s + nS\rho_w + n(1 - S)\rho_g \tag{5-18}$$

ρ is the multiphase medium, a function of the solid ρ_s, water ρ_w and gas ρ_g densities, the degree of saturation S and the porosity n, g is the gravity acceleration. The total stress σ for partially saturated soil is given by:

$$\sigma = \sigma' + pm \tag{5-19}$$

Where σ' is the effective stress, m is the identity tensor and p the average pore pressure, a function of pore water p_w and pore gas pressure p_g and the degree of saturation of water and gas.

$$p = S_w p_w + S_g p_g = S p_w + (1 - S) p_g \tag{5-20}$$

By substituting the average pore pressure p in Equation 5-20 and replacing the degree of saturation with the matric suction coefficient χ, Bishop's stress (average stress) can be calculated with the following equation:

$$\sigma = \sigma' + \left(\chi p_w + (1-\chi)p_g\right)m \tag{5-21}$$

χ depends on the degree of saturation, porosity and the matrix suction and can be determined experimentally. Because pore gas pressure p_g and atmospheric pressure are assumed to be equal and the pore gas pressure is assumed to be constant the second term in the brackets can be neglected.

Using the effective stress σ' the constitutive relation can be written as:

$$d\sigma' = M:(d\varepsilon - B_{DT}mdT) \tag{5-22}$$

where M is the material stress-strain matrix, ε is the total strain of the skeleton. The second part in the brackets represent the thermal strain, which is caused by temperature increase and defined as a function of the thermal expansion coefficients in x, y, and z directions.

This leads finally to the governing equation for the deformation model, which is:

$$\nabla \cdot [M:(d\varepsilon - B_{DT}m\,dT) + \chi dp_w m] + d(\rho g) = 0 \tag{5-23}$$

The heat balance equation for a porous medium can be written in the following form:

$$\frac{\partial}{\partial t}\left(nS\rho_w e_w + n(1-S)\rho_v e_v + (1-n)\rho_s e_s\right) = -\nabla \cdot \left(J_{A\omega} + J_c\right) + Q_T \tag{5-24}$$

in which e_w, e_v, and e_s are the internal energy in water, vapour and solid phases, respectively. Q_T is the heat source term which is defined as the heat generation rate per unit volume and which includes the mechanical energy conversions in fluid and solid phases. The source term can be neglected in most practical applications. J_c is the conductive heat flow which can be expressed with Fourier's law:

$$J_c = -\lambda \nabla T \tag{5-25}$$

λ is the thermal conductivity of the porous medium, which depends on the solid, the water and the gas thermal conductivity. J_{Aw} is the advective internal energy flux in water, which can be formulated with the following equation:

$$J_{Aw} = \rho_w C_w V_w T \tag{5-26}$$

Where, C_w is the specific heat capacity of water and V_w the water phase velocity. The total heat flux is the summation of conductive and advective heat flux. Neglecting the source term Q_T and

inserting the equation for the conductive and advective heat flux the right-hand side of the heat balance equation can be expanded to:

$$-\nabla(\lambda\nabla T) + \nabla \cdot (\rho_W C_w V_w T) \tag{5-27}$$

The left-hand side of the heat balance equation can be simplified to:

$$\frac{\partial}{\partial t}\left(nS\rho_w e_w + n(1-S)\rho_v e_v + (1-n)\rho_s e_s\right) = \rho C \frac{\partial T}{\partial t} \tag{5-28}$$

ρC is the heat capacity of the porous medium, which depends on the solid, water and gas specific heat capacities. At the end, the heat balance equation can be written as:

$$-\nabla(\lambda\nabla T) + \nabla \cdot (\rho_W C_w V_w T) = \rho C \frac{\partial T}{\partial t} \tag{5-29}$$

The phase change when liquid turns to ice, due to temperatures below 0 °C is considered by modifications of the storage term because additional energy must be provided. This energy depends on the latent heat of water and the unfrozen water content, which can be defined by the user. (Plaxis 2015)

6 Case Study: Baydara Bay

In this section, information about the coast at Baydara Bay and the Thermodenudation Model of Baydara Bay are presented as well as a description of the climate change in Arctic areas. The coast of Baydara Bay was used to calibrate and validate the newly developed Thermodenudation Model and to study the effect of climate change regarding the coastal retreat, the active layer thickness and the volume of eroded soil. The available measured data at Baydara Bay, which was obtained during the “Baydara Bay – Field investigations and laboratory testing" field campaign for the international research project SAMCoT in September 2015 is summarized as well.

6.1 Site description

The Baydara Bay is situated on the west coast of the Baydara gulf of the Kara Sea in western Siberia in Russia. The site is located 3.6 km North West of the Bovanenkovo-Ukhta gas pipeline, which was constructed from 2008 - 2017 and is threatened by coastal erosion and landfall, which makes the study of the erosion processes at Baydara Bay important. Figure 6-1 shows the location of the Study site.

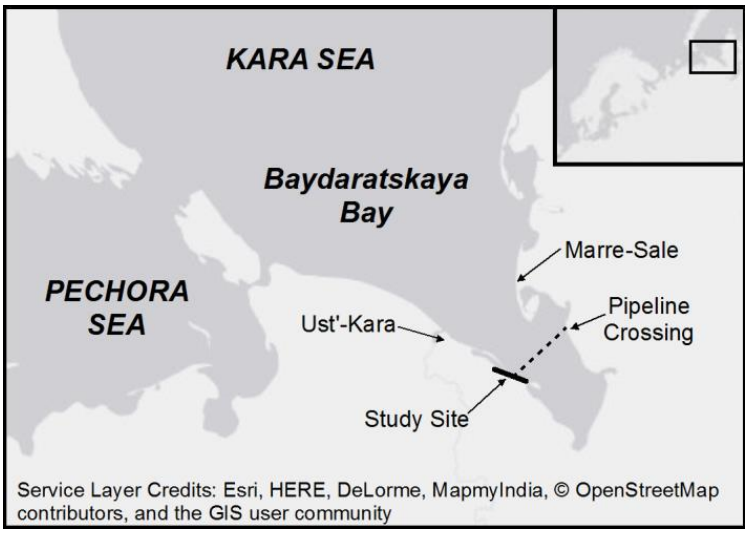

Figure 6-1: Location of the study site (Pearson, Lubbad and Le 2016)

The study site is subdivided into Site 1 and Site 2 and consists of three geomorphological formations. Site 1 is situated in the northwest, where there is a low marine terrace with a height of 5 - 6 m and a length of 1,2 km, which mainly consists of sandy clay with a smoothly sloping

surface, covered with grass and minor swamped hollows. A picture of the low marine terrace is presented in Figure 6-2.

Figure 6-2: Picture of the low marine terrace (Isaev et al. 2016)

The low marine terrace declines into a laida with a height of 1.5 - 2 m and a length of 1.3 - 1.4 m which is followed by Site 2, a high terrace with a height of 10 - 17 m and a length of 1.2 m along the coastline. The high terrace is composed of marine dusty sands, with peat layers and icy layers. (Pearson, Lubbad and Le 2016, Isaev et al 2016)

The shape of the seabed is shallow with a maximum depth of approximately 23 m and partly underlaid with sea permafrost down to a depth of -25 m. Sea ice usually appears between mid- and end October and reaches a maximum thickness of about 1.2 m at the west coast of the bay. There is a continuous sea ice cover over 7 months, whereas only for 2 months the sea is completely ice-free. The tidal range of Baydara Bay is about 70 cm and average annual wave heights lie between 1.3 - 1.8 m. The area is thinly populated with only a few roads and buildings. (Pearson, Lubbad and Le 2016, Isaev et al 2016)

The climate conditions are harsh with an average annual temperature of about -8 °C, a long and chilly winter with a mean temperature in January of -22 °C, short mid-season and cold summer with a mean temperature in June of +7 °C. The annual precipitation ranges from 300- 500 mm. Thermometric measurement and soil determinations were done in 2 boreholes one at the low marine terrace (Site 1) and the high marine terrace (Site 2) respectively with thermistor strings. The coastal retreat was obtained by time laps shooting and GPS mapping. Historical erosion rates vary from 0.5 - 1.5 m/year to 5 - 10 m/year when massive ground ice is present. (Isaev et al. 2016, Pearson, Lubbad and Le 2016)

6.2 Profile description

To calibrate the model, Profile #3 at Site 1, the low marine terrace, was chosen, because the low marine terrace is mainly subjected to thermodenudation, whereas at the high coast also thermoabrasion is present (Isaev et al. 2016).

The geometry of Profile #3 was determined by Trimble DGPS measurements with re-levelling in June 2014, September 2015 and September 2016. Profile #3 has a height of approximately 6 m and a slope angle of about 26,7 degrees. In front of the bluff, there is a level beach with a length of approximately 30 m and a slope angle of about 3 degrees. The whole beach and parts of the bluff are covered with a snowbank, which was about 1.5 - 2 m thick in June 2013 and 2014 respectively. The size of the snowbank is highly varying with climate conditions, there are no information when the snowbank appears and when it has melted away. Borehole #4 is placed at the top and Borehole #5 at the toe of the bluff. The geometry of Profile #3 is shown in Figure 6-3.

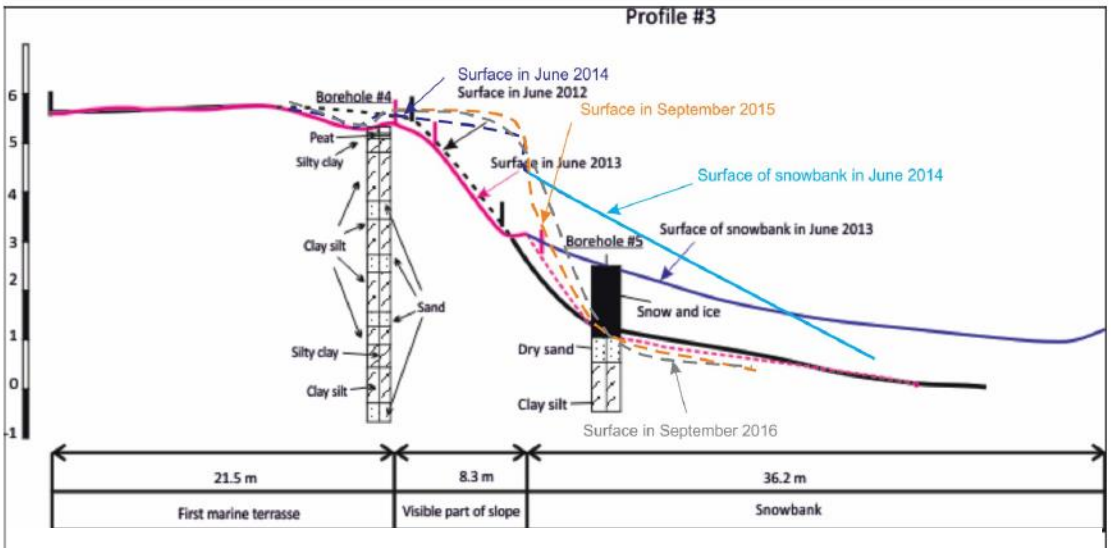

Figure 6-3: The geometry of Profile#3

Borehole #4 was drilled in June 2013 and reinstalled in 2015, due to coastal retreat, it has a depth of 6.2 m. In Borehole #4 the temperature was measured with a thermistor string every 4 hour from 19.06. 2013 - 06.06.2014 in different depths, starting at the ground surface and down to a depth of -2.43 m in steps of 5 - 23 cm. The temperature measurement showed positive temperatures from June to September, where the freezing already started. Maximum temperature of +11 °C was reached in July, whereas the minimum temperature of -25 °C was reached in January. The average temperature from 2013 - 2014 was -4.8 °C. The average temperature of the permafrost was -3.6 °C at a depth of -2.4 m. The active layer thickness can be obtained from the temperature measurement by selecting the maximum depth with positive

temperatures. From 2013 - 2014 the active layer was between 0.86 and 1.0 m thick. (Isaev et al. 2016)

Additionally, there was a temperature measurement from 2014 - 2015 at the high coast at Site 2 available, where the measurements were taken every 6 hours. Positive temperatures were obtained during 5 months from mid-May until mid-October with a maximum temperature of +20 °C in July. The minimum temperature of -37 °C was reached in December. The measured temperatures varied much within a day and in general the climate conditions seem more extreme compared to Site 1in 2013. The average temperature of the permafrost was -3.5 °C at a depth of -2,4 m. The active layer thickness was between 1.3 and 1.5 m from 2014 - 2015. (Isaev et al. 2016)

In Borehole #4 of Profile #3 the geocryological texture of the soil was analysed down to a depth of -3.4 m. The soil mainly consists of fine grained sandy clay with some layers with ice lenses but mainly a massive cryostructure (Isaev et al. 2016). The term massive means in this context that pore ice is predominant, which indicates a relatively low total ice content. (Harris et al. 1988) The surface is covered with a peat layer and overgrown with grass and liches. (Isaev et al. 2016)

The cliff retreat of Site 1 and Site 2 were determined with GPS mapping from 2012 to 2016. The results at Profile #3 are shown in Figure 6-3. At Profile #3 the erosion rate from 2014 - 2015 was only 1.1 m, but the climatic conditions from 2014 to 2015 were reported as very cold. For 4 years an erosion of 5 m was observed, resulting in an average erosion of about 1.25 m per year. The high coast showed an erosion of 6 m during the 4 years of study, which means an average erosion of 1.5 m per year. (Isaev et al. 2016)

6.3 Thermodenudation Model of Baydara Bay

6.3.1 Geometry

Because only temperature measurements from 2013 to 2014 at Profile #3 are available the geometry of the model represents the situation in 2013. Therefore, the surface of June 2013, which is pictured in pink in Figure 6-3 was chosen as the geometry. The influence of the snow bank was neglected, since modelling the behaviour of snow is only possible by applying a thermal boundary condition in Plaxis, for which not enough information e.g. date of appearance and disappearance, thickness, temperature was available. Additionally, erosion can only take place when the snow has melted away, so by neglecting snow the calculations of erosion are on

a higher side for design purposes. Figure 6-4 shows the geometry and dimensions of the Thermodenudation Model of Baydara Bay.

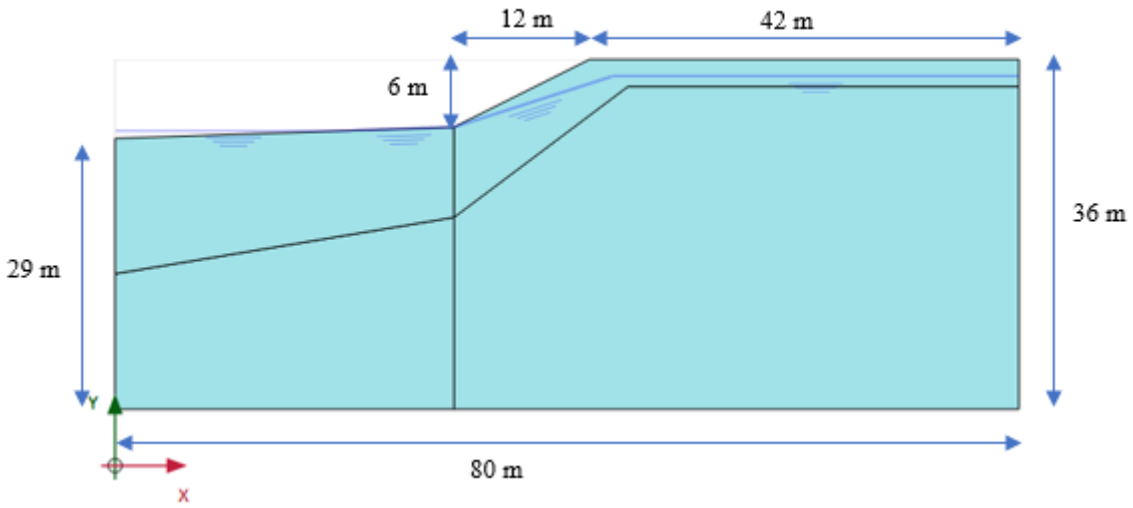

Figure 6-4: Geometry of the Thermodenudation Model

6.3.2 Boundary conditions

6.3.2.1 Thermal boundaries

For the Thermodenudation Model, the temperature measurements directly at the ground surface were transformed to mean daily temperatures and applied as thermal boundary conditions at the ground surface. The reference temperature was set to 273.15 Kelvin (K). The vertical boundaries were set close to prevent thermal flow and the bottom boundary was applied with a constant temperature of 272.15 K, to simulate the continuing permafrost. This temperature was chosen because permafrost temperatures can vary between 0 °C and -3 °C, with a large fraction at -1 °C at the Ob river basin in western Siberia, near the study site as studies of Zang et al. (2005) showed. An additional thermal boundary condition was installed in a depth of -2.4 m below the top of the bluff and applied with the temperature measured at a depth of -2.4 m. The reference temperature was set to 271.15 K. This temperature distribution was used to model the temperature variation within the permafrost.

There was no information available about the sea water temperature. So, the temperature of the sea water was simulated with a harmonic thermal boundary condition with an amplitude of 6 and a period of one year. The reference temperature was set to 274.15 K.

6.3.2.2 Hydraulic boundaries

There was no information about hydraulic conditions at Profile #3 available, so it was assumed that the groundwater level would follow the shape of the slope to the sea. Most hydraulic

boundary conditions were set to close and deactivated during calculation, only when the water level was above the ground surface the boundary type head was used to consider the hydraulic pressure.

The boundary conditions of the Thermodenudation Model of Baydara Bay are shown in Figure 6-5.

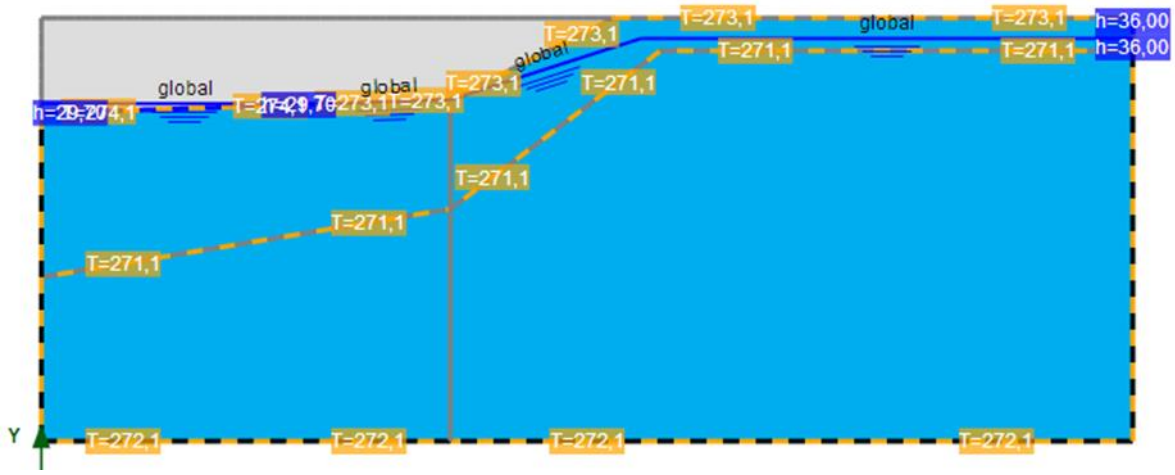

Figure 6-5: Boundary conditions of the Thermodenudation Model

The values high lightened in yellow are the thermal boundary conditions, the hydraulic boundaries are presented in blue.

6.3.3 Soil parameters

In the Thermodenudation Model of Baydara Bay the soil was assumed as sandy clay, the layering was neglected to simplify the model and because, besides the soil type, no soil parameters were available. Table 6-1 shows important parameters required for the Mohr Coulomb model and the thermal analysis, which were found in literature and used in the Thermodenudation Model of Baydara Bay:

Table 6-1: Soil parameters used in the Thermodenudation Model

Parameter		Value	Unit
Friction angle	φ	30	°
Effective cohesion	c’	1	kPa
Particle density	ρ_s	2600	kg/m^3
Specific heat capacity	c_s	945	J/kgC
Thermal conductivity	λ	2,5	W/mK
Unit weight sat/unsat	γ	20/20	kN/m^2

The friction angle for sandy clay was found to range from 30 - 34 ° (Geotechdata.info 2013 (1)). The particle density is a measure of the mass per unit volume of only the solid particles of the soil, it usually ranges from 2600 – 2750 kg/m^3. The specific heat capacity of a soil describes the amount of heat, which can be stored in the solid material, it was assumed as 945 J/kgC for clay (The Engineering Toolbox 2017 (1)). The thermal conductivity describes the rate of energy which can be transported in the material, for saturated clay values from 0.6 - 2.5 W/mK are possible, whereas for saturated sand values from 2 - 4 W/mK can be reached. A value of 2.5 W/mK was used in the model (The Engineering Toolbox, 2017 (2)). The unit weight is defined as the weight per unit volume of a soil and can be calculated by multiplying the soil density with the acceleration due to gravity in the unsaturated state, where the soil pores are filled with air. In the saturated sate, the pores are fully or partly filled with water, then the unit weight depends on the water content of the soil. The unit weight was assumed as 20 kN/m^2 in the saturated as well as in the unsaturated state (Geotechndata.info 2013 (2)).

6.3.4 Calculation phases

In the Thermodenudation Model of Baydara Bay only the calculation time of the Flow Model was adapted to the situation at Baydara Bay. For example, the time of the *two years phase* was reduced, since temperature measurements were only available for 352 days in a year. The calculation time of the *Quarter year cycle* was maintained, since three months are a reasonable time period for the thawing season and the results represent then a condition in mid-September. The Stability Model was not changed, since there, time is not considered. To provide a better overview, the calculation phases are presented in Figure 6-6. For a detailed description see chapter 5.2.

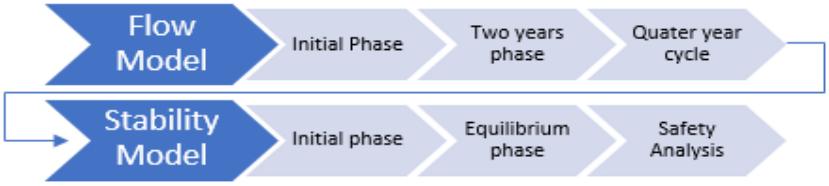

Figure 6-6: The calculation phases of the Thermodenudation Model

6.4 Climate change scenarios

6.4.1 Climate change in Arctic regions

The climate change in Arctic regions takes place more than twice as fast as in the rest of the world. According to Zetsche, Faller and Broich (2005) main reasons are:

- the snow- and ice melt leaves darker surfaces behind, which absorb a bigger part of the solar radiation, leading locally to an acceleration of the melting process.
- The part of the radiation which gets absorbed by greenhouse gases directly contributes to atmospheric warming in the Arctic whereas in temperate climate a part of the energy goes into evaporation.
- The atmosphere above the pols is thinner as above the rest of the world and therefore gets heated up faster.
- The heat exchange between ocean and atmosphere is intensified when the sea ice cover decreases, leading to a higher heat intake of the ocean during summer and a higher heat dissipation in the winter months.

As a result, the annual mean temperature in the Arctic has increased in the last 50 years by about 4 °C. A further increase by 3-7 °C over land areas and 4 -7 °C over the sea is expected until the end of the century. The sea ice cover decreased the last 30 years (state 2005) by about 8 %, which corresponds to an area of about 1 million km^2 (larger than the areas of Norway, Sweden and Denmark altogether) and a further reduction by up to 50 % is expected until 2100. (Zetsche, Faller and Broich 2005, ACIA 2005). The temperature increase is subjected to high local variations, reaching highest values in the Canadian Beaufort Sea and the Russian Arctic. Additionally, it is expected that especially in near shore areas the temperature increase in autumn and winter is higher than the increase in the summer, because of effects due to the heat storage of the Arctic ocean, which extends the thawing period. (ACIA 2005)

Figure 6-7 shows the projected surface air temperature development until 2100 in the Arctic from the IPCC (Intergovernmental Panel on Climate Change).

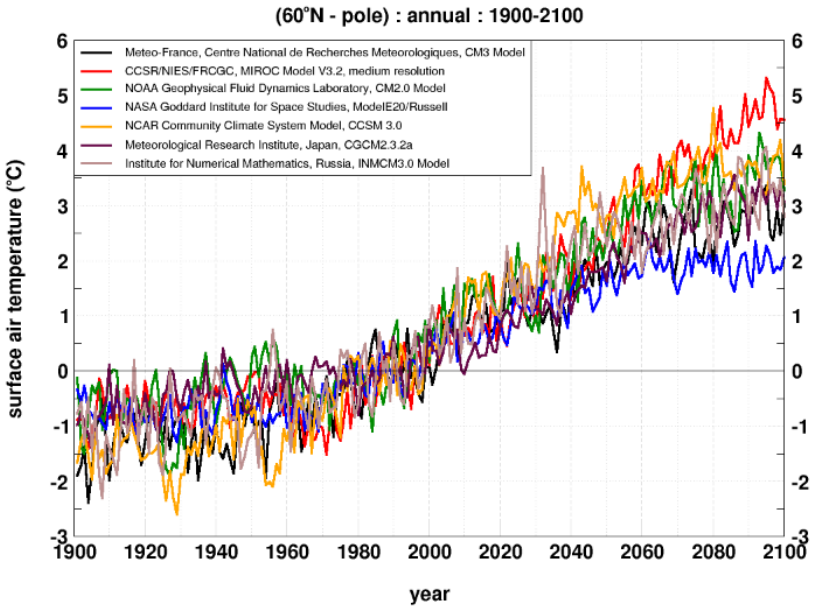

Figure 6-7: IPCC projected Arctic surface air temperature, based on the B2 emission scenario (IPCC 2001)

These values correspond to the temperatures which were obtained from the Arctic Climate Impact Assessment (ACIA) commissioned by the Arctic Council. In the frame of the ACIA research project five models were developed to simulate climate change in the Arctic. (ACIA 2005)

In the ACIA report, the mean temperature increase predicted by the five models are +1.2 °C from 2011 - 2030, +2.5 °C from 2041 - 2060 and +3.7 °C from 2071 - 2090. This forecast was based on the B2 emission scenario of the IPCC. (ACIA 2005)

Using the more extreme A2 emission scenario a temperature increase of about + 3 °C until 2050 and +7 °C until 2100 both relative to 1981 - 2000 was projected by the five ACIA designed models. (ACIA 2005)

The permafrost table also experiences a temperature increase. According to Pavlov (1994) the permafrost temperature at a depth of -6 m in the continuous permafrost area of the European part of northern Russia increased about +1.6 to +2.8 °C from 1973 to 1992. The five models developed from ACIA predicted a further increase of the permafrost temperature at the Russian Arctic coast by +2 to +2.5 °C from 1981 - 1990 to 2050, while the air temperature increase in this area was + 2 - 3 °C. The prediction was based on the B2 emission scenario (ACIA 2005)

The temperature increase also is a major contributor to the sea level rise, which is caused by the thermal expansion of the warming ocean, the loss of ice by glaciers and ice sheets and the reduction of liquid water storage on land (Gregory 2013, ACIA 2005). Figure 6-8 shows the projected sea level rise until 2100 from the IPCC.

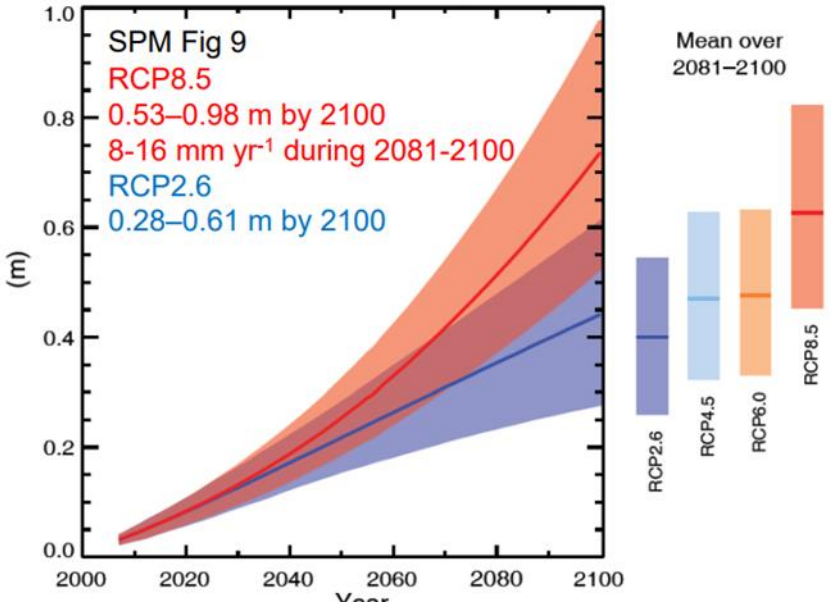

Figure 6-8: Projection of global mean sea level rise (Gregory, 2013)

The projections of climate change vary much depending on the chosen climate model and the climate change scenario. (ACIA 2005)

The B2 and A2 emission scenarios are two of the four main groups of the climate scenarios, which were developed by the IPCC. They consider the influence of economic and social development, population growth, technological change, the consumption of resources and environmental management on the emission of main greenhouse gases in the 21th century and can therefore be used to predict the future temperature increase. In the B2 emission scenario solutions to economic, social and environmental oriented problems are found locally or regionally, the population is growing but less strong than in other scenarios with a moderate economic development and a locally different and slower technological change. The A2 emission scenario assumes a heterogenic world in which local characteristics are maintained, the birth rate is locally different and the population therefore growing constantly. The economic and technologic development is primarily regional determined and slower than with the other scenarios. The development of renewable energy and improvements in energy efficiency happen delayed compared to other scenarios. (IPCC, 2001)

The Arctic Climate Impact Assessment report (ACIA 2005) contains also some predictions of the active layer thickness. The five ACIA designated models obtained an increase of the seasonal thawing depth by more than 50 % for the Russian Arctic coast from 1981 - 1990 to 2050. For northern Alaska, also projections of the maximal active layer thickness until 2100 were conducted and showed an increase by 1 m in coarse grained areas with high conductivity and 0.5 m elsewhere. Lawrence et al. (2015) developed maps of the maximal active layer thickness for the years of 1850, 2000, 2100 and 2300 in Russia and northern Alaska, using the community land model, which formalizes and quantifies concepts of ecological climatology. The active layer thickness in 2100 in the west of Russia, where the study site is located was about 2 m an increase of about 1 m compared to the thickness in 2000. Thus, an active layer increase until 2100 of up to 2 m seems reasonable. (ACIA 2005, Lawrence et al. 2015)

6.4.2 Climate change scenarios Baydara Bay

For the modelling of Baydara Bay in 2013, 2050 and 2l00 two different scenarios were simulated: Scenario 1 simulates the climate conditions according to an average temperature and sea level increase based on the B2 emission scenario. Scenario 2 simulates an extreme development of temperature and sea level rise, using temperature values according to the A2 emission scenario and the highest projected sea level values. In Scenario 1 an overall temperature increase of about +3.5 °C compared to the temperature in 1990 is chosen until the

end of the century, whereas for Scenario 2 the temperature increases by +7 °C until 2100. The Thermodenudation Model simulates the climate conditions from 2013 to 2014; from 1990 to 2013 the temperature increased already by about +1 °C as can be seen from Figure 6-7, this means that from 2013 to 2050 only a temperature increase of +1.5 °C is left. From 2050 to 2100 a further temperature increase by +1 °C is predicted, as can be seen in Figure 6-7. For Scenario 2 the temperature also increases by about +1 °C until 2013 so that from 2013 to 2050 a further increase by +2 °C is left and from 2050 to 2100 an increase by +4 °C.

The permafrost temperature is assumed to increase from 2013 to 2050 and from 2050 to 2100 by about 1 °C for Scenario 1. For Scenario 2 the permafrost temperature increases from 2013 to 2050 by about 1 °C as well, but from 2050 to 2100 an increase by +2 °C is assumed, because of the stronger increase in the air temperature.

For the climate Scenario 1, an average sea level rise of 0.5 m until the end of this century is assumed. From 2013 - 2050 the sea level rises about 20 cm the remaining increase of 30 cm happens from 2050 to 2100. In Scenario 2 the water level rises until 2100 by about 1 m. From 2013 to 2050 an increase of 40 cm and from 2050 until 2100 an increase of 60 cm is assumed. The maximum tide of 0.7 m is added to the sea level to simulate worst case scenarios and obtain the water level. Table 6-2 summarizes the water level and the temperature increase for the three different simulation cases and two different climate scenarios in relation to the situation at Baydara Bay in 2013.

Table 6-2: Climate change scenarios at Baydara Bay

	Baydara Bay 2013	Baydara Bay 2050		Baydara Bay 2100	
	Reference	Scenario 1	Scenario 2	Scenario 1	Scenario 2
Water level [m]	0.7	0.9	1.1	1.2	1.7
Air temperature increase [°C]	0	+1.5	+2.0	+2.5	+6
Permafrost temperature increase [°C]	0	+1	+2	+1	+3

The water level consists of the sea level, which is at 0 m in 2013, and the maximum tide of 0,7 m. It was assumed that the maximum tide remains 0.7 m in 2050 and 2100. A temperature increase of the sea water was neglected as well as a possible extension of the thawing period, which remained three months for all climate change scenarios.

7 Results and Discussion

7.1 Calibration of the model

To calibrate the originally developed Thermodenudation Model to the situation at Baydara Bay, the geometry of the model, the boundary conditions and the soil parameters were adjusted in a way that reasonable values for active layer thickness and coastal retreat were obtained, which comply with the measured values.

To match the active layer thickness observed in the field and to simulate the temperature distribution of the permafrost, an additional boundary condition was set at a depth of -2.4 m below the top of the slope and applied with the temperature measurement at -2.4 m. The depth of the boundary condition increases below the inclined slope from -3 to -6 m and reaches below the beach a depth between -8 and -12 m. The reference temperature of this boundary condition was set to 271.15 K to match the active layer thickness observed in the field. A reason why a reduction of the reference temperature to -2 °C was necessary (usually 273.15 K) could be the neglection of snow, vegetation and soil layering within the Thermodenudation Model. Snow and vegetation can have an insulating effect on the permafrost, slowing down the thawing in the summer. By neglecting the soil layering, the thermal conductivity of different soil types is not considered. The thermal conductivity of fine grained soil is for example lower as for coarser soil (Blanck, 1929), neglecting layers of finer soil, can lead to higher thermal conductivities and higher thawing depths in the Thermodenudation Model, where only an average thermal conductivity was used. The different depths below the inclined surface and the beach were chosen because there the effects of the boundary condition should be minimized, since the thawing depth below the beach can be significantly higher because of the influence of the warm seawater. The thawing depth below inclined surfaces can also be higher due to the more intensive radiation of the sun, which stands low on the horizon in Arctic areas. Additionally, the thawing depth was only measured on top of the slope, thus no comparative values of the active layer thickness for the beach or the inclined surface were available.

The model parameters presented in Table 6-1 were used in the Thermodenudation Model of Baydara Bay. They were determined by varying the parameters within reasonable limits until best results were obtained. The thus adjusted model was applied with the temperature measurement at Baydara Bay. Figure 7-1. shows the temperature distribution in mid-September as an output of the calculation phase *Quarter year cycle* of the Flow Model. The white line is

the frost line, which separates the frozen part of the soil from the unfrozen. Thereby the active layer thickness on top of the slope can be determined and equals 0.88 m.

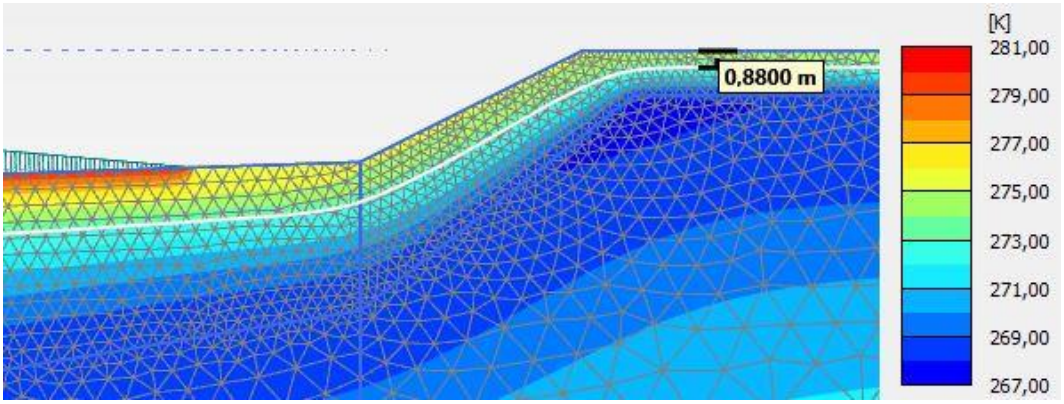

Figure 7-1: Active layer thickness in 2013

The active layer thickness determined with the temperature measurements was between 0.86 and 1.0 m thick, thus the Thermodenudation Model delivers reasonable results regarding the active layer thickness. As an output of the Stability Model, the mesh deformation can be obtained which is presented in Figure 7-2.

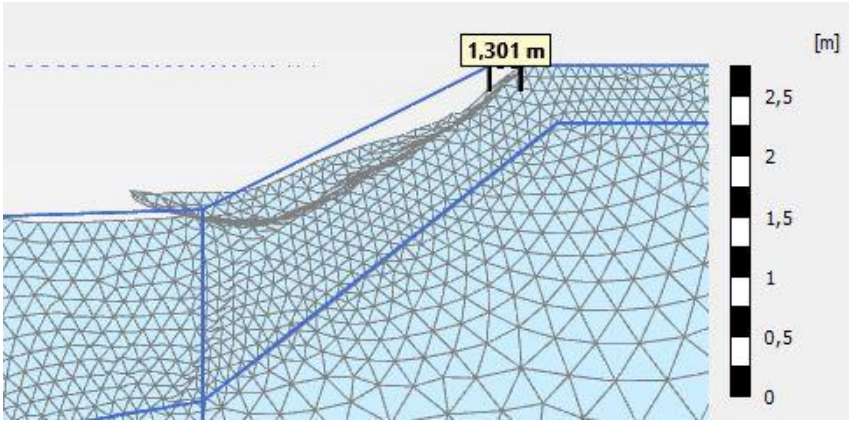

Figure 7-2: Coastal retreat in 2013

Thereby the coastal retreat rate can be determined, which was 1.3 m from 2013 to 2014. There are no measurements regarding the coastal retreat rate from 2013 to 2014, but from 2014 to 2015 the retreat rate was 1.1 m and the average erosion rate, determined over the 4 years of study was 1.25 m. The erosion rate calculated with the Thermodenudation Model seems therefore reasonable. Additionally, there are settlements in front of the bluff. Although this was not reported at Baydara Bay it seems reasonable, since thawing of soil often leads to settlements.

The amount of eroded soil could be determined using the area calculation Excel sheet. Using a displacement limit value of 0.16 m the volume of the soil was 44.46 m^2/m. This value seems reasonable considering the dimensions of the slope and the area of displacements which is shown in Figure 7-3.

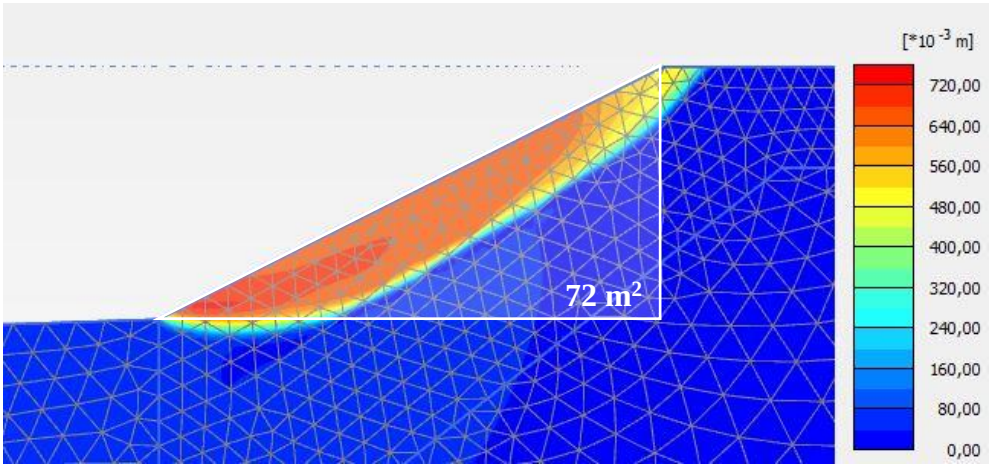

Figure 7-3: Area of displacement in 2013

The eroded soil volume of Profile #3 was measured from 2013 to 2014 to 21.09 m^3, this is the soil volume which is effectively removed from the coastline by waves and currents during high water conditions due to extreme weather phenomena. An explanation for the difference between the calculated and measured values is, that the calculated value includes all soil which experiences a certain displacement, but parts of the soil accumulate in front of the bluff or get deposited on the slope surface and therefore do not account for to the eroded soil volume. Additionally, the mass of eroded soil strongly depends on the occurrence of extreme weather conditions, since the sea water has no contact with the bluff under normal conditions. The parts of the soil which experience a displacement of more than 0.67 m represent a mass of 24.58 m^2/m, which is composed of soil of the lower part of the bluff, pictured in red in Figure 7-3. This is probably also the part of the soil that gets removed by waves and currents first.

7.2 Validation of the model

To validate the Thermodenudation Model of Baydara Bay the calibrated model was applied with the temperature from 2014 to 2015 measured at the high coast at Site 2, because for Site 1 no additional measurements were available. As a result, the active layer thickness was calculated to 1.26 m. The temperature measurements indicated an active layer thickness between 1.30 and 1.45 m, which is a little higher. Anyway, the calculated result still is in a reasonable range. A reason for the difference could be the different soil type at Site 2, where sand is present (Pearson 2016). Since sand usually is coarser than clay, the thermal conductivity

could be higher than assumed in the Thermodenudation Model. The erosion rate at site 2 was on average 1.5 m per year. With the thermodenudation model a coastal erosion of 1.80 m was obtained, which is a little high but still in a reasonable range, considering the different geometry of Site 2.

It should be noted that the Thermodenudation Model was not validated with data from Site 1 and the temperature at Site 2 was considerably higher than at Site 1. Additionally, the bluff at Site 2 is approximately 12 m high and has a slope angle of approximately 45 degrees. Higher cliffs tend to erode more slowly than lower ones, due to their bigger mass, whereas a steeper cliff experiences more erosion than a flatter one (Edil and Vallejo, 1979). Except the temperature and the calculation time, which was extended to match the thawing period at Site 2, nothing else was adjusted to the situation at Site 2. The Thermodenudation Model is thus considered as only validated regarding the active layer thickness. (Pearson 2016)

7.3 Climate change scenarios

7.3.1 Water level increase

The results of the coastal retreat rates show a significant dependence on the position of the water level. An increase of the water level leads to a reduction of the slope stability, which made it necessary to increase the friction angle to 32 degrees to obtain results for all climate change scenarios. Otherwise, the calculation phase *Safety Analysis* could not be conducted, since soil body collapse was reported as an error message in the previous *Equilibrium* phase. Additionally, an increase of the water level leads to a reduction of the coastal retreat rates, compared to calculations, where the water level remained at the position of Baydara Bay in 2013 but with an adapted friction angle of 32 degrees. This is not reasonable, because in the nature, water at the toe of the bluff would lead to the removal of soil through waves and currents and a further destabilization of the bluff, which is also called the thermoabrasion (see chapter 2.2 for more information). Plaxis is not able to simulate the effects of waves and currents and considers a water level only as hydrostatic pressure and temperature. Especially in the extreme scenarios, where the water has a certain depth at the toe of the bluff and the water temperature is below the air temperature during the thawing period the water level leads to a reduction of the erosion. In fact, for the extreme scenario in 2100 only a coastal erosion of 1.3 m was calculated when considering the increased water level, whereas otherwise the erosion was 3.2 m, which is much more reasonable. But also, an increase of the water level below the ground surface reduces the erosion rate, thus considering a water level directly at the ground surface

leads to an erosion rate of 1.2 m for Baydara Bay 2013, whereas the erosion rate was 1.3 m, when the water level was placed 0.3 m below the ground level, which is a more reasonable location.

The position of the water level does not show any influence on the thawing depth or the temperature distribution of the bluff.

To obtain comparable and reasonable results for all climate change scenarios and to model the worst-case scenario, the water level increase was neglected, instead the water level of the situation at Baydara Bay in 2013 was selected for all climate change scenarios and only the temperature increase as shown in Table 6-2 was applied. A friction angle of 30 degrees was used as shown in Table 6-1.

7.3.2 Coastal erosion

The active layer thickness for the year 2050 could be determined to 1.24 m, which is an increase by about 39 % towards the situation in 2013. The obtained value is in a reasonable dimension, since projections of the ACIA predicted an increase of the active layer thickness by more than 50 % for the Russian Arctic coast from 1981 - 1990 to 2050 (ACIA 2005).

The coastal retreat rate is shown in Figure 7-4. For the year 2050 it was determined to 1.793 m, which is an increase by 38 % relative to the coastal erosion in 2013. The coastal erosion is therefore strongly related to the active layer thickness.

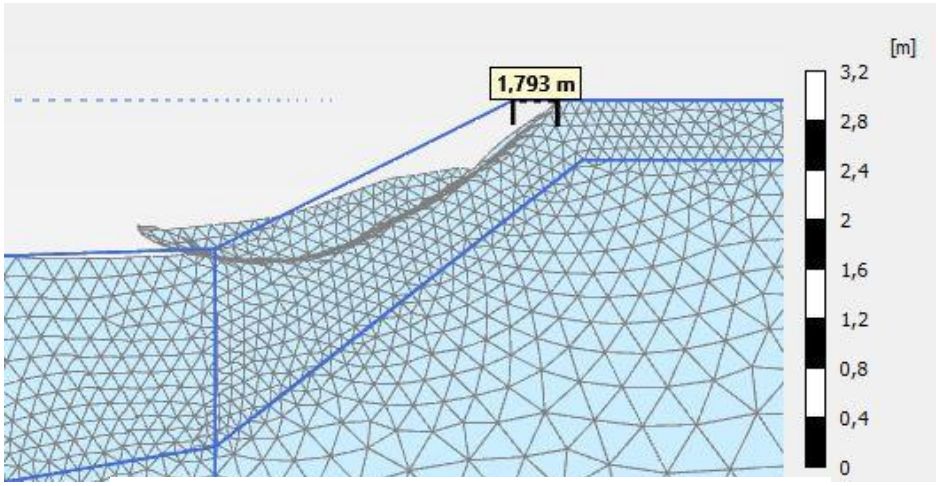

Figure 7-4: Coastal retreat in 2050 for Scenario 1

The potential volume of eroded soil, which includes the whole area of displacements and which represents the worst case, was calculated to 52.49 m^2/m in the year 2050 for Scenario 1. This is an increase by 18 % compared to 2013.

The extreme climate change scenario for 2050 is quite like the average scenario. The temperature increase is only 0.5 °C higher. The coast retreats about 1.867 m per year, while the active layer thickness is about 1.28 m. That is an increase by 44 % compared to 2013 in both cases. The potential volume of eroded soil was calculated to 56.56 m^2/m, which is an increase of 27 % compared to 2013.

For the year 2100, in the average climate change scenario an active layer thickness of about 1.512 m was calculated. According to Lawrence et al. (2015) an active layer thickness up to 2 m is reasonable for the Russian Arctic. Since only an average temperature increase was simulated, the obtained value seems reasonable. The coastal retreat rate was about 2.4 m. This is an increase of 71 % and 85 % respectively compared to the situation in 2013. The volume of potentially eroded soil was 60.87m^2/m, an increase by 37 % compared to 2013.

For Scenario 2, the active layer thickness was 1.9 m, which still is below the maximum predicted active layer thickness of 2 m, this is an increase by 113 % compared to 2013. The coastal retreat was about 3.2 m, which is an increase by 146 % compared to 2013. The potential volume of eroded soil was 69.48 m^2/m, which is an increase by 56 % compared to 2013. Figure 7-5 shows the coastal retreat in 2100 for Scenario 2.

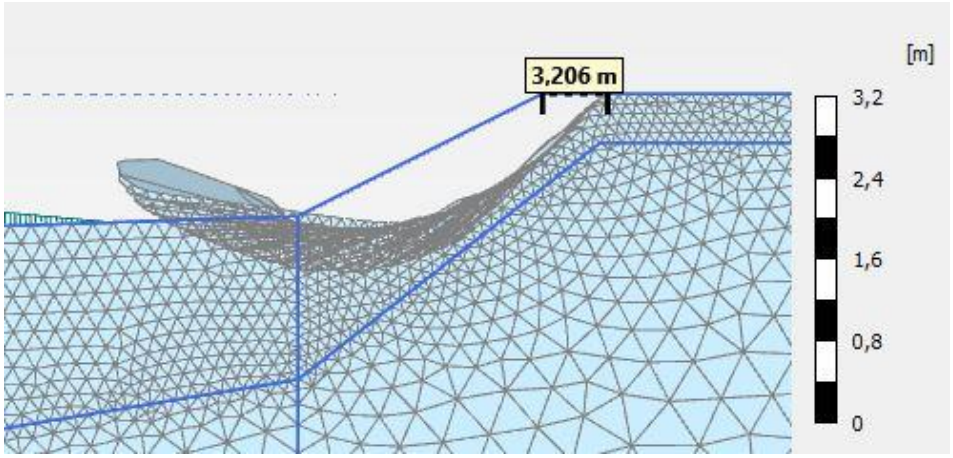

Figure 7-5: Coastal retreat in 2100 for Scenario 2

The results show that there is generally a strong correlation between active layer thickness increase and coastal retreat rate increase, but for higher temperatures, the costal retreat rate exceeds the increase in active layer thickness.

The results of the climate change scenario are summarized in Table 7-1.

Table 7-1: Results of the climate change scenarios

	Baydara 2013	Baydara 2050		Baydara 2100	
		Scenario 1	Scenario 2	Scenario 1	Scenario 2
Active layer thickness [m]	0.89	1.24	1.28	1.51	1.90
Coastal retreat rate [m]	1.30	1.79	1.87	2.4	3.2
Potential eroded soil volume [m^2/m]	44.46	52.49	56.56	60.87	69.48

Figure 7-6 shows the development of the active layer thickness (red) and the coastal retreat rate (blue) from 2013 to 2100 for Scenario1 and 2. On the abscissa the time from the year 2000 to the year 2100 is shown, whereas the axis of ordinates presents optionally the coastal retreat rate or the active layer thickness in m.

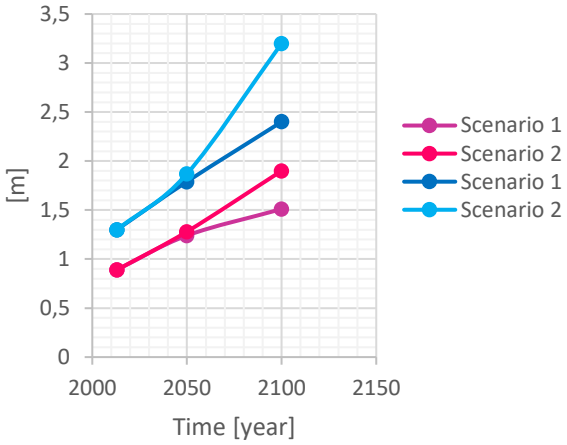

Figure 7-6: Development of active layer thickness (red) and coastal retreat rate (blue) from 2013 -2100

For Scenario 1 the development of the active layer thickness follows a flattening curve, indicating that the rate of increase is reduced to the end of this century, whereas for Scenario 2 the active layer thickness increases linearly. The coastal retreat rate follows for both secenarios for lower temperatures until 2050 quite closely the curves for the active layer thickness, then the coastal retreat rate exceeds the active layer thickness. For Scenario 1 the coastal retreat rate increases linearly, whereas the rate of increase for Scenario 2 is larger and nonlinear.

7.3.3 Bearing capacity and slope stability

An indication for the slope stability is the factor of safety (FS), which is defined as the ratio of mobilized strength to strength at failure. For design purposes the FS is usually set to 1.5. The FS calculated for the different climate change scenarios is presented in Table 7-2.

Table 7-2: FS for the climate change scenarios

	Baydara Bay 2013	Baydara Bay 2050		Baydara Bay 2100	
		Scenario 1	Scenario 2	Scenario 1	Scenario 2
FS	1.1	1.05	1.05	1.05	1.04

The factor of safety is in all cases lower than the required 1.5. This means that the slope itself is unstable and the bearing capacity is very low and not sufficient for additional structural measures.

To obtain dimensions of the available bearing capacity line loads were applied on top of the bluff. Thereby two cases were distinguished. In Case 1 a line load of 5 m length was placed directly at the crest, in Case 2 the same line load was placed 15 m from the crest away, thereby the strength of the soil, depending on the active layer thickness without the influence of the slope can be investigated. In the calculation process, the load was increased in steps of 1 kN/m for Case 1 until failure occurred.

For Case 2 the strength was much higher so steps of 5 kN/m were chosen. Since the FS calculated in the loading scenarios was close to 1.0, the maximum loads were reduced according to a FS of 1.5. The results are presented in Table 7-3. The extreme Scenario 2 was only considered for the year 2100.

Table 7-3: Maximum load for Case 1 and 2

	Case 1 [kN/m/m]	Case 2 [kN/m/m]
Baydara 2013	31.333	231.933
Baydara 2050	25.867	221.667
Baydara 2100, 1	16.640	215.333
Baydara 2100, 2	12.800	206.667

In both cases, the bearing capacity decreases with increasing active layer thickness. The maximum load in Case 1 is reduced from 2013 to 2100 by 47 % for Scenario 1. For Scenario 2 only 40 % of the original bearing capacity is left, which means a reduction of 60 %. The loading capacity in Case 2 shows a much less strong decrease of the maximum loading capacity. Thus, from 2013 to 2100 only about 7 % of the bearing capacity is lost for Scenario 1, whereas for Scenario 2 the maximum load is reduced by 11 % in the same period.

Additionally, the loading capacity in Case 2 is in general much higher, since most of the load

is carried by the stable permafrost and there is no tendency of the active layer to slide. The maximum load in Case 2 causes deformations at the edges of the load, which sink into the soil until their reach the permafrost table. This is reasonable, since the active layer usually has a soft consistence and can easily be squeezed away.

7.4 Protection measure: Thermosyphon

In order to investigate the effect of a thermosyphon as a protection measure, a thermosyphon was installed in the model below the slope to follow the shape of the slope in a depth of -1 m in 2013. The thermosyphon is equipped with a fluid which has a maximum temperature of 273.15 K, which means the cooling effect starts at this temperature. The temperature variation of the fluid follows a harmonic curve with an amplitude of 15 and a phase of one year, because this also is the amplitude of the air temperature at Baydara Bay in 2013. The reference temperature is set to -5 °C, because this is approximately the average temperature at Baydara Bay in 2013. Because the cooling effect of the thermosyphon develops progressively over a period of several seasons, the calculation time of the *Quarter year cycle* phase was extended to 3 years.

Figure 7-7 shows a section of the temperature variation from the second to the third year at a point between thermosyphon and the ground surface. The pink line represents the temperature variation without the influence of the thermosyphon, whereas the blue line shows the effect of the thermosyphon on the temperature development.

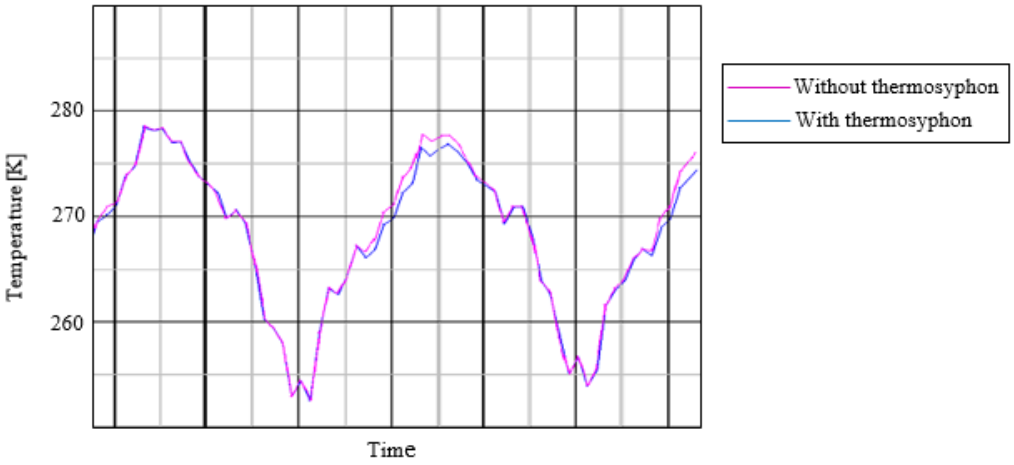

Figure 7-7: Temperature variation with and without thermosyphon

As visible, from the second year on, the thermosyphon reduces the temperature in the summer, because it slows down the thawing of the soil due to its passive cooling function, which starts at a temperature of 273.15 K. Although the temperature reduction is quite small, about 2 °C,

the active layer thickness could be reduced to 0.5 m on the slope, whereas without the thermosyphon the active layer thickness was about 1 m at the same location. Figure 7-8 shows the temperature distribution.

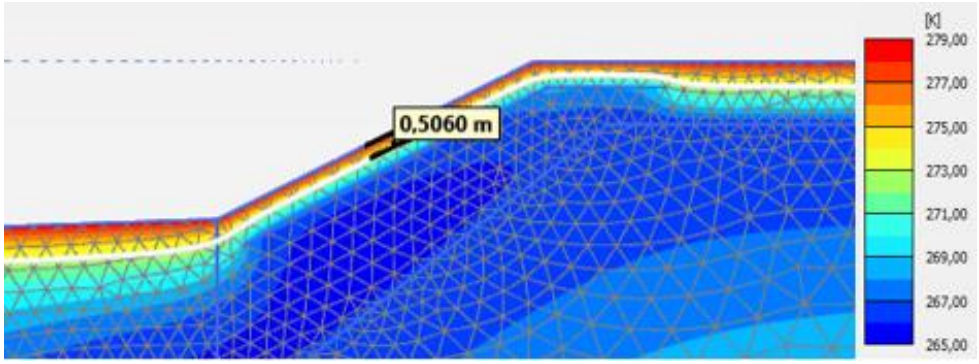

Figure 7-8: Temperature distribution with a thermosyphon

The maximum thawing depth at the slope at the end of the thawing period is 1.2 m with the thermosyphon and 1.9 m without. This prevents any coastal retreat as Figure 7-9 shows, but still leads to some erosion at the slope.

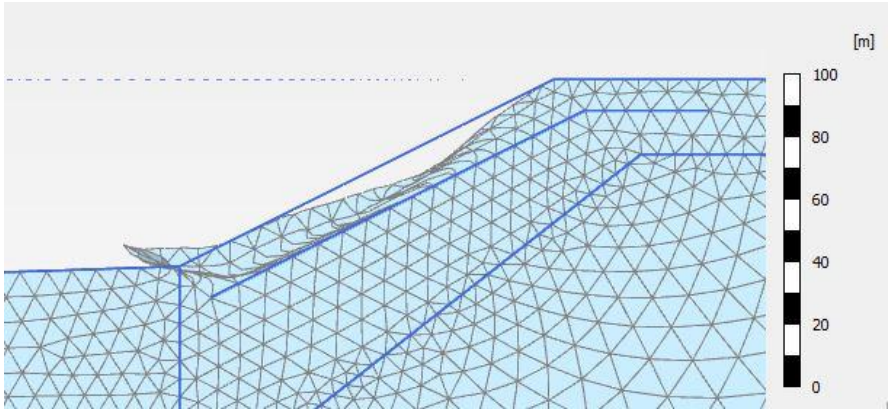

Figure 7-9: Coastal retreat with a thermosyphon

This also leads to a reduction of the volume of eroded soil, which is only 27.85 m^2/m when considering the whole failure plane. Without the thermosyphon the volume was 44.46 m^2/m. Furthermore, also the bearing capacity of the slope could be significantly increased by using a thermosyphon, so the maximum load in Case 1 (5 m line load directly at the crest) could be determined to 76 kN/m/m, which nearly is 2.5 times the maximum load in Case 1 of Baydara Bay in 2013 without the thermosyphon. To investigate the effect of a thermosyphon also when high temperatures are present, the temperature of the extreme Scenario 2 in 2100 was simulated. Hereby the thermosyphon could not prevent coastal erosion, in fact the coastal retreat was still 2.7 m, compared to 3,2 m without the thermosyphon. The active layer thickness was only reduced by 50 cm to 2.5 m on the slope. The maximum load in Case 1 for this Scenario was accordingly lower with only 16.467 kN/m. But compared to the situation in 2100, Scenario 2 without the thermosyphon, the bearing capacity still increased by more than 25 %.

This example shows, that thermosyphons can be an effective measure to reduce or even prevent coastal erosion in Arctic areas when relatively low temperatures during the summer period are present. For higher temperatures additional measures to stabilize the slope, e.g. slope reinforcement, bulkheads, are necessary. Thermosyphons only protect a slope against thawing, so in addition a toe protection should be constructed if an erosion due to waves and currents is expected.

7.5 Parameter variation

The following parameters were varied to investigate their effect on the active layer thickness, the coastal retreat rate, the slope stability and the volume of eroded soil.

- Friction angle
- Particle density
- Slope angle
- Specific heat capacity
- Thermal conductivity
- Unit weight

Additionally, by doing this, the parameters which have a considerable influence on the results and which therefore need to be determined carefully can be identified. For the parameter variation, the model of Baydara Bay in 2013 was used. The original values of the parameters mentioned above are mainly summarized in Table 6-1. The slope angle of the Thermodenudation Model at Baydara Bay was 26.57 degrees.

The friction angle was varied between 27 and 33 degrees and showed a strong correlation with the factor of safety. An increase in the friction angle leads to an increase in the factor of safety e.g. for a friction angle of 27 degrees the factor of safety only was 0.98 whereas a friction angle of 33 degrees leads to a factor of safety of 1.25. The coastal retreat rate varied between 1.3 and 1.6 m, but showed no clear correlation with the friction angle.

The particle density was varied between 1500 and 3500 kg/m^3 and had an influence on the active layer thickness and the factor of safety. An increase in the particle density leads to an increase in active layer thickness, e.g. the active layer thickness with a particle density of 1500 kg/m^3 was 0.78 m, compared to 0.91 m with a particle density of 3500 kg/m^3. The factor of safety increased from 1.11 to 1.24 respectively. This can be explained physically, since the thermal conductivity of a material is correlated to its density. In a soil with a lower density less contact surfaces between soil grains are present to transmit heat. But, because the change in the

active layer thickness due to variation of the particle density is relatively low, no clear influence on the coastal retreat rate could be determined. Therefore, it is sufficient to calculate with the common particle density of 2600 kg/m^3 if no measured values are available.

During the slope angle variation, the angle was gradually reduced to 10 degrees, because an increase was not possible due to soil body collapse in the Thermodenudation Model of Baydara Bay. The slope angle had a major influence on the coastal erosion rate and the factor of safety. The slope angle of Baydara Bay in 2013 was 26.57 degrees, a reduction to 18 degrees lead to a decrease of the coastal erosion to 0.4 m compared to the originally 1.3 m. The factor of safety increased to 1.4. At a slope angle of 10 degrees there was no coastal retreat at all. The factor of safety was 2.3. To investigate the effects of a steeper slope angle, the friction angle was increased to 34 degrees. This made it possible to increase the slope angle to 27.6 degrees, resulting in an increased coastal erosion of 1.4 m and a factor of safety of 1.05. A further increase of the slope angle was not possible due to the low stability of the bluff. In sum, a reduction of the slope angle reduces the retreat of the bluff. An increase in the slope angle also leads to increased coastal retreat rates. This is reasonable, because at steeper slopes the weight forces of the soil reinforce the tendency of the soil to slide down rather than to experience horizontal displacements.

The specific heat capacity, which was varied from 500 - 2000 J/kg/K has an influence on the active layer thickness. A decrease in the specific heat capacity also leads to a decrease in the active layer thickness, whereas the coastal retreat and the factor of safety remained nearly constant. With a specific heat capacity of 500 J/kg/K the active layer was 0.82 m deep and with a specific heat capacity of 2000 J/kg/K the active layer thickness was about 1 m. This is reasonable since the specific heat capacity of a soil describes the amount of heat, which can be stored in the solid material. If a soil can store more heat the active layer thickness will be higher because refreezing is slowed down. However, except for the active layer thickness the influence of this parameter on slope stability and retreat rate is negligible.

The thermal conductivity was varied from 1 to 3 W/mK and mainly influenced the active layer thickness. Hereby an unreasonable behaviour could be noticed, because an increase in the thermal conductivity led to a decrease in the active layer thickness. Thus, with a thermal conductivity of 3 W/mK the active layer thickness was 0.81 m, whereas with 1W/mK it was about 1.05 m. The reason for this behaviour was the presence of the second thermal boundary condition which simulates the temperature variation in the permafrost. Because of this, two opposite heat sources, a cold one from the permafrost and a warm one from the ground surface,

occur. Without considering the second thermal boundary condition the active layer thickness was 2.7 m deep with a thermal conductivity of 2.5 W/mK, then the coastal retreat increased to approximately 2.6 m. An active layer thickness of 1.9 m was calculated with a thermal conductivity of 1 W/mK.

The saturated and unsaturated unit weight was varied from 15 - 23 kN/m^2. The unit weight showed a clear effect on the coastal retreat and on the deformation. This also influenced the volume of eroded soil, which was therefore calculated as well. A decrease in the unit weight leads to a decrease in the coastal retreat rate, but to an increase in the volume of the eroded soil, because the shape of the deformation becomes more curved. So, with a saturated and unsaturated unit weight of 15 kN/m^2 there was no coastal retreat, whereas the eroded soil volume was 26.11 m^2/m. An increase in the unit weight leads to an increase in coastal retreat rate and eroded soil volume. For example, with a saturated and unsaturated unit weight of 23 kN/m^2 the coastal retreat was 1.62 m and the eroded soil volume 37.21 m^2/m. Here the shape of the deformation does not differ much from the original situation of Baydara Bay, where the unit weight was 20 kN/m^2. The ratio between saturated and unsaturated unit weight doesn't have much influence on the coastal retreat rate, but leads to higher volumes of eroded soil. This could be because a difference indicates a soil, which is partially saturated, and a certain water content could have a destabilizing effect on the slope.

Table 7-4 summarizes the results of the parameter variation.

Table 7-4: Results of the parameter variation

Parameter	Main influence on:	Description
Friction angle	Factor of safety	Increase leads to a higher slope stability
Particle density	Active layer thickness, factor of safety	Increase leads to an increase in active layer thickness and factor of safety. Negligible effect on erosion rate
Slope angle	Coastal retreat rate, factor of safety	Increase leads to higher coastal retreat
Specific heat capacity	Active layer thickness	Increase leads to an increase of active layer thick-ness. No significant effect on the coastal retreat
Thermal conductivity	Active layer thickness, coastal retreat rate	increase leads to an increase of active layer thickness and coastal retreat rate
Unit weight	Coastal retreat rate, volume of eroded soil	Decrease leads to a decrease of the coastal erosion rate but an increase of eroded soil volume increase leads to an increase of both parameters

In general, most of the investigated parameters had no clear influence on the coastal retreat rate, because the changes in the active layer thickness were too small to have an effect. For the determination of the active layer thickness they are however important. The slope angle and the unit weight had a major influence on the coastal retreat rate and the deformation. The thermal conductivity also is important but leads to changes in the retreat rate only when the variation in the active layer thickness is high enough. Very important also are the location and values of the thermal and hydraulic boundary conditions and the position of the water level. There a small displacement could cause huge differences in the output results.

8 Conclusion

The objective of this thesis was the development of a thermo-hydro-mechanical model in Plaxis, to simulate the thermodenudation erosion process in Arctic areas and to obtain the mass of eroded soil.

The objective of the thesis has been archived by developing a new modelling approach, which consists of a thermo-hydro-mechanical coupling with a conventional Mohr Coulomb soil model to model the response of the unfrozen soil and a combination of the Mohr Coulomb model with the cryogenic suction in the frozen domain. The thermal and hydraulic elements of the thermo-hydro-mechanical model are calculated in a 'Flow Model'. Among various thermal and hydraulic properties, the Flow Model evaluates the cryogenic suction according to the Clausius-Clapeyron equation. The thermal and hydraulic model properties are coupled with a mechanical 'Stability Model' via Python program codes. The, thus developed Thermodenudation Model allows the modelling of thermo-hydro-mechanical processes including instabilities of coastal slopes and coastal retreat rates. The model assumes that failure only takes place in the unfrozen part of the soil and does not consider the development of excess pore pressures due to the thawing of soil. Another limitation of the model is its inability to consider the effects of a water level, e.g. waves and currents on the erosion, therefore it can only be used at slopes, which don't have direct contact with water. The volume of eroded soil is calculated separately with an Excel sheet, in which all element areas, which experience a certain displacement are summed up.

The Thermodenudation Model was successfully calibrated and partly validated to the coast of Baydara Bay and used to study the effects of climate change scenarios on the active layer thickness, the erosion rates and the volume of eroded soil. The calculated results showed a reasonable behaviour of all investigated parameters and a strong correlation between active layer thickness and coastal retreat rate. This is reasonable and corresponds to the predicted development, so that the applicability of the model for such a purpose can be confirmed. Additionally, the bearing capacity of the slope was investigated. The obtained results seem reasonable and showed that the bearing capacity of the bluff was also strongly correlated to the active layer thickness. Away from the bluff the bearing capacity was much higher, because there the loads are mainly carried by the stable permafrost ground and the soil shows less tendency to slide. The Thermodenudation Model also was used to successfully simulate the effects of a thermosyphon as a coastal protection measure on the active layer thickness, which

could be reduced significantly preventing any coastal retreat, for lower temperatures. For high temperatures additional measures are necessary. Additionally, a parameter variation was conducted, by which the slope angle of the bluff, the unit weight of the soil and the location of the boundary conditions and the water level were identified as most important.

Although further research in developing more advanced models of the thermodenudation process can be conducted, the Thermodenudation Model provides one of the first possibilities to simulate the thermodenudation erosion process.

8.1 Recommendation for further work

The recommendations for further work mainly result from the limitations of the developed model and the paucity of the available data and are summarized as follows:

- The Thermodenudation Model was only partly validated. A full validation should be conducted when sufficient temperature measurements and more information about the soil parameters are available.
- The model does not consider excess pore pressure due to the thawing of the soil, possibilities can be investigated to include that into the model code
- The mass of the eroded sediment is calculated in a separate Excel sheet, possibilities can be investigated to include that in the program code.
- The Frozen and Unfrozen Soil Model can be extended so that also a stability analysis with c’ phi’ reduction is supported.

References

Abaqus, (2017): "*Abaqus/CAE User's Guide*", http://abaqus.software.polimi.it/v6.14/books/usi/default.htm, accessed: 26.05.2017

ACIA, (2005): "*Arctic Climate Impact Assessment*", (Cambridge Univ. Press, Cambridge, 2005) http://www.acia.uaf.edu/pages/scientific.html, accessed 15.09.2017

ACIA, (2004). "*Impacts of a Warming Arctic - Arctic Climate Impact Assessmen*t". Cambridge University Press, New York

Amiri, S.A.G., Grimstad, G., Kadivar, M., Nordal, S., (2016): "*A constitutive model for rate-independent behaviour of saturated frozen soils*", Canadian Geotechnical Journal, (53)10, p. 1646 – 1657, DOI: 10.1139/cgj-2015-0467

Amiri, S.A.G., Grimstad, G., Kadivar, M., (2015): "*A thermo-hydro-mechanical constitutive model for saturated frozen soils*", Conference Paper, DOI: 10.3233/978-1-61499-601-9-1024, Trondheim, Norway.

Andersland, O.B., Ladanyi, B., (2004): "*Frozen Ground Engineering* ", 2nd ed., ISBN 0471615498, John Wiley & Sons, New Jersey

Aukenthaler, M., Brinkgreve, R.B.J., Haxaire, A., (2016): "*Evaluation and application of a constitutive model for frozen and unfrozen soil*", Geovancouver 2016

Barnhart, K.R., Anderson, R.S., Overeem, I., Wobus, C., Clow. G.D., Urban, F.E., (2013): "*Modeling erosion of ice-rich permafrost bluffs along the Alaskan Beaufort Sea coast*", Journal of Geophysical Research: Earth Surface, research article 10.1002/2013JF002845, p. 1155 - 1179

Bates, N.R., Mathis, J.T., (2009): "*The Arctic Ocean marine carbon cycle: evaluation of air-sea CO2 exchanges, ocean acidification impacts and potential feedbacks*", Biogeosciences, 6, p. 2433 - 2459

Blanck. E., (1929): "*Handbuch der Bodenlehre: Band 1: Die naturwissenschaftlichen Grundlagen der Lehre von der Entstehung des Bodens*", Springer Verlag, ISBN 978-3-540-01083-8, DOI 10.1007/978-3-642-45801-9

Building Research Advisory Board (1963): Proceedings, Permafrost International Conference, 11-15 November 1963, Indiana

Briaud, J., (2013): "*Geotechnical Engineering: Unsaturated and Saturated Soils*", ISBN: 9780470948569, John Wiley & Sons, Inc. New Jersey

Carson, M.A. (1971): "*The mechanics of erosion. Monographs in spatial and environmental systems analysis*", Pion Publisher, London.

Cheng, G., Zhang, J., Sheng, Y., Chen, J., (2004): „*Principle of thermal insulation for permafrost protection*", Cold Regions Science and Technology 40 (2004), p. 71 -79

Clarke, J., Fenton, C., Gens, A., Jardine, R., Martin, C, Nethercot, D., Nishimura, S., Olivella, S., Reifen, C., Rutter, P., Strasser, F., Toumi, R., (2008): "*A Multi-Disciplinary Approach to Assess the Impact of Global Climate Change on Infrastructure in Cold Regions*", International Conference on Permafrost. "9th International Conference on Permafrost". 2008, p. 279 - 284.

CODE_BRIGHT, (2017): "*User's Guide*", www.etcg.upc.edu/recerca/webs/code_bright, Department of Geotechnical Engineering and Geosciences, Technical University of Catalonia accessed: 28.05.2017

COMPASS, (2017): Homepage University of Cardiff, http://grc.engineering.cf.ac.uk/facilities/compass/, accessed: 01.06.2017

COMSOL Multiphysics ®, (2017): "*User's Guide*", http://people.ee.ethz.ch/~fieldcom/ppscomsol/documents/User%20Guide/COMSOLMultiphysicsUsersGuide.pdf, accessed: 26.05.2017

Craig B., Leidersdorf, M., Peter E., Gadd, M., William G., Mcdougal, M., (1990): "*Arctic slope protection methods*", Coastal Engineering Proceedings, 1(22).

Dagher, E. E., Su, G., Nguyen, T.S., (2014): "*Verification of the Numerical Simulation of Permafrost Using COMSOL Multiphysics® Software*", Canadian Nuclear Safety Commis-sion, Ottawa, ON, Canada

De Goede, E., De Graaff, R., (2014): "*Ice modelling in Delft3D, with application to the North Sea and to lakes*", Presentation JONSMOD2014, Brussels

Depina, I., Guégan, E.B.M., Sinitsyn, A., (2017): "*Arctic coastal erosion protection measur*es", a state of the art report, SAMCOT

Edil, T.B. And Vallejo, L.E., (1979): "*Mechanics of coastal landslides and the influence of slope parameters*", Engineering Geology, 16 (1980), p. 80 - 96

Elias, V.; Christopher, B.R. (1997): "*Mechanically stabilized earth walls and reinforced soil slopes - design and construction guidelines*". August. Tech. Rep. No. FHWA-SA 96-071,

reprinted September 1998. FHWA Demonstration Project 82. Washington, DC: Department of Transport., Federal Highway Administration. Pp 369, http://www.fhwa.dot.gov/bridge, accessed 21.09.2017

Frauenfeld, O.W., Zhang, T., Mc Creight, J.L., (2007): "*Northern hemisphere freezing/thawing index variations over the twentieth century*", International Journal Of Climatology, 27: p. 47 - 63 (2007), Published online 17 July 2006 in Wiley InterScience (www.interscience.wiley.com) DOI: 10.1002/joc.1372

Fritz, M., Vonk, J.E., Lantuit, H., (2017): "*Collapsing Arctic Coastlines*", Nature Climate Change 7, p. 6 - 7 (2017) doi:10.1038/nclimate3188, Published online 04 January 2017

GeoStudio, (2017): Homepage of GeoSlope, https://www.geoslope.com/products/geos tudio, accessed 22.05.2017

Geotechdata.Info, (2013) (1): "*Angle of Friction*", http://geotechdata.info/ parameter/angle-of-friction.html (as of December 14.2013), accessed: 21.08.2017

Geotechdata.Info (2013) (2): "*Dry unit weight*", http://geotechdata.info/parameter/soil-dry-unit-weight.html (as of August 29, 2013), accessed: 21.08.2017

Gholamzadehabolfazl, A., (2015): "*A Numerical Study of a Highway Embankment on Degrading Permafrost*", Master thesis, University of Manitoba

Glendinning, M.C., (2007): "*Modelling the Freezing and Thawing Behaviour of Saturated Soils*", dissertation, Cardiff University

Gregory, J., (2013): "*Projections of sea level rise*", Climate Change 2013: The Physical Science Basis, Working Group I, contribution to the IPCC Fifth Assessment Report

Guégan, E. B. M. and Christiansen, H. H., (2016): "*Seasonal Arctic Coastal Bluff Dynamics in Adventfjorden, Svalbard*", Permafrost and Periglaclacial Processes 28: p. 18 - 31 (2017), DOI: 10.1002/ppp.1891

Guégan, E., (2015): "*Erosion of permafrost affected coasts: rates, mechanisms and modelling*", doctoral thesis, Norwegian University of Science and Technology, Norway

Harris, C. and Lewkowicz, A.G., (2000): "*An analysis of the stability of thawing slopes, Ellesmere Island, Nunavut*", Canadian Geotechnical Journal, Volume37, p. 449 - 462

Hoque, Md. A.L. and Pollard, W. H., (2009): "*Arctic coastal retreat through block failure*", Canadian Geotechnical Journal (Revue Canadienne de Géotechnique), 2009, Vol.46(10), p.1103 - 1115

Hoque, Md. A.L and Pollard, W. H., (2016): "*Stability of permafrost dominated cliffs in the Arctic*", Polar Science, March 2016, Vol.10(1), p.79 - 88

IPCC, (2001): Climate Change 2001: The Scientific Basis. Summary for Policy makers and Technical Summary of the Working Group I Report, Cambridge 2001

Isaev, V. Koshurnikov, A., Pogorelov, A., Amangurov, R., Podchasov, O., Sergeev, D, Kioka, A., (2016):" *Field investigation and laboratory analyses; Baydaratskaya bay 2016",* SAMCOT report

Jørgensen, A.S., Doré, G., Voyer, É., Chataigner, Y., Gosselin, L., (2007): "*Assessment of the effectiveness of two heat removal techniques for permafrost protection* ", Cold Regions Science and Technology 53 (2008), p. 179 - 192

Kobayashi, N., (1985): "*Formation of thermoerosional niches into frozen bluffs due to storm surges on the Beaufort Sea coast*." J. Geophys. Res., 90(C6), 11983 - 11988.

Lantuit, H. and Pollard, W.H., (2008): *"Fifty years of coastal erosion and retrogressive thaw slump activity on Herschel Island southern Beaufort Sea; Yukon Territory; Canada*", Geomorphology 95, p. 84 - 102

Lawrence, D. M. Koven, C. D., Swenson S. C., Riley, A. G., Slater, W. J., (2015): "*Permafrost thaw and resulting soil moisture changes regulate projected high-latitude CO2 and CH4 emissions*", Environmental Research Letter, Volume10, 094011

Linzbach, A., (2013): "*Coastal erosion on Vestpynten, Svalbard; Engineering measures for shore protection*" LWR Degree Project p.59

Liu, Z. and Yu, X., (2011): "*Coupled thermo-hydro-mechanical model for porous materials under frost action: theory and implementation*", Acta Geotechnica (2011) p. 651. - 65, DOI 10.1007/s11440-011-0135-6

Mathis, J.T., Cross, J.N., Evans, W., And Doney, S.C., (2015): "*Ocean acidification in the surface waters of the Pacific-Arctic boundary regions*", Oceanography 28(2): p. 122 - 135, http://dx.doi.org/10.5670/oceanog.2015.36.

McRoberts, E.C., and Morgenstern, N.R., (1974): "*The stability of thawing slopes*", Canadian Geotechnical Journal, Volume 11.

Na, S.H., and Sun, W.C., (2017): "*Computational thermo-hydro-mechanics for multiphase freezing and thawing porous media in the finite deformation range*", Computer Methods in Applied Mechanical Engineering 318 (2017), p. 667 - 700

Nairn, R. B., Soloman, S. M., Kobayashi, N., Vidrine, J. (1998): "*Development and testing of a thermal-mechanical numerical model for predicting arctic shore erosion process*", Proceedings of the 7th International Conference on Permafrost, Yellowknife, N.W.T., 23–27 July 1998. Edited by A.G. Lewkowitz and M. Allard. Laval University, Que ´bec City, Que. Nordicana No. 57. p. 789 - 795.

Nishimura, S., Gens, A., Olivella, S., Jardine R. J., (2009): "*THM-coupled finite element analysis of frozen soil: formulation and applicatio*n", Géotechnique 59, No. 3, p. 159 - 171 DOI: 10.1680/geot.2009.59.3.159

Oda, M., Iwashita, K., (1999): "*Mechanics of Granular Materials: An Introduction*", ISBN: 90 5410 461 9, AA Balkeema, Rotterdamm

O'Neill Jr, C. R., (1986): "*Structural methods for controlling coastal erosion*", Inform. bull./New York state college of agriculture and life sciences.

Pavlov, A.V., (1994): *"Current changes of climate and permafrost in the Arctic and sub-Arctic of Russia*", Permafrost and Periglacial Processes, 5, p. 101 - 110

Pearson, S.G., Lubbad, R., Le, T.M.H, Nairn, R.B., (2016): "*Thermomechanical erosion modelling of Baydaratskaya Bay, Russia with COSMOS*", Conference Paper, International Conference of Scour and Erosion, At Oxford, UK, DOI: 10.1201/9781315375045-34

Pearson, S., (2015): *"Erosion in the Arctic: A Coastal Engineering Perspective*", Sustainable Arctic Marine and Coastal Technology (SAMCoT), Norwegian University of Science and Technology Trondheim, Norway

PLAXIS, (2017) (1): "*Reference Manual*", https://www.plaxis.com/support/manuals/plaxis-2d-manuals/, accessed: 10.06.2017

PLAXIS, (2017) (2): "*Scientific Manual*", https://www.plaxis.com/support/manuals/plaxis-2d-manuals/, accessed: 10.06.2017

PLAXIS, (2017) (3): "*Material Models Manual*", https://www.plaxis.com/support /manuals/plaxis-2d-manuals/, accessed: 10.06.2017

PLAXIS, (2016): "*The Frozen and Unfrozen Soil Model*", https://www.plaxis.com/support/ models/frozen-and-unfrozen-soil-model/, accessed: 27.06.2017

PLAXIS, (2015): "*Thermal and coupled THM analysis*", https://www.plaxis.com /content/uploads/import/kb/kb-publications/Thermal_and_coupled_THM_analysis.pdf, accessed: 26.09.2017

Ravens, R. M., Jones, B. M., Zhang, J., Arp, C. D., Schmutz, J. A., (2012): "*Process-Based Coastal Erosion Modelling for Drew Point, North Slope, Alaska*", DOI: 10.1061/(ASCE)WW.1943-5460.0000106

Smith, O. and Hendee, M., (2011): "*Responses to Coastal Erosion in Alaska in a Changing Climate: A Guide for Coastal Residents, Business and Resource Managers, Engineers, and Builders*", Alaska Sea Grant College Program.

Thomas, H.R., Vardon, P.J., Li, Y.C., (2009): *"Coupled thermo-hydro-chemo-mechanical modelling for geoenvironmental phenomena*", Proc. of Int. Symp. on Geoenvironmental Eng., ISGE2009, September 8-10, 2009, Hangzhou, China

Thomas, H.R., Cleall, P.J., Li, Y., Harris, C., Kern-Luetschg, M., (2009): "*Modelling of cryogenic processes in permafrost and seasonally frozen soils*", Géotechnique, 59(3), p. 173 - 184

The Engineering Toolbox, (2017) (1): "*Specific Heat of common Substances*", http://www.engineeringtoolbox.com/specific-heat-capacity-d_391.html, accessed 21.08.2017

The Engineering Toolbox, (2017) (2): "*Thermal Conductivity of common Materials and Gases*", http://www.engineeringtoolbox.com/thermal-conductivity-d_429.html, accessed: 21.08.2017

Tsegaye, A. B. (2014): "*Modelling the strength of saturated frozen soil*", [internal report].

WAVEWATCH III, (2017): homepage of the National Oceanic and Atmospheric Administration, U.S. Department of Commerce, http://polar.ncep.noaa.gov/waves/wavewatch/, accessed 05.06.2017

Weihong, H., Jungchun, W., Xizhao, W., Wenjiang, L., (2006): *"Effect of Slope Protection of Crushed Stone on Subgrade in Permafrost*", Cold Regions Engineering 2006: Current Practices in Cold Regions Engineering

Yandong, H., Qingbai, W., Yongzhi, L., Zhongqiong, Z., Siru, G., (2015): "*The thermal effect of strengthening measures in an insulated embankment in a permafrost region*". Cold Regions Science and Technology 116 (2015), p. 49 - 55

Zhang, Y., (2014): "*Thermal-hydro-mechanical model for freezing and thawing of soils*", dissertation University of Michigan

Zhang, T., Frauenfeld, O.W., Serreze, M.C., Etringer, A., Oelke, C., Mccreight, J., Barry, R.G., Gilichinsky, D., Yang, D., Ye, H., Ling, F., Chudinova, S., (2005): "*Spatial and temporal*

variability in active layer thickness over the Russian Arctic drainage basin", Journal of Geophysical Research, Volume 110, Issue D16, 27 August 2005

Zetsche, S., Faller, C., Broich, U., (2005): „*Klimawandel in der Arktis, ein Resümee des ACIA Berichts*" Hintergrundpapier, Germanwatch e.V., http://www.germanwatch.org/rio/acia05 .htm, accessed: 21.08.2017

Zhi, W., Yu, S., Wei, M., Jilin, Q., Wu, J., (2005): "*Analysis of effect of permafrost protection by two-phase closed thermosyphon and insulation jointly in permafrost region*s", Cold Regions Science and Technology 43 (2005), p. 150 - 163

Appendix

Location of Profile #3

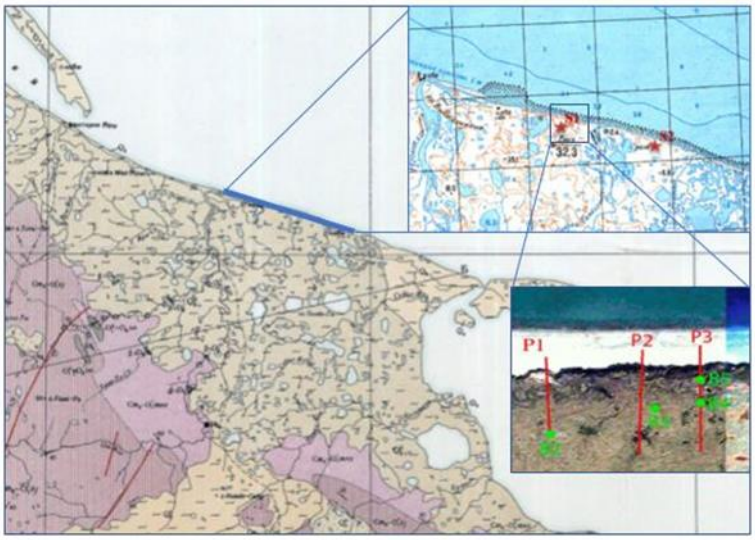

Figure A-1: Location Profile #3

Validation

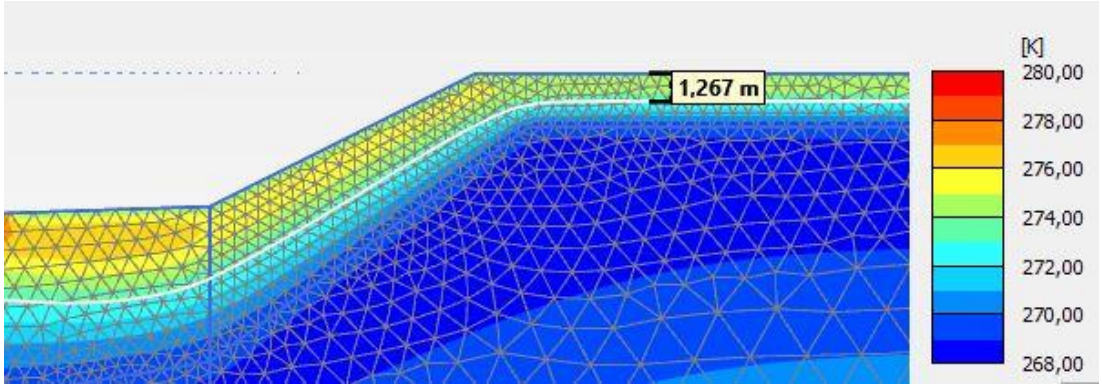

Figure A-2: Temperature distribution at Baydara Bay 2014-2015

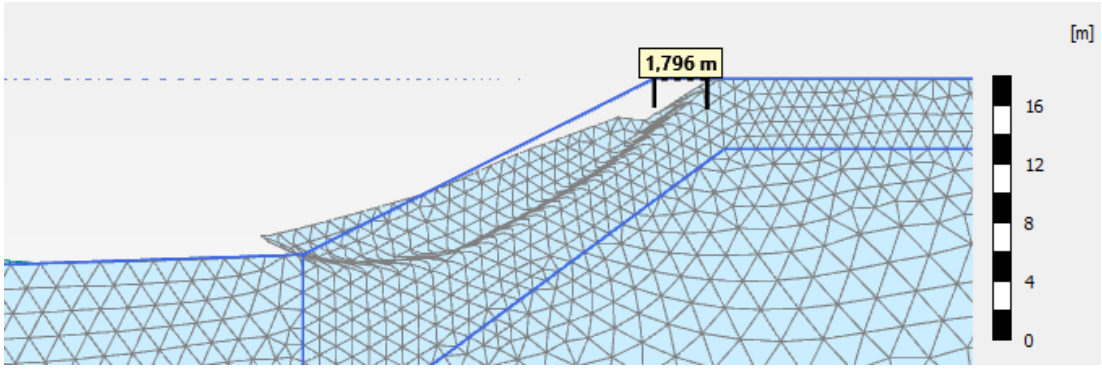

Figure A-3: Coastal retreat at Baydara Bay 2014-2015

Temperature distributions

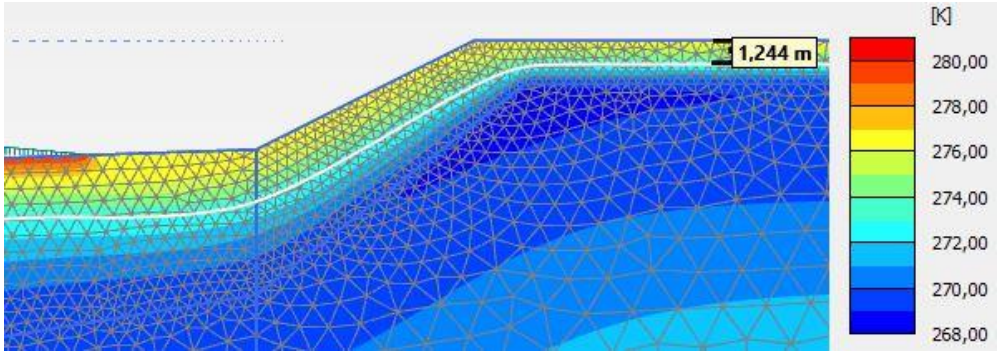

Figure A-4: Temperature distribution 2050, Scenario 1

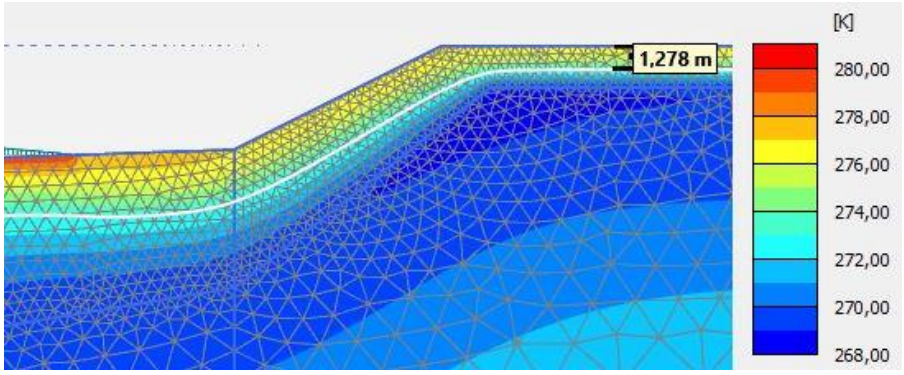

Figure A-5: Temperature distribution 2050, Scenario 2

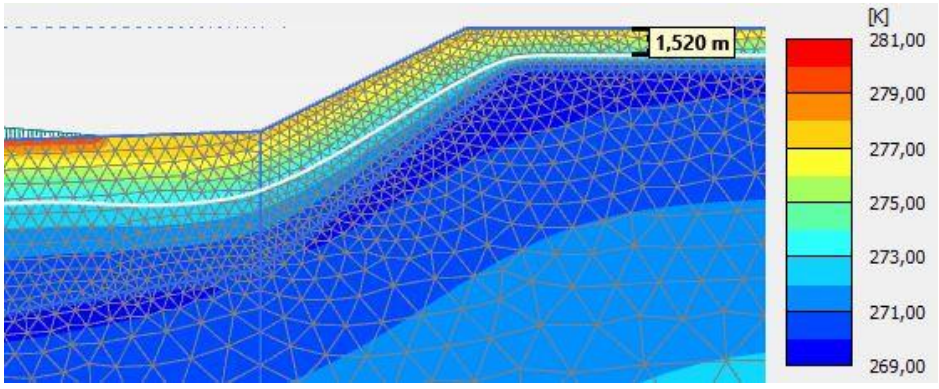

Figure A-6: Temperature distribution 2100, Scenario 1

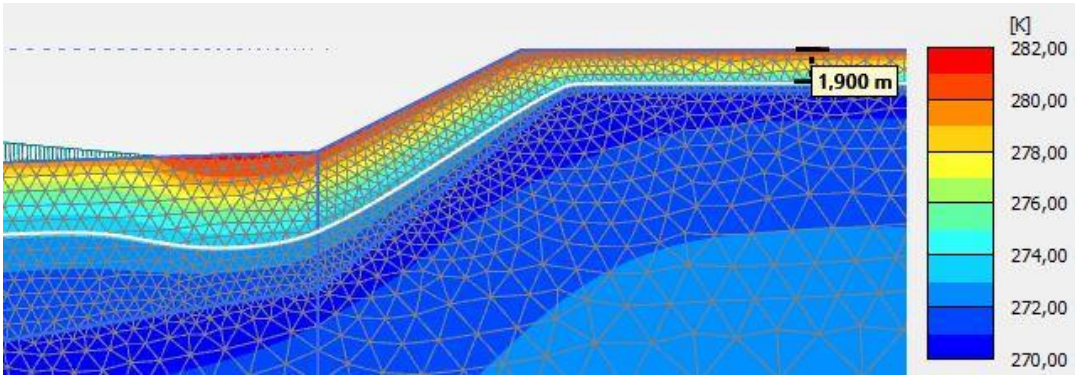

Figure A-7: Temperature distribution 2100, Scenario 2

Deformations

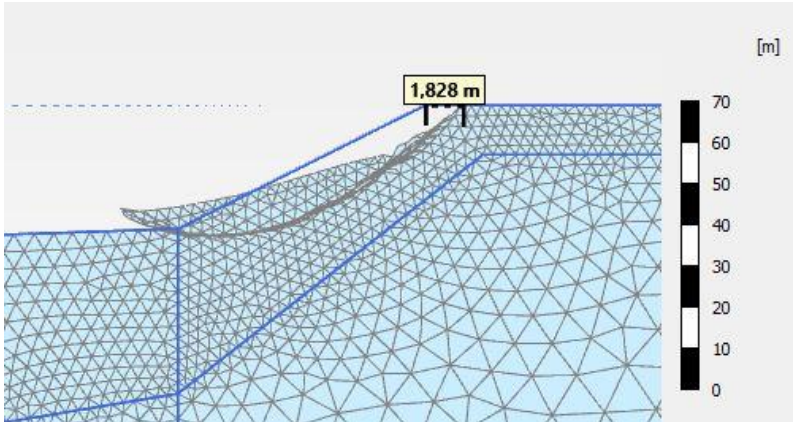

Figure A-8: Deformation 2050, Scenario 2

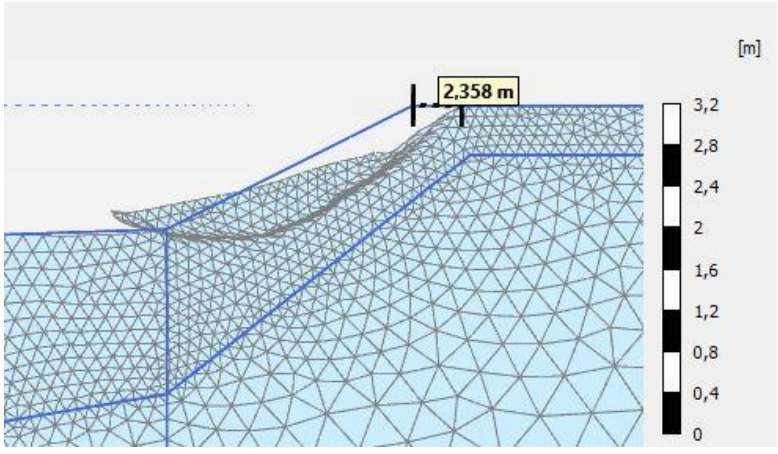

Figure A-9: Deformation 2100, Scenario 1

Areas of displacement

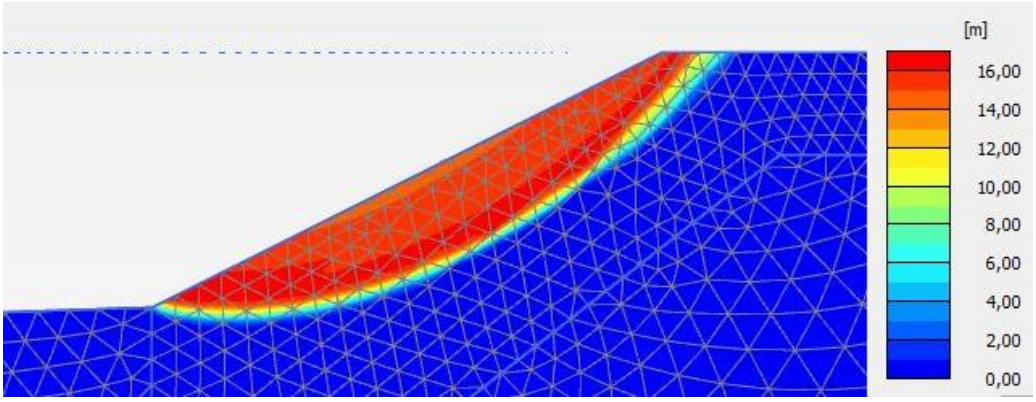

Figure A-10: Area of displacement, 2050, Scenario 1

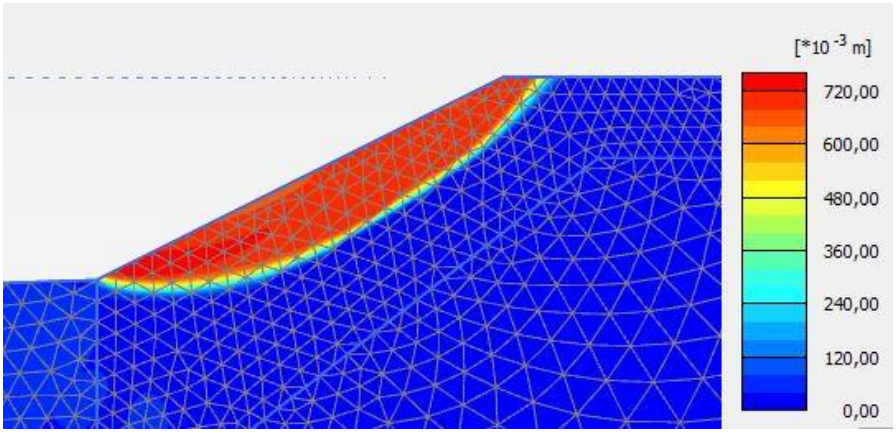

Figure A-11: Area of displacement 2050, Scenario 2

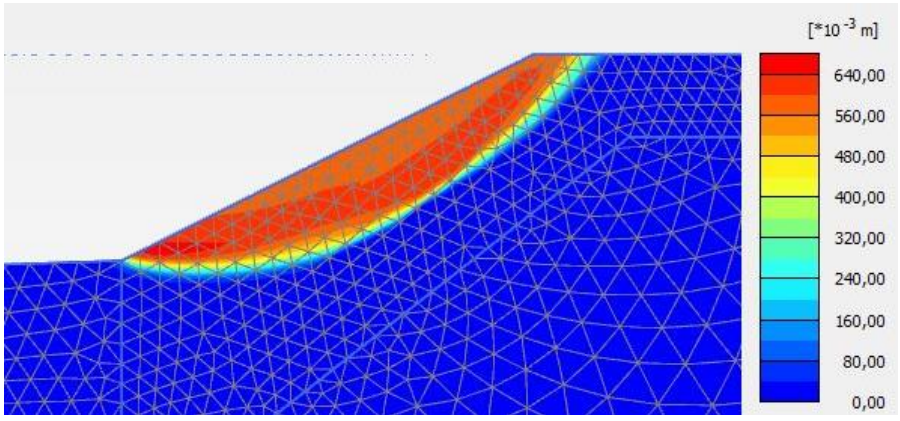

Figure A-12: Area of displacement, 2100, Scenario 1

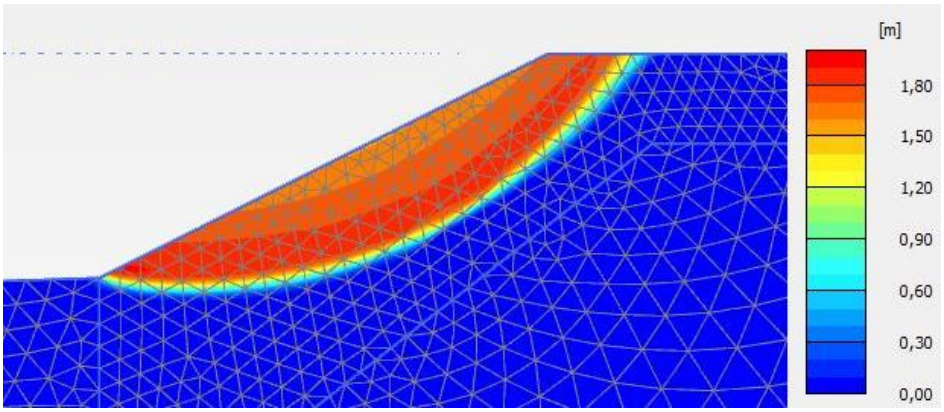

Figure A-13: Area of displacement, 2100, Scenario 2

Bearing capacity investigation

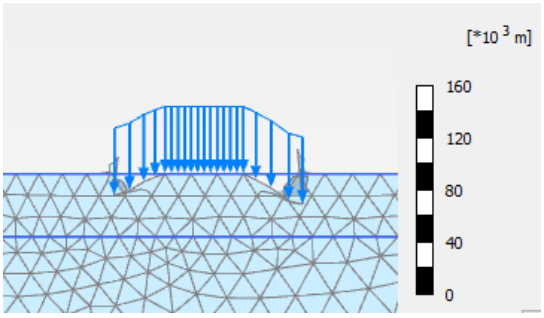

Figure A-14: Deformation in loading scenario Case 2